

Big Sky Regional Carbon Sequestration Partnership – Kevin Dome Carbon Storage FC26-05NT42587

Lee Spangler
Montana State University

U.S. Department of Energy

National Energy Technology Laboratory

Mastering the Subsurface Through Technology Innovation, Partnerships and Collaboration:
Carbon Storage and Oil and Natural Gas Technologies Review Meeting

August 13-16, 2018

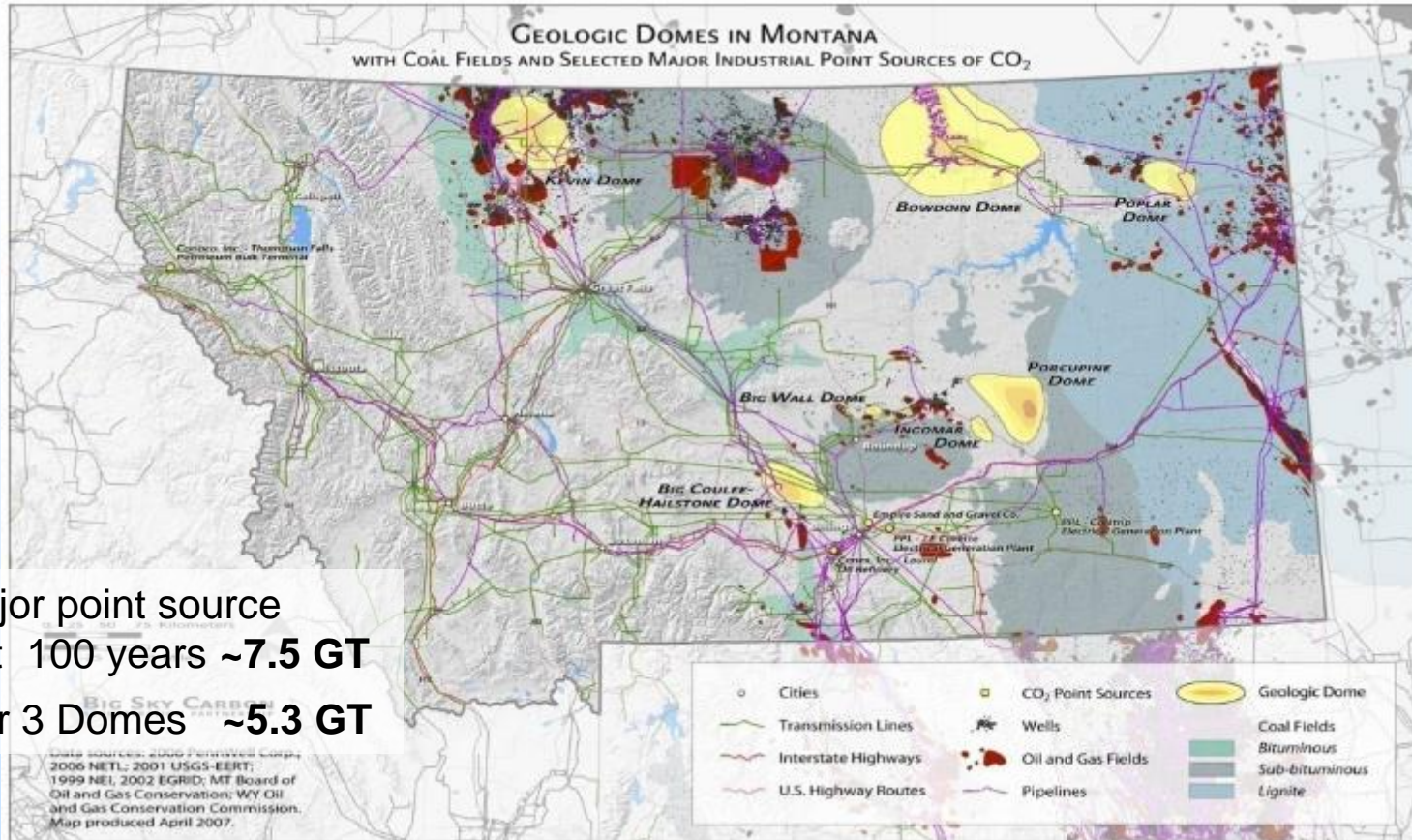


Acknowledgments

- US Department of Energy
- Altamont Oil & Gas, Inc.
- Columbia University & Barnard College
- Idaho National Laboratory
- Los Alamos National Laboratory
- Lawrence Berkeley National Laboratory
- Schlumberger Carbon Services
- SWCA Environmental Consultants
- Vecta Oil and Gas, Ltd.
- Washington State University
- Montana State University

Dave Bowen
Colin Shaw
Omotayo Omosebi
Lianjie Huang
Minh Nguyen
Phil Stauffer
Bryan DeVault
Wade Zaluski
Harry Lisabeth
Jonathan Ajo-Franklin
Tim Kneafsey
Chun Chang
Quanlin Zhou
Curt Oldenburg
Lehua Pan
Bill Carey

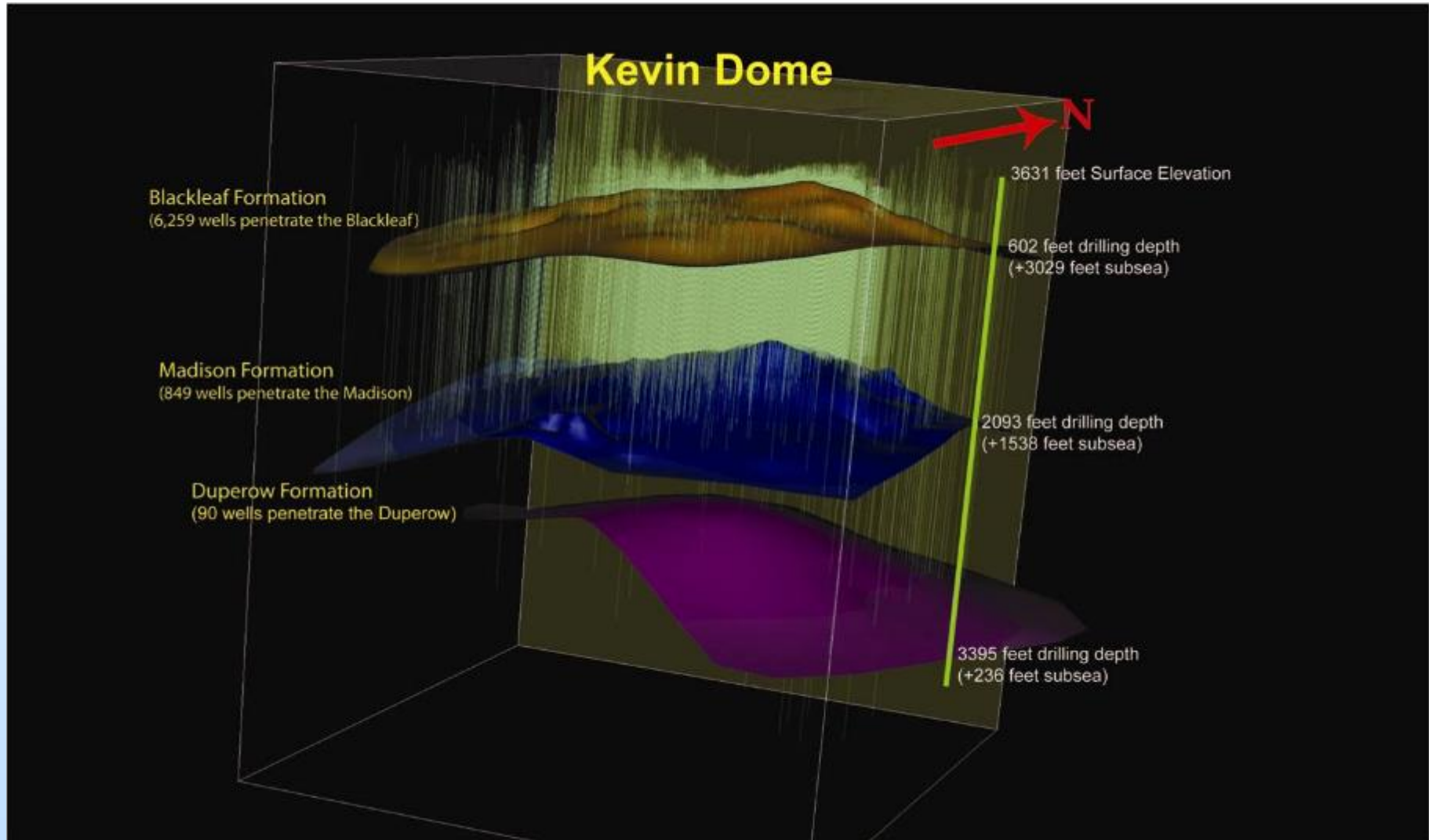
Domes Are Attractive Early Storage Target



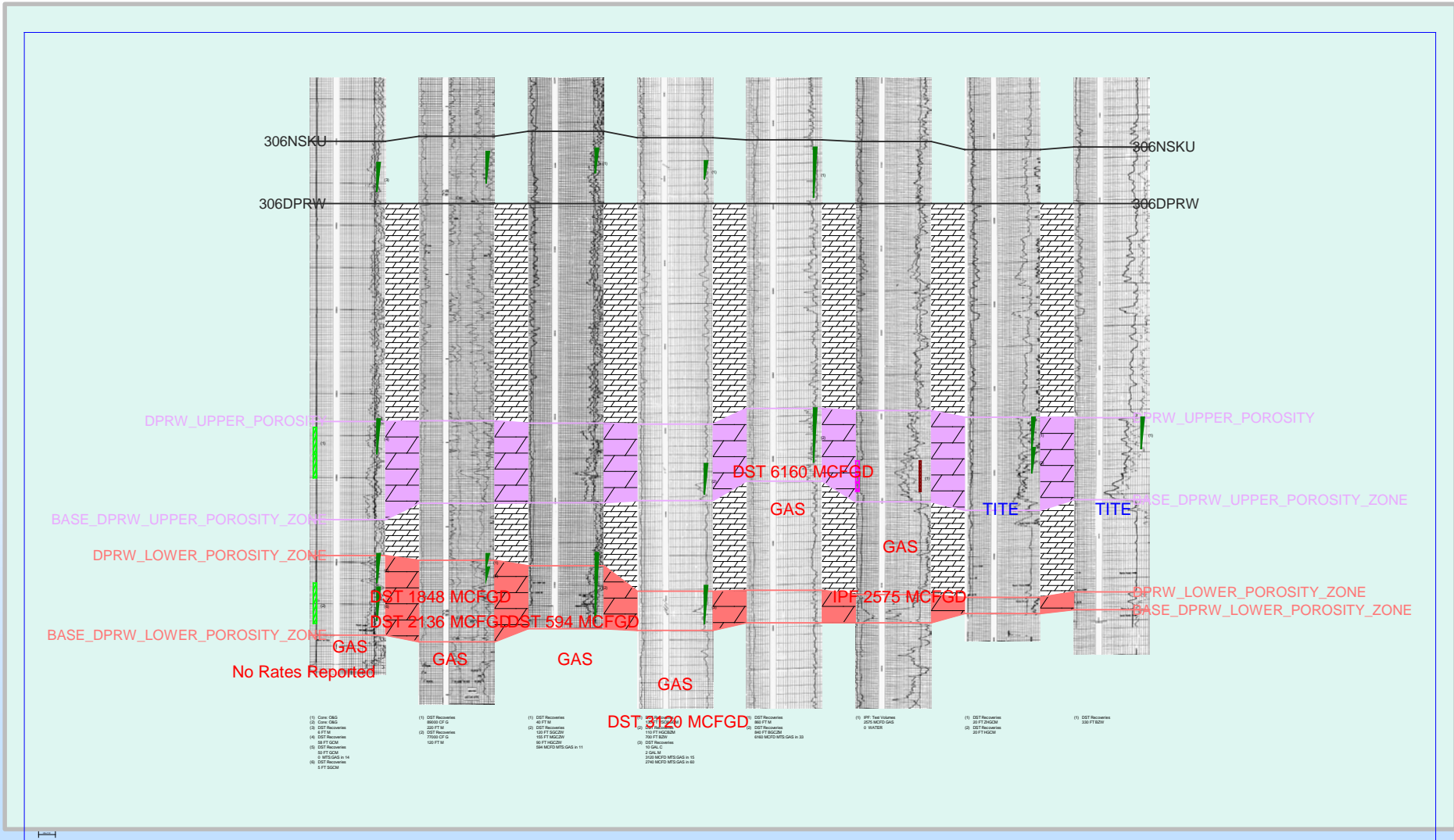
Half of the current major point source emissions for the next 100 years ~7.5 GT
Resource Estimate for 3 Domes ~5.3 GT

- Prevent trespass issues – buoyancy flow will take CO₂ to top of dome
- Potential use as carbon warehouse – decouple anthropogenic CO₂ rate from utilization rate

Kevin Structure Tops & Well Penetrations



NW - SE Cross Section Kevin Dome



PETRA 11/4/2009 4:13:39 PM (Duperow_XS_11_4_CSP)

Site Characteristics – Scientific Opportunities

Natural CO₂ production

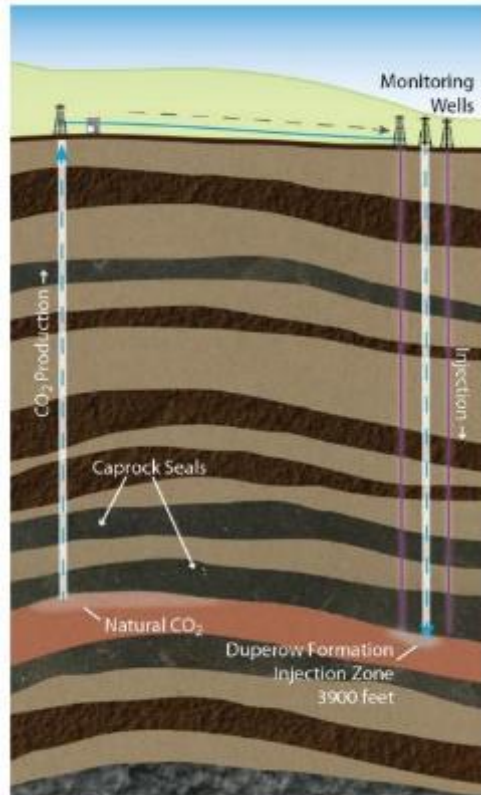
- Opportunity to study the natural accumulation and long term effects

CO₂ in a reactive rock

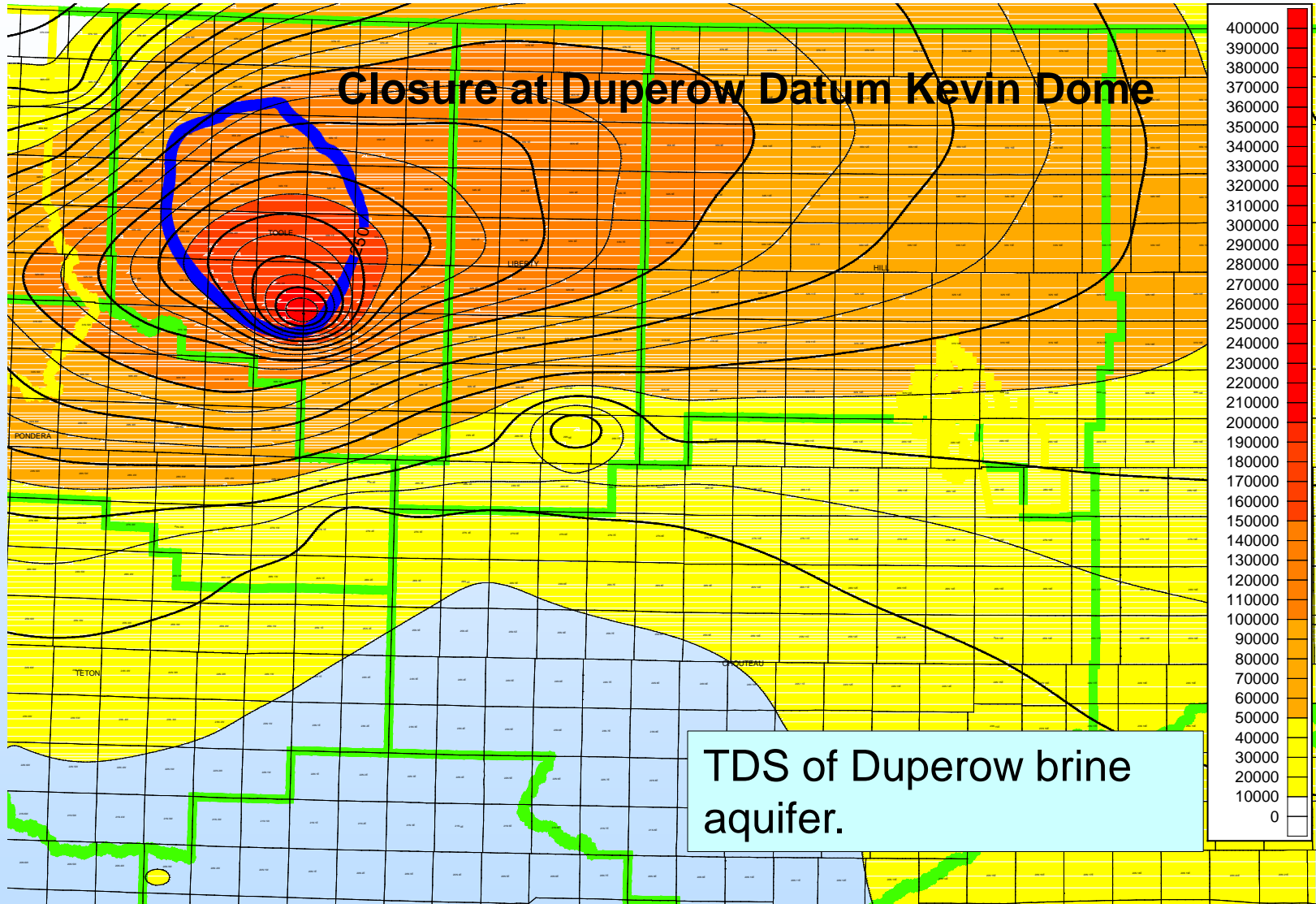
- Opportunity to study geochemical effects on both reservoir rock (long term fate of CO₂) and caprock (storage security)
- To accomplish this, injection should be in water leg of the same formation
- Still retain engineered system learnings on injection, transport, capacity, etc.

Duperow is a fractured reservoir with very secure caprock

- Opportunity to investigate impact of fracture permeability



Regional Water Quality Data



Project Re-Scope

Project Re-scope: Maximize Learnings from Samples and Data

- Complete the core descriptive work and core flood experiments to characterize the pore and fracture geometry of the Duperow formation;
- Measure the fracture-permeability of evaporite and dolomite caprock;
- Perform laboratory measurements of seismic properties as a function of CO₂ saturation;
- Perform laboratory measurements of fracture-matrix flow to inform modeling of two-phase flow in fractured carbonate reservoir rock;
- Complete seismic processing and interpretation including use of quantitative interpretation techniques to determine if pore fluid differences in the reservoir zone can be discerned spatially without time lapse techniques;
- Apply full waveform inversion to develop a high resolution velocity model;
- Complete analysis of the geologic framework and stratigraphic architecture of the reservoir;
- Produce a final geostatic model with descriptive metadata;
- Improve phase change modeling using the production well data, assess applicability to leakage scenarios and CO₂ / EOR storage hub concept.

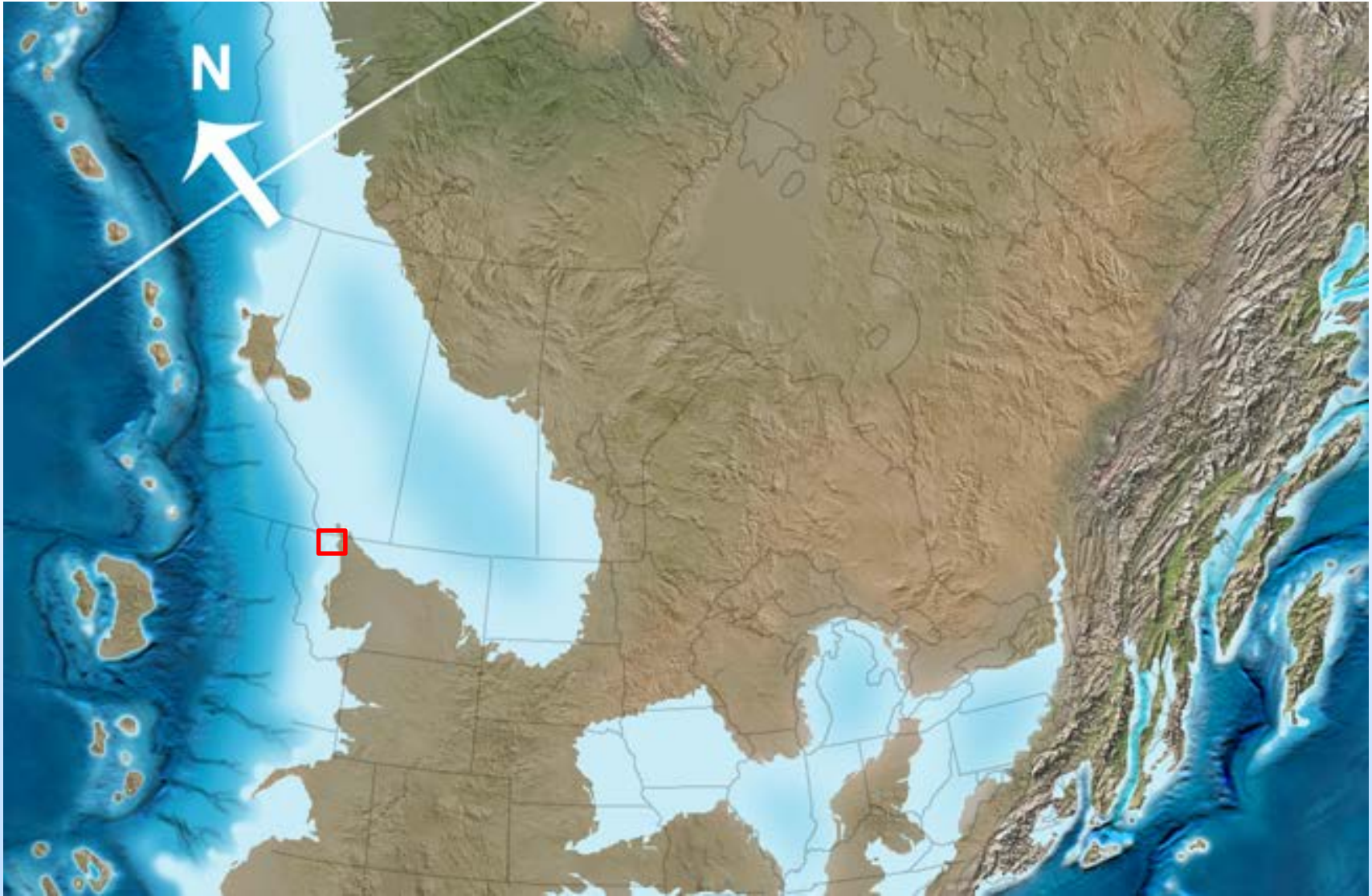
Project Re-Scope

Project Re-scope: Maximize Learnings from Samples and Data

Continued...

- Further develop fracture–matrix permeability interaction models incorporating data previously mentioned;
- Use the dual permeability model to refine reservoir performance for fractured carbonate reservoirs including capacity, injectivity and storage efficiency;
- Apply an integrated assessment model to Kevin Dome as a test case for NRAP tools;
- Process and analyze the surface monitoring data, assess baseline variability;
- Modify assessments of regional and national storage resources with information gained through the Kevin Dome project;
- Capture lessons learned from the permitting, risk, and management components of the Kevin Dome project through continued analyses and the development of peer-reviewed publications and web-based applications for information sharing and
- **Use the Kevin Dome project to illustrate unanticipated geologic scenarios to inform EPA’s scheduled evaluation of the UIC Class VI rule.**

Middle Devonian Paleogeography



Enlarged Devonian Paleogeography – Western U.S. by Ron Blakey, <http://cpgeosystems.com/wnam.ht>



Duperow Facies Model

West

East

Limestone

Dolomitized
Facies

Limestone

Basin

Slope

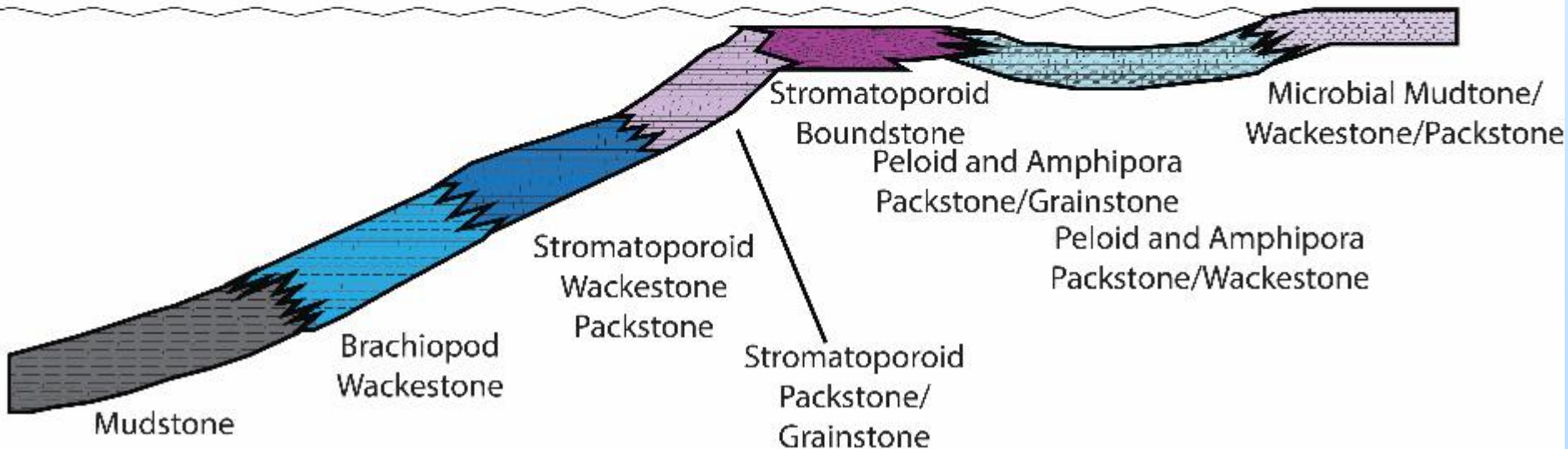
Fore-Reef

Shallow
Reef Front

High-Energy Shoal/
Biostrome/Reef

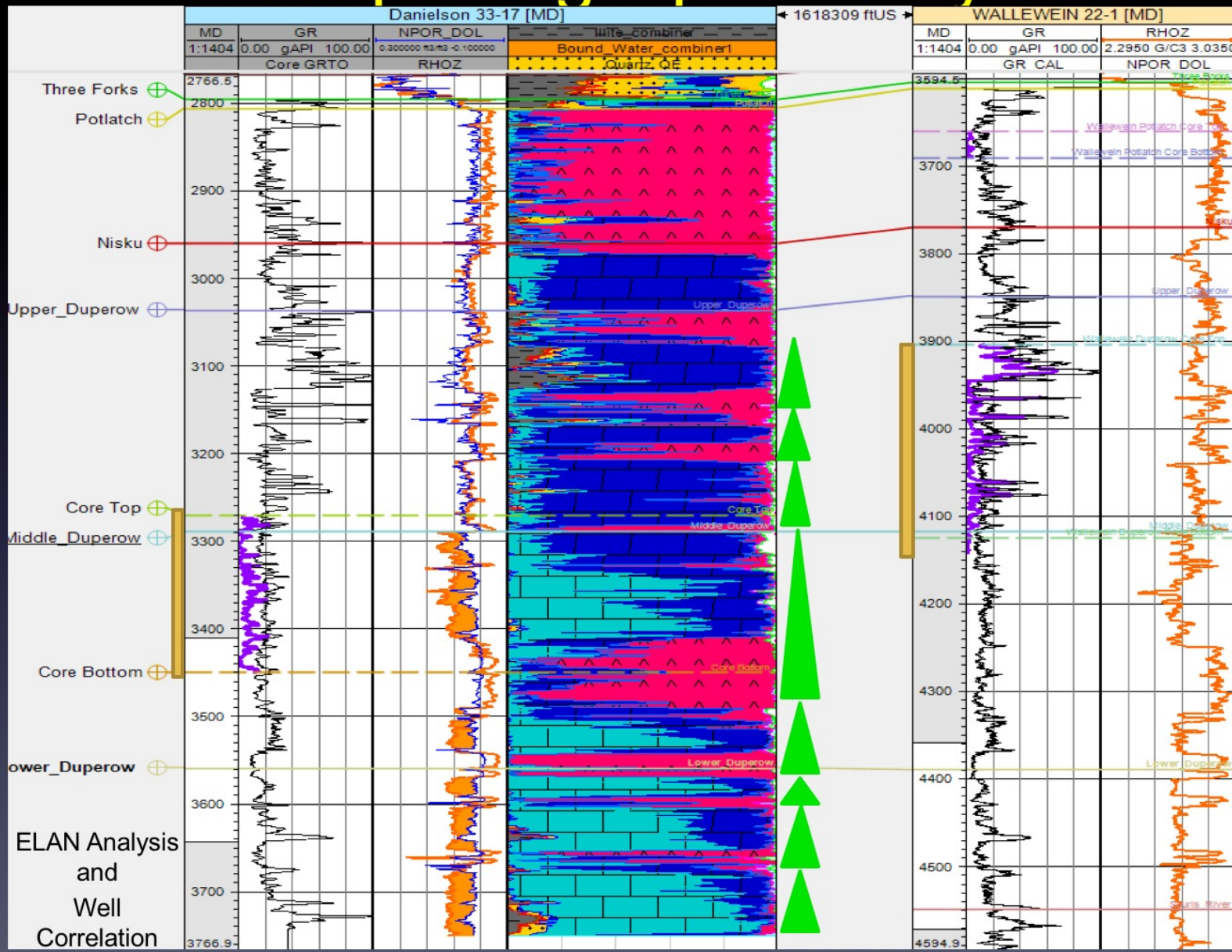
Lagoon

Tidal Flat

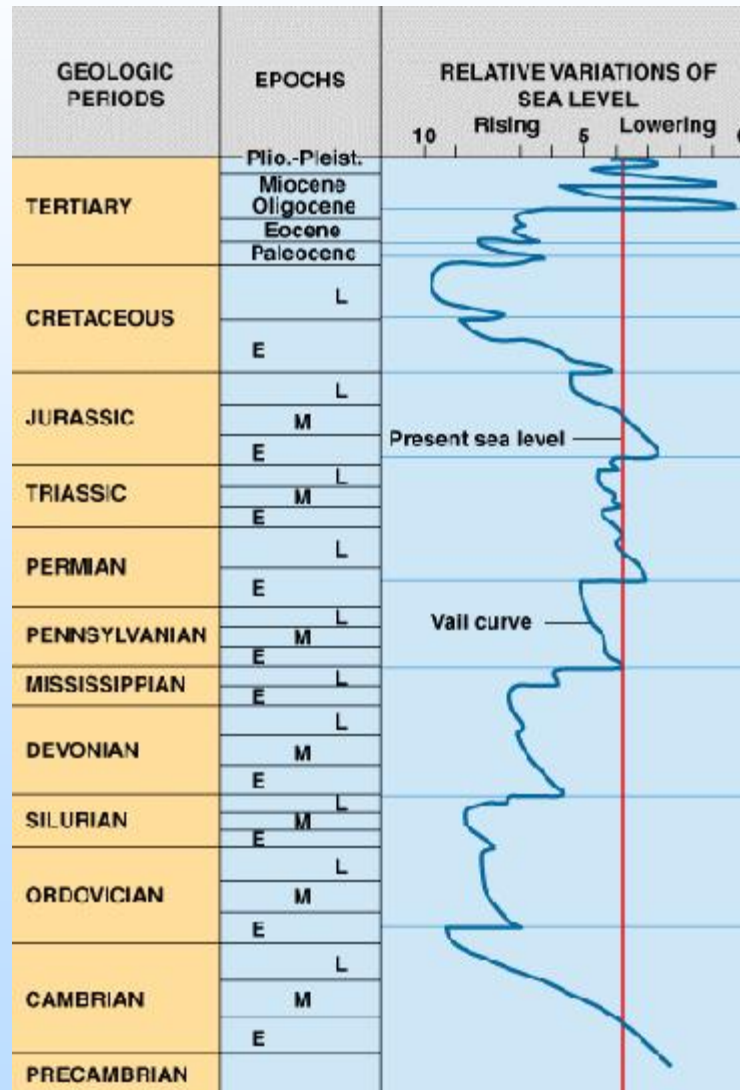


Danielson – Wallewein

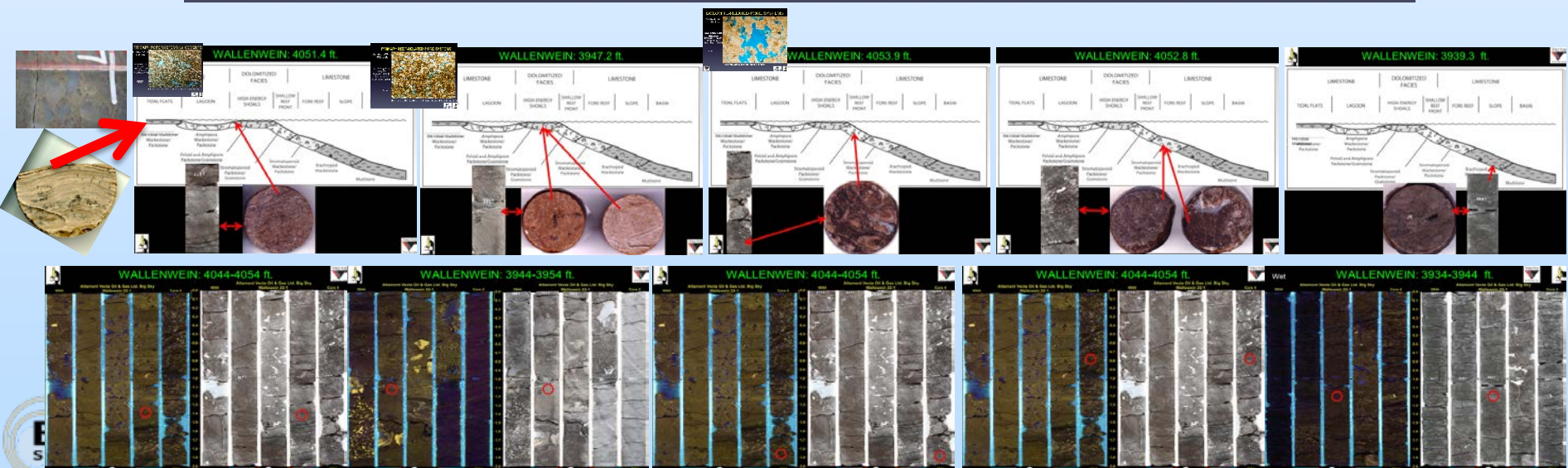
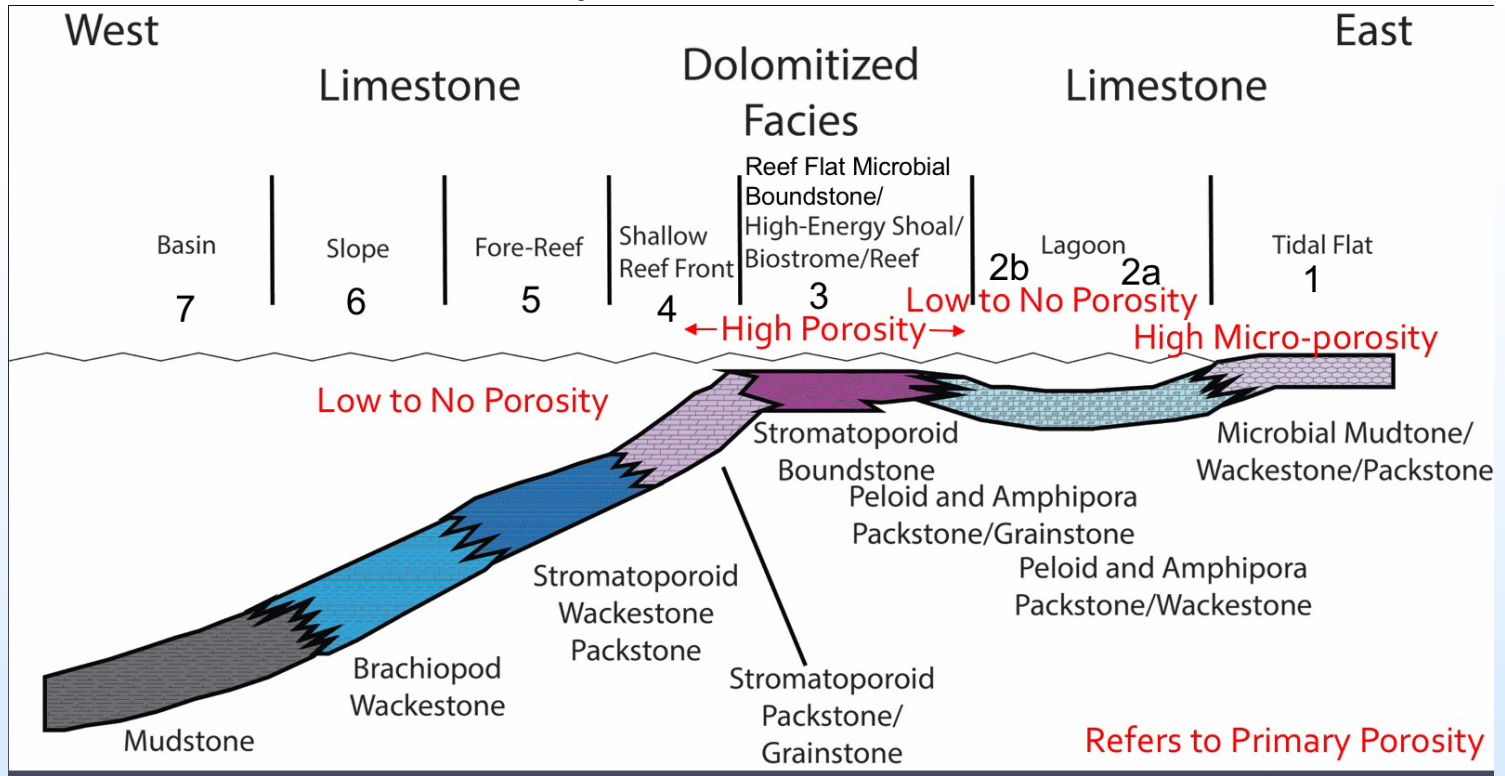
8 Deepening Upward Cycles



Global Sea Level Curve



Duperow Facies Model



Duperow Lagoonal Facies



Laminated, organic-rich, fetid, dolomite

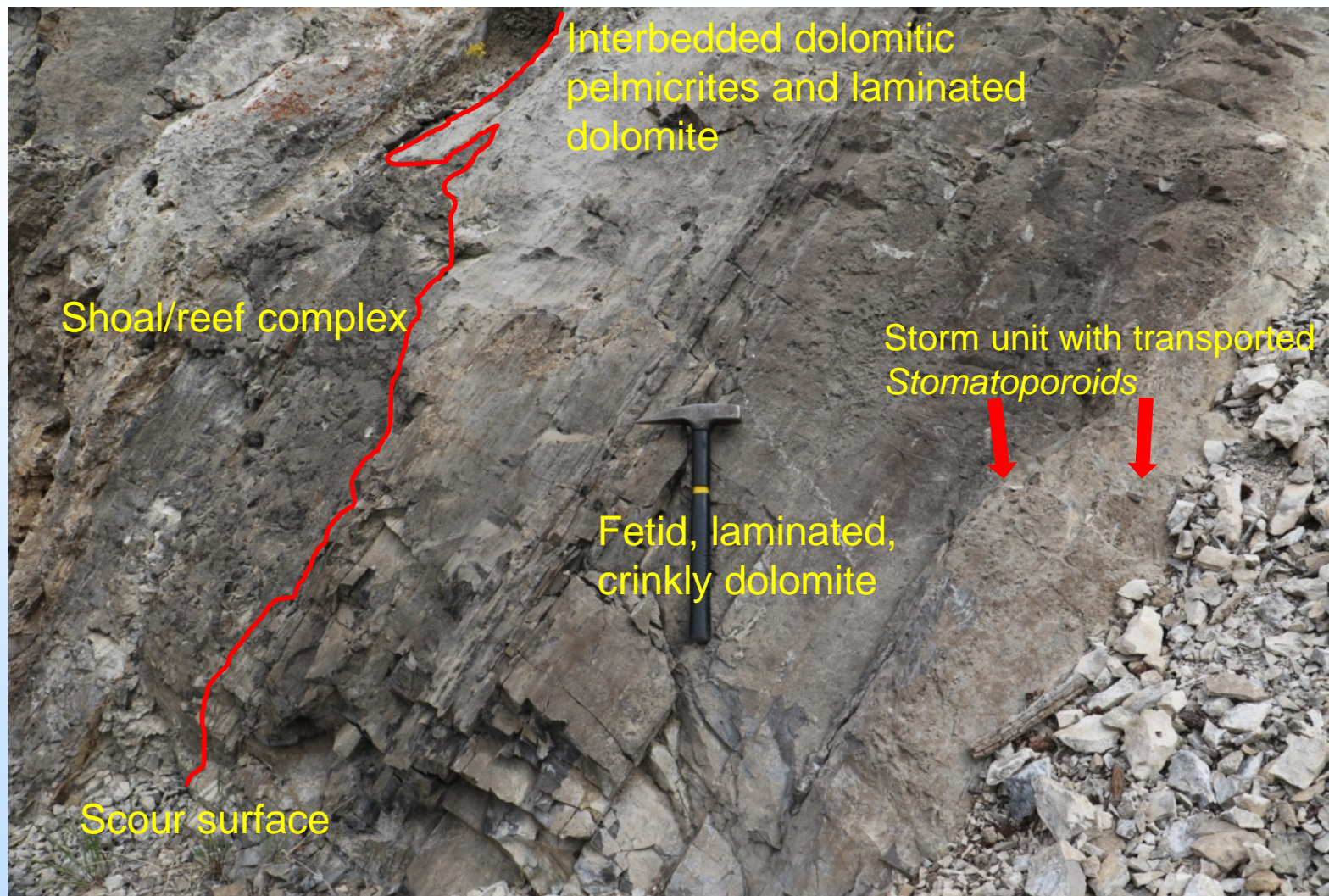
Inter-bedded lagoonal evaporite/laminites

Evaporite dissolution/collapse breccia zone

Fetid, organic, finely-crystalline dolomite laminites



Back-reef stromatoporoid heads washed into lagoon



Stromatoporoid reef topped by reef-flat “microbialites”



Reef Flat



Stromatoporoid dominated reef facies – Little Belt Mtns.



High Energy Shoal



Cross-bedded grainstones – Little Belt Mtns.

Deepening upward cycle

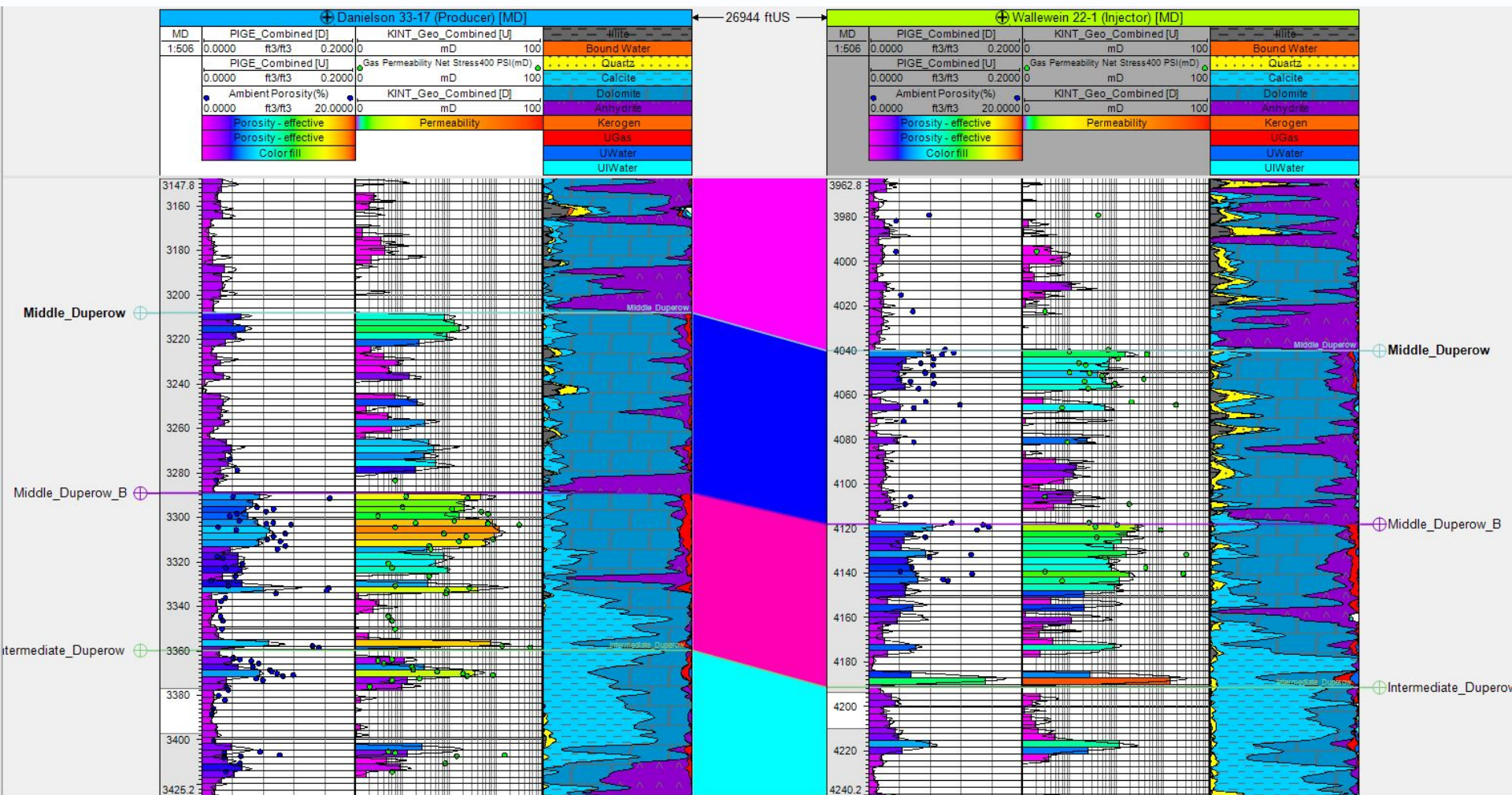


Reef

Lagoonal mudrocks with storm debris

Laminated lagoonal mudrocks

Site Characterization: ELAN Analysis and Well Correlation

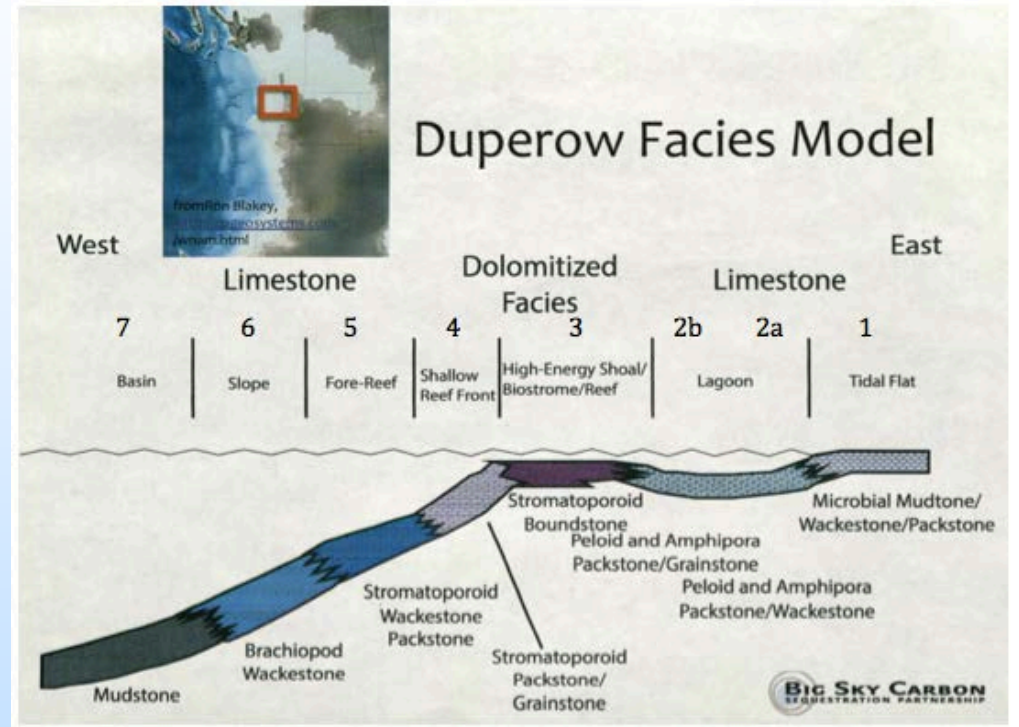


Excellent correlation for wells 12.8 km apart

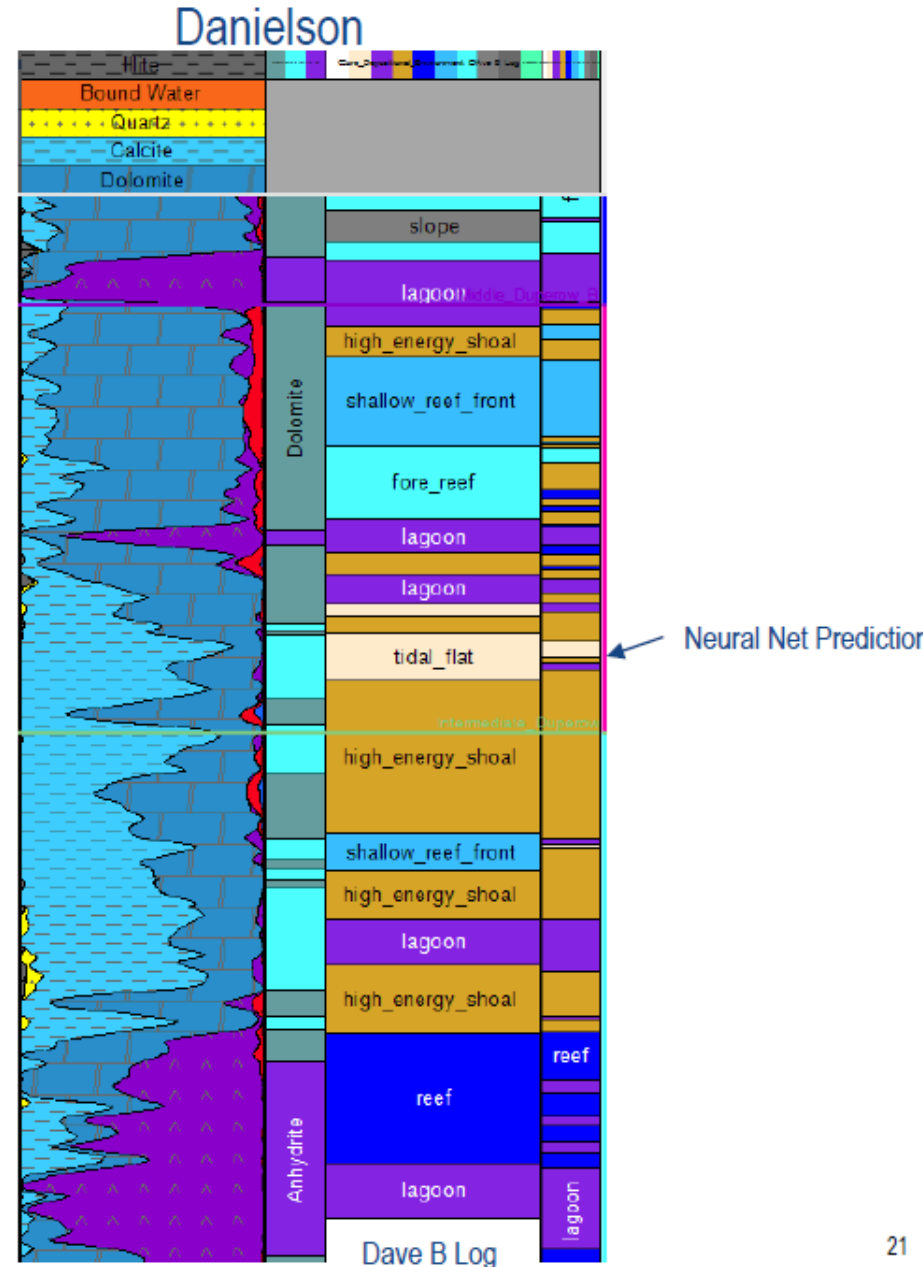
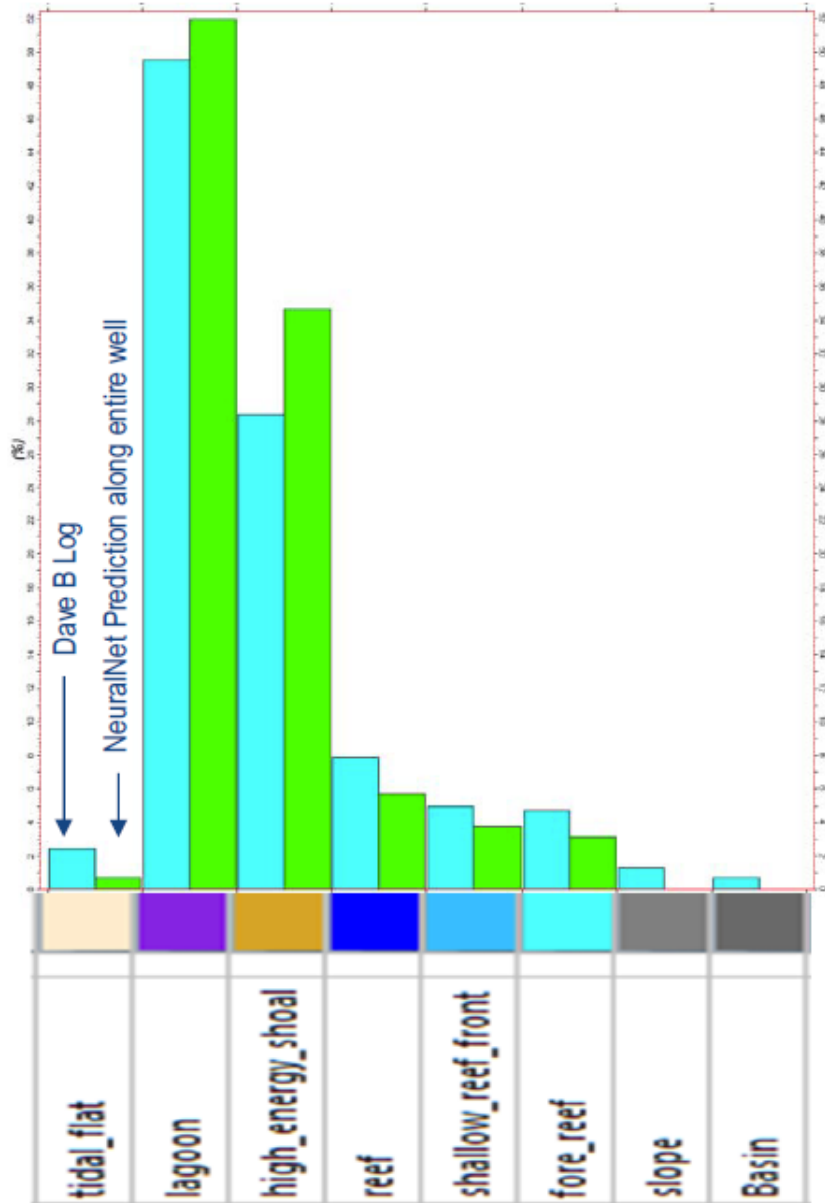
Geostatic Model: Refine Model Based on Geologic Interpretation

Depositional Environment

tidal_flat	
lagoon	
high_energy_shoal	
reef	
shallow_reef_front	
fore_reef	
slope	
Basin	
back_reef	

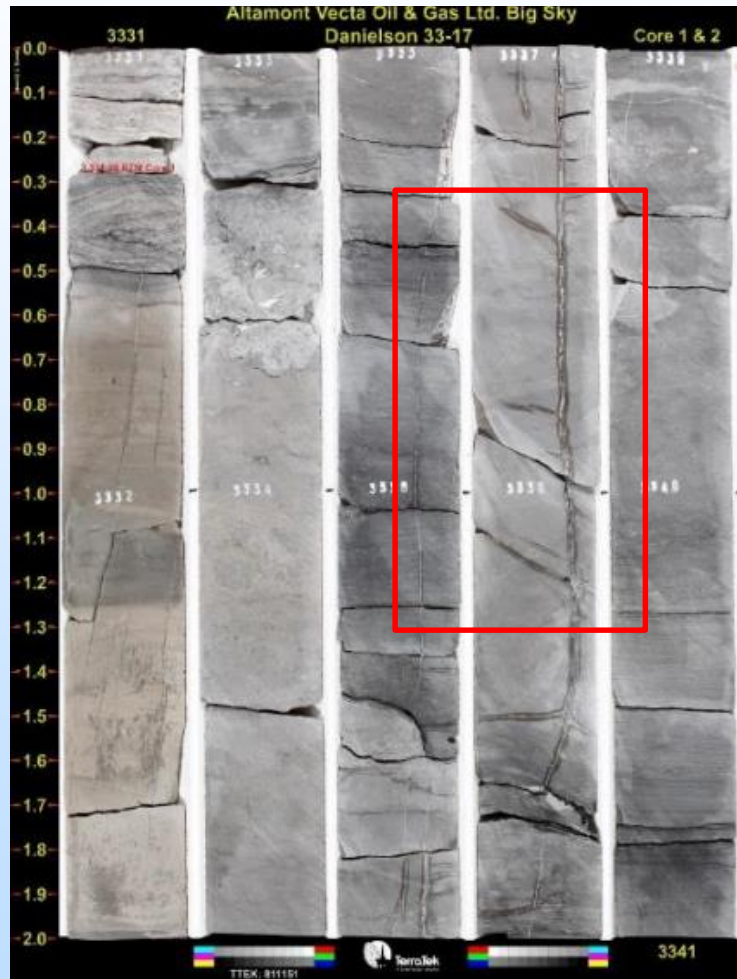


Good Neural Net Match Along Core Interval



Middle Duperow – Fractures

Site Characterization: Core Fracture Analysis



Lumicon UHC

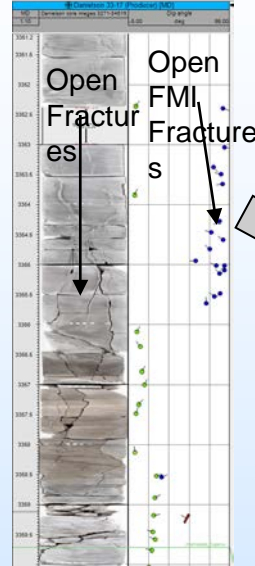
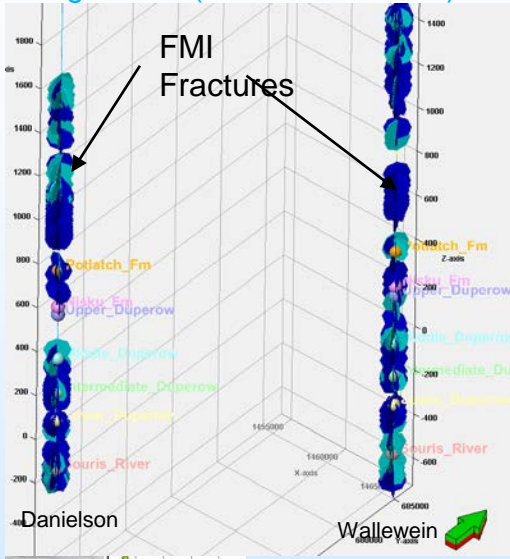


Natural Fracture Model

Inputs

Outputs

Dark Blue (Open Fractures)
Light Blue (Closed Fractures)

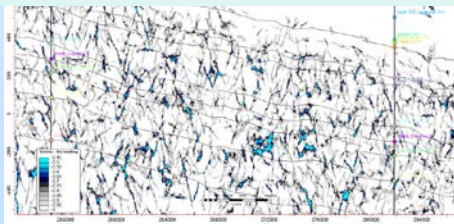


Open natural fracture model of Middle Duperow (3 Fracture Sets)

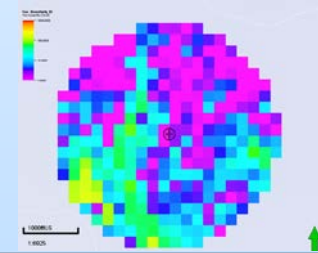
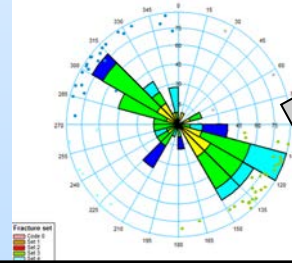


Seismic Ant Tracking Attribute

Potential fracture corridors (Light Blue)



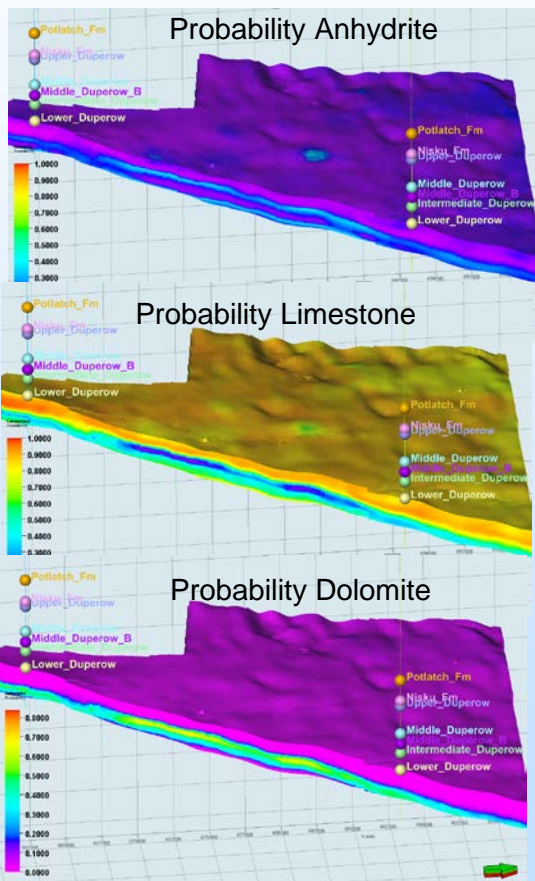
Fracture Set Stereonet



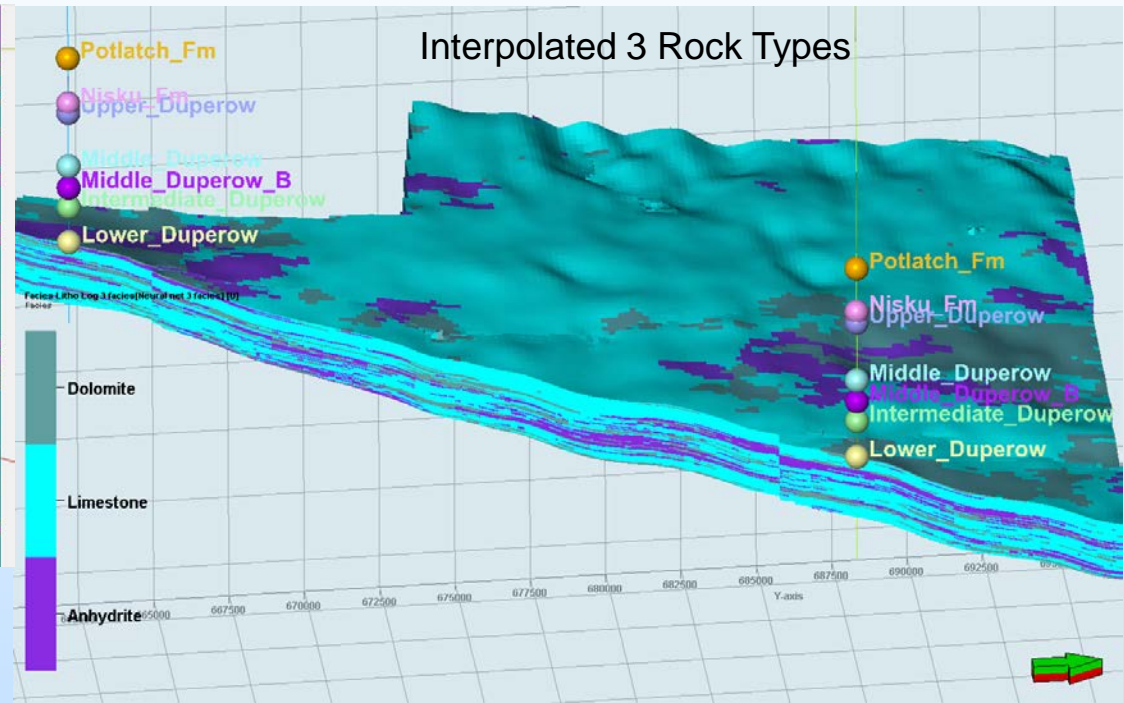
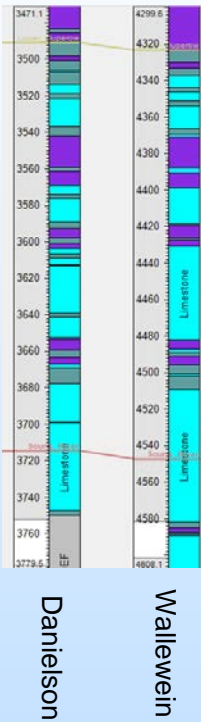
Fracture Cell
• Permeability IJK
• Porosity

Lithology Prediction Using Seismic Inversion

3D probability lithology prediction volumes as a trend for rock type interpolation



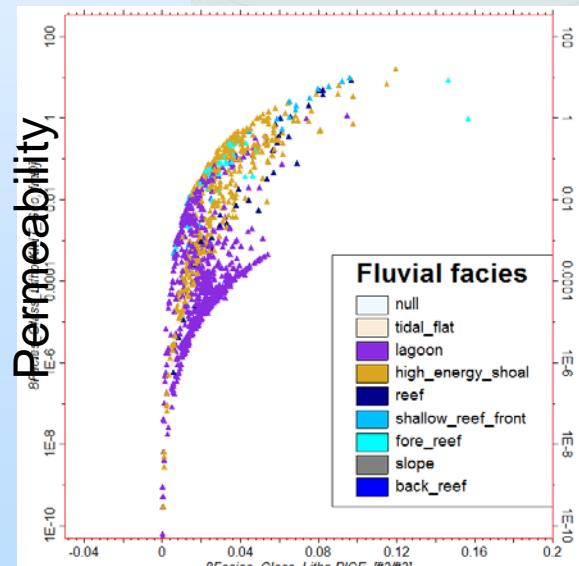
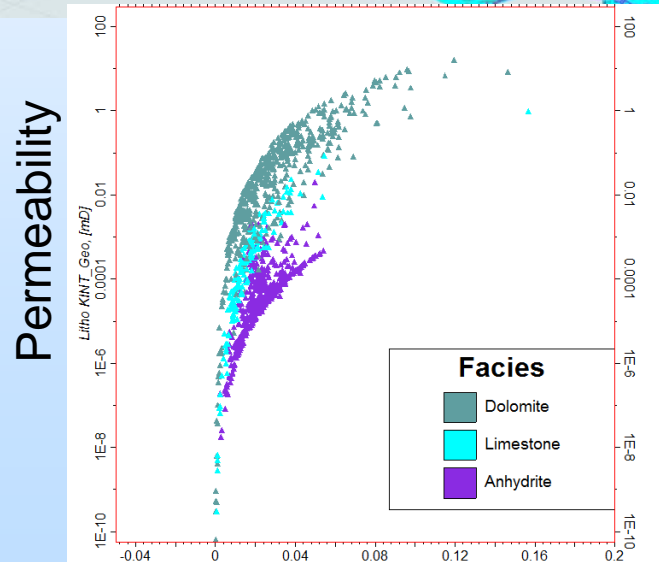
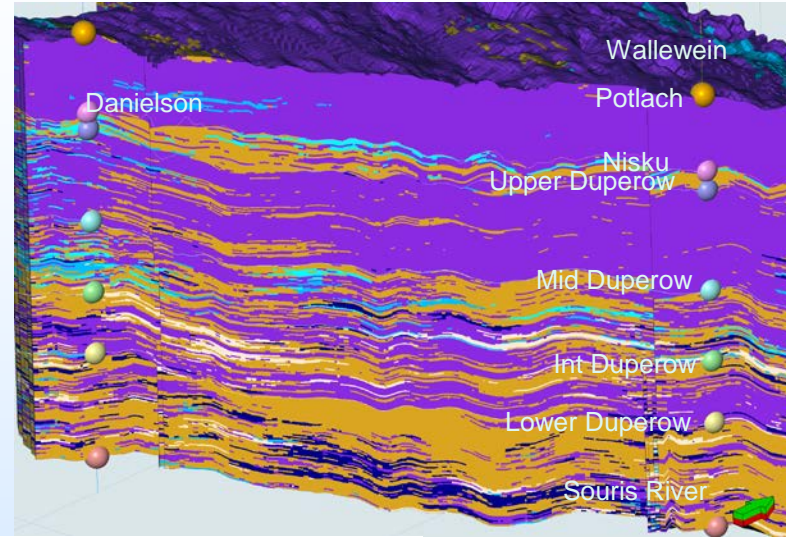
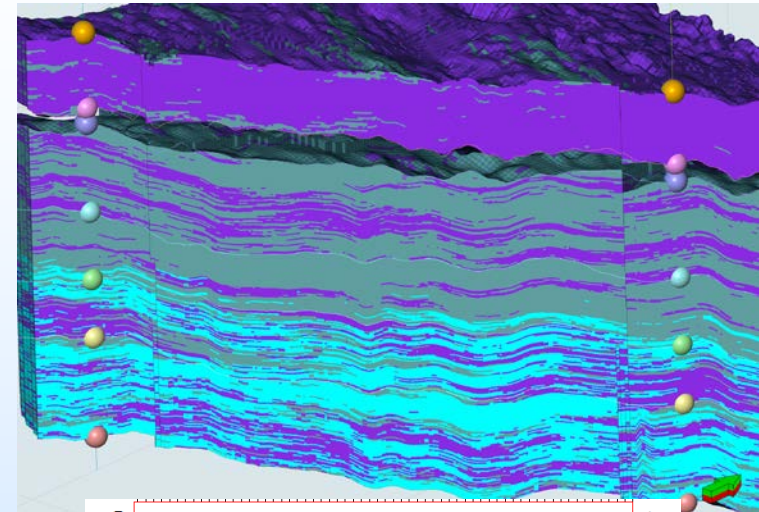
Rock Type Logs



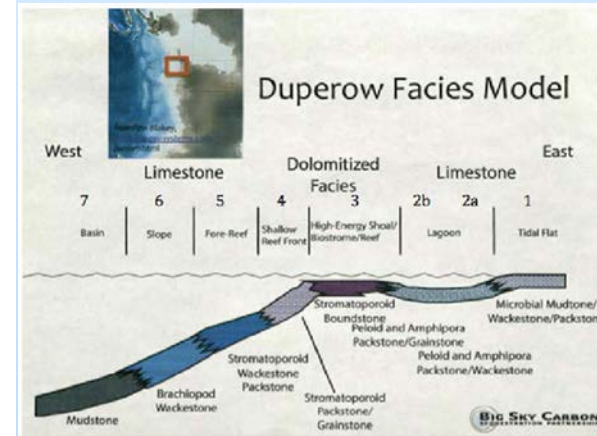
Facies, Porosity and Permeability Interpolation

3-Rock Type

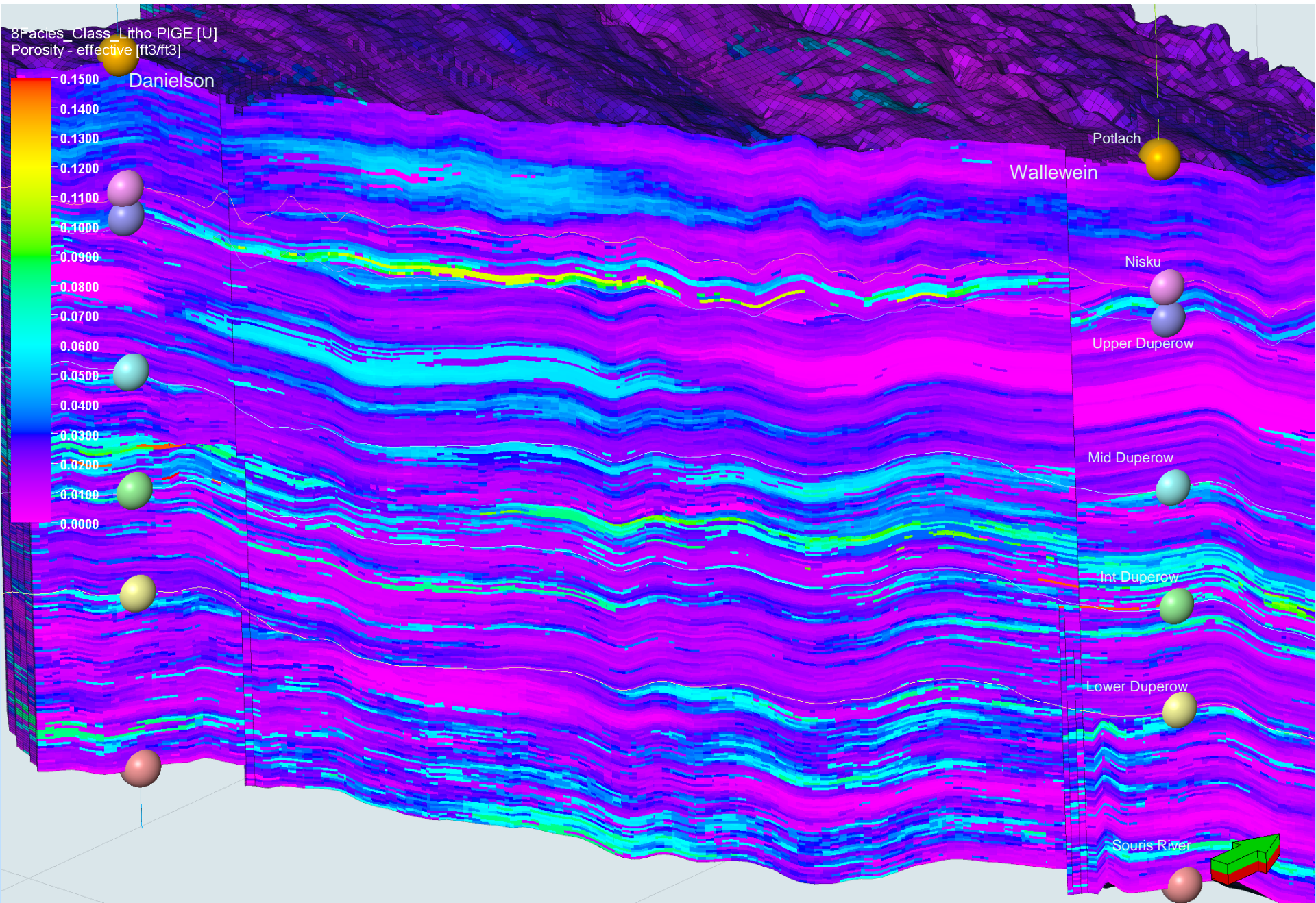
8-Rock Type



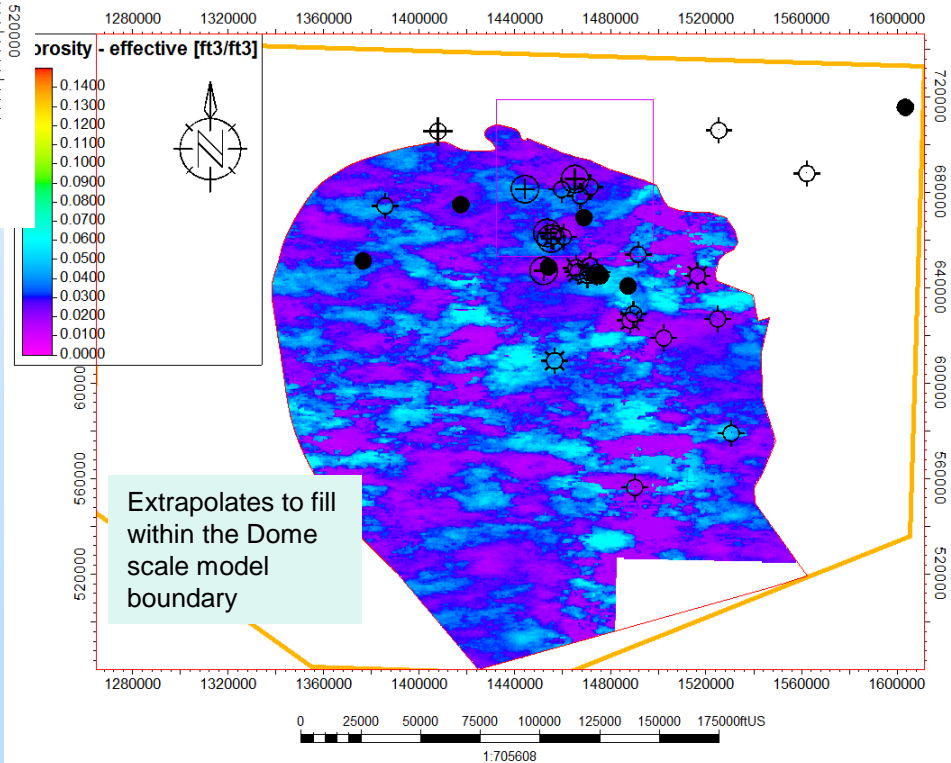
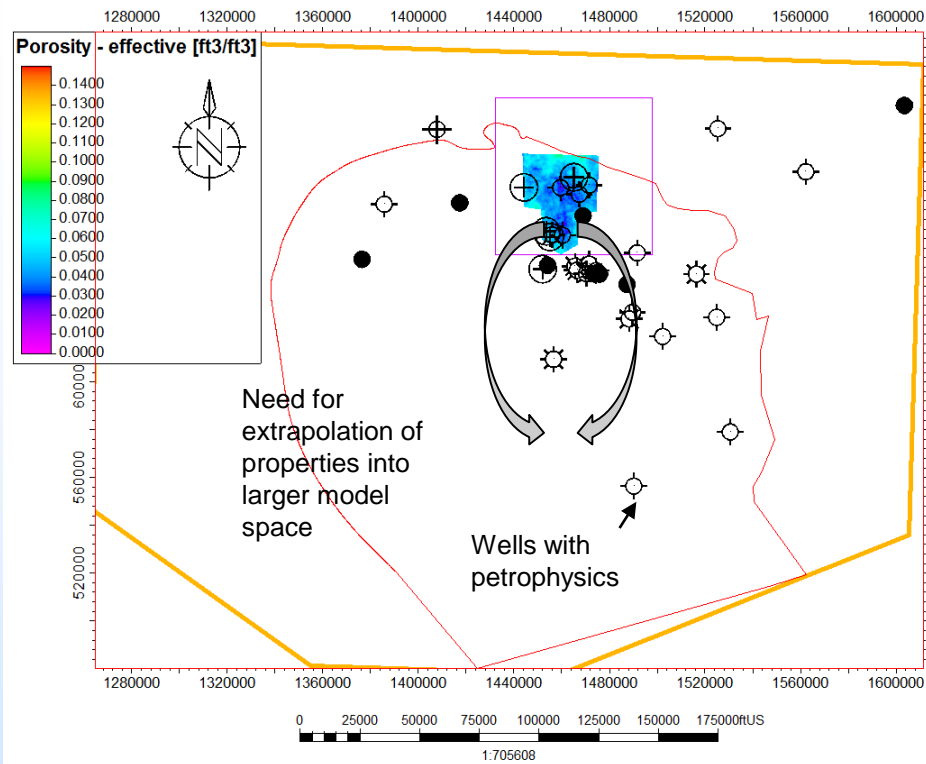
8 Rock Type model calibrated to geologist's (Dave Bowen) facies log and facies model



Property Interpolation (Porosity)



Dome Scale Model Property Extrapolation



Motivation for lab seismic study



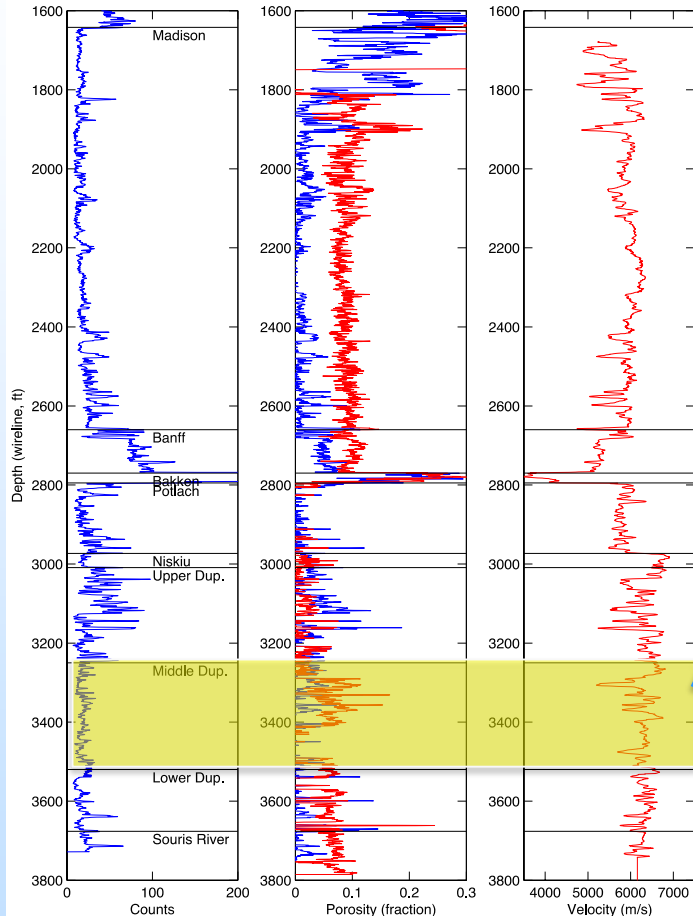
Harry Lisabeth, Jonathan Ajo Franklin

- Time-lapse (4D) seismic monitoring is one of the best tools we have to see dynamic changes in the subsurface
- Most of our understanding of changes in seismic response due to fluid replacement and stress perturbation are from studies of porous sandstones. We have much less understanding of these effects in low porosity, fractured carbonate reservoirs
- Measurements in the laboratory allow us to deconvolve complex effects of geology and gain understanding of the fundamental physics at play during fluid substitution and pressure changes

Laboratory study of structure and broadband seismic characteristics of fractured, fluid-filled reservoir material



Danielson Well (Production Pad)



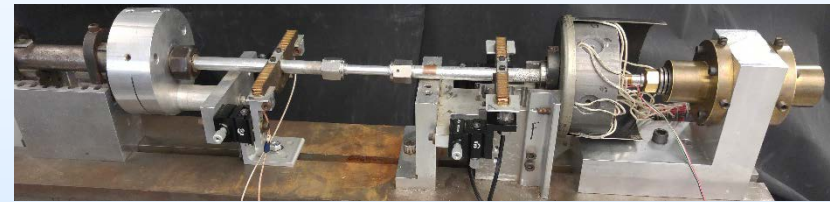
Gamma

Neutron

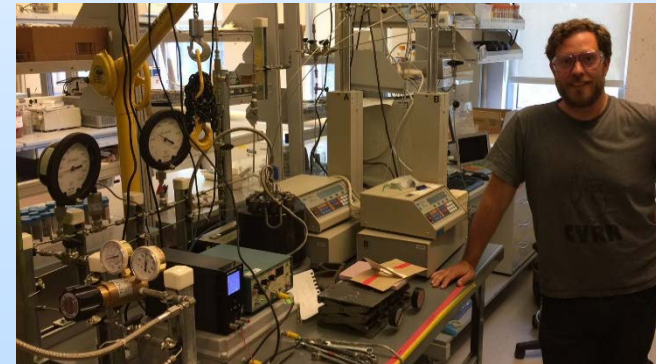
Sonic



Low frequency modulus/attenuation



Fluid replacement/ultrasonic characterization

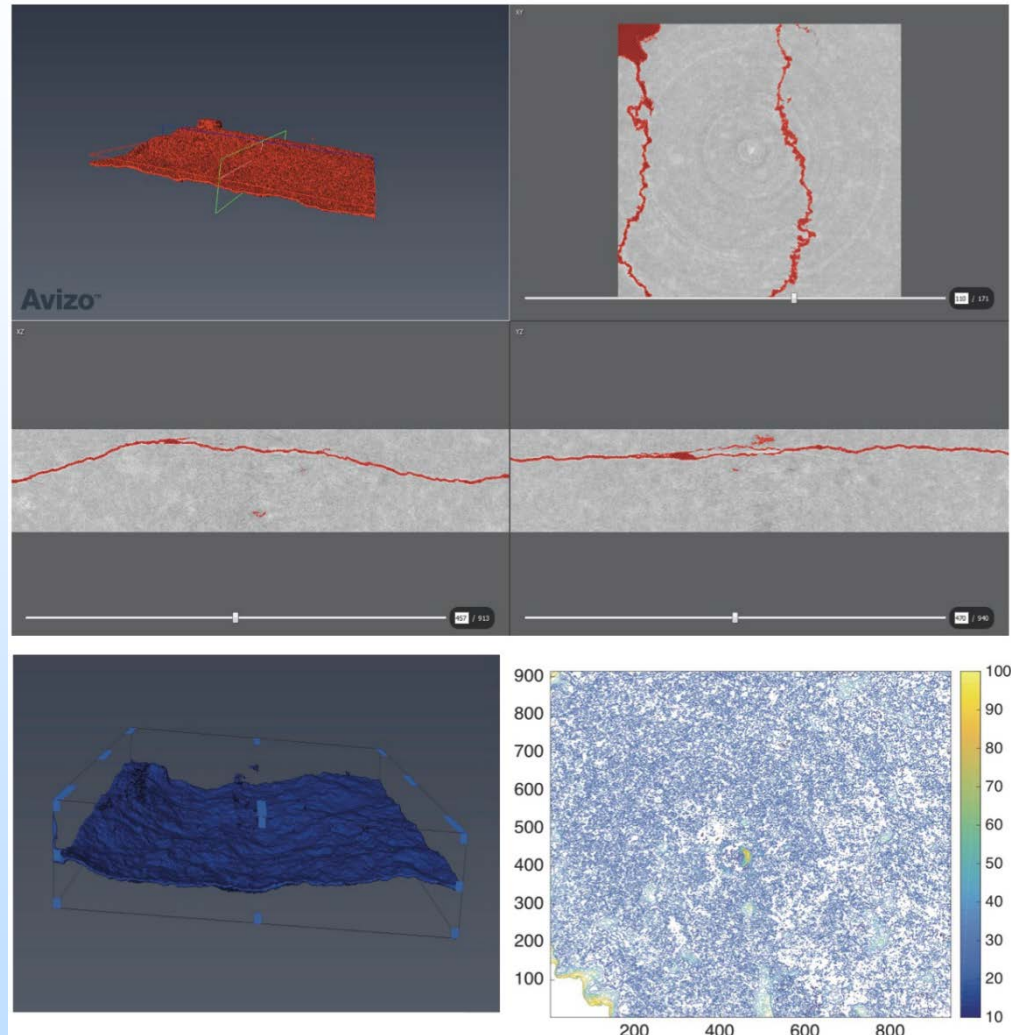


Synchrotron x-ray microtomography of fractured Duperow dolomite

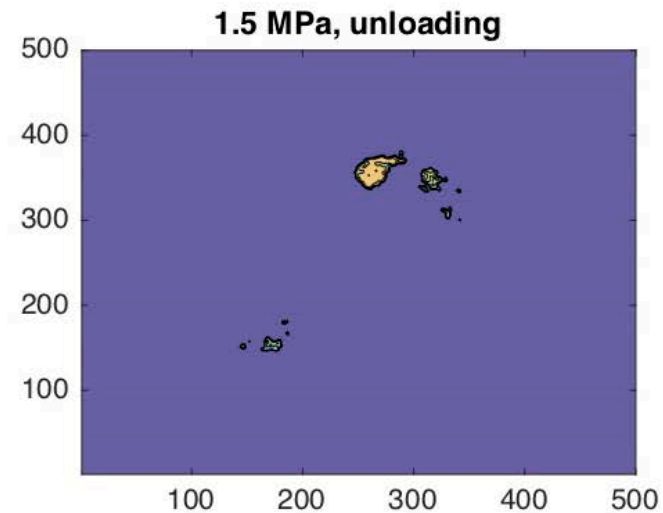
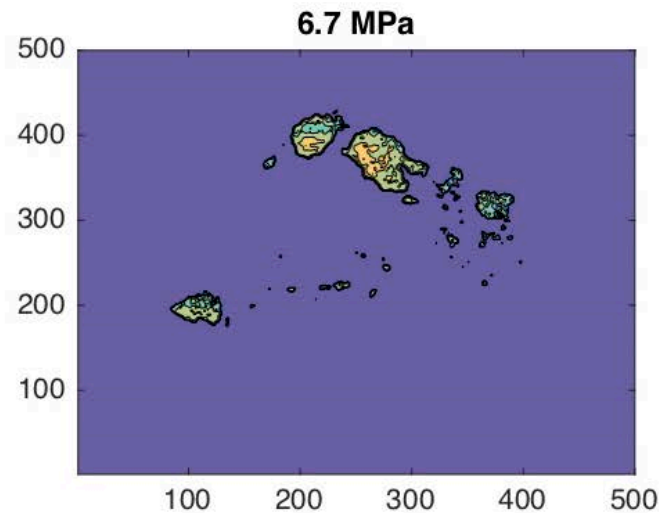
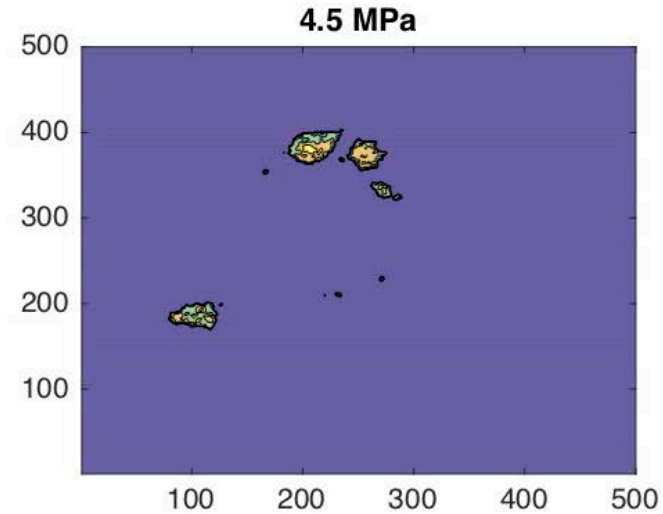
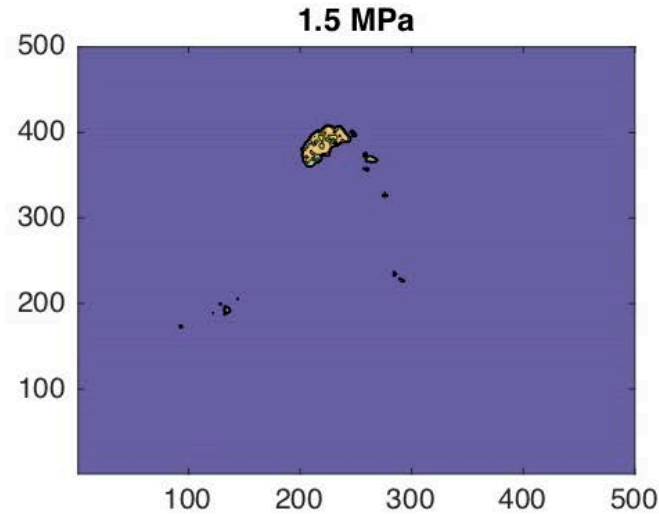


- Fracture shows multiscale roughness, with undulations at the scale of the sample (9mm)
- Secondary fractures sub-parallel to primary fracture are evident
- At 0 pressure, aperture ranges from 10 to 100 microns
- mCT conducted to identify features of natural fractures which differ from induced tensile fractures.

[Conducted at beamline 8.3.2,
Advanced Light Source]

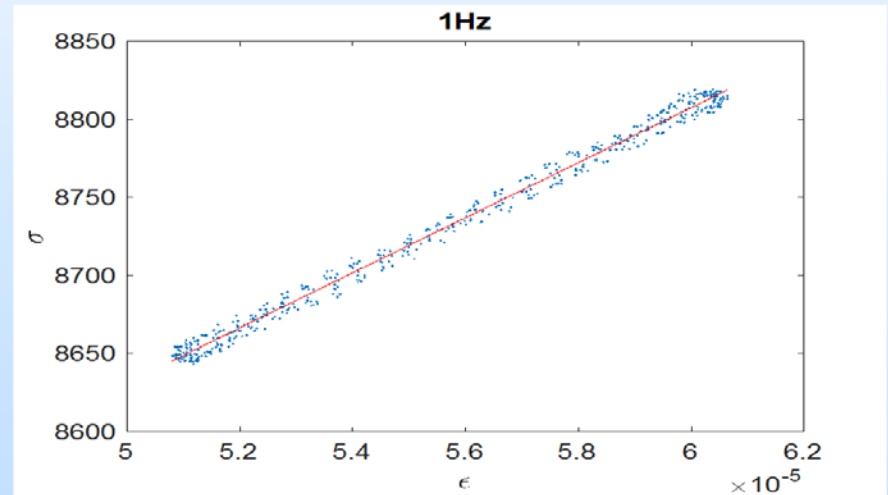
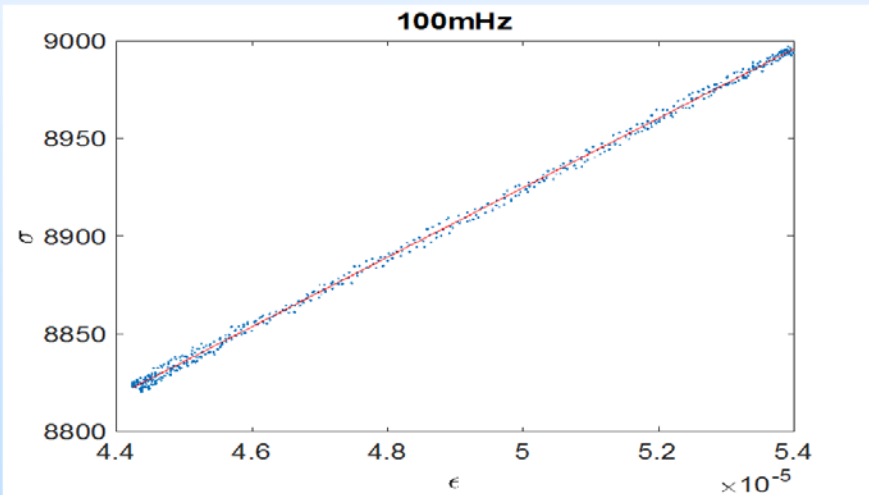
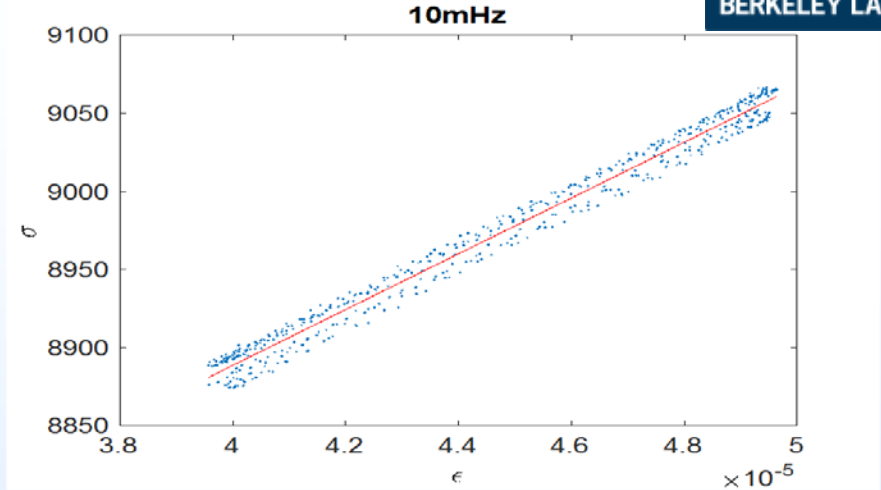
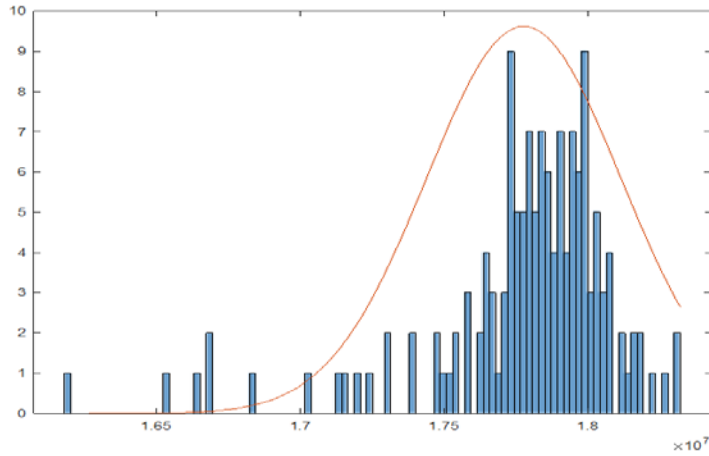


Pressure-sensitive film measurements



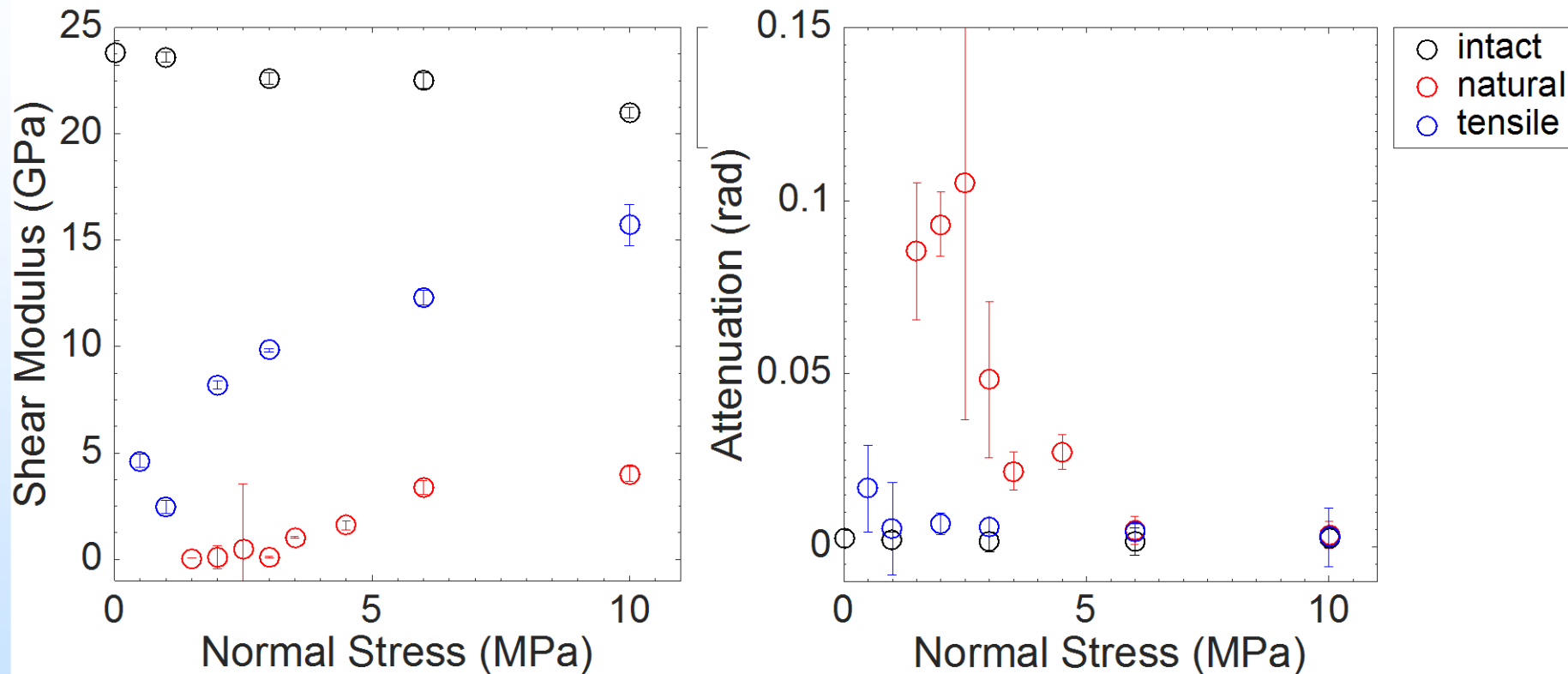
With increasing normal stress, asperities grow and local stresses are intensified

Low frequency measurements of Duperow dolomite



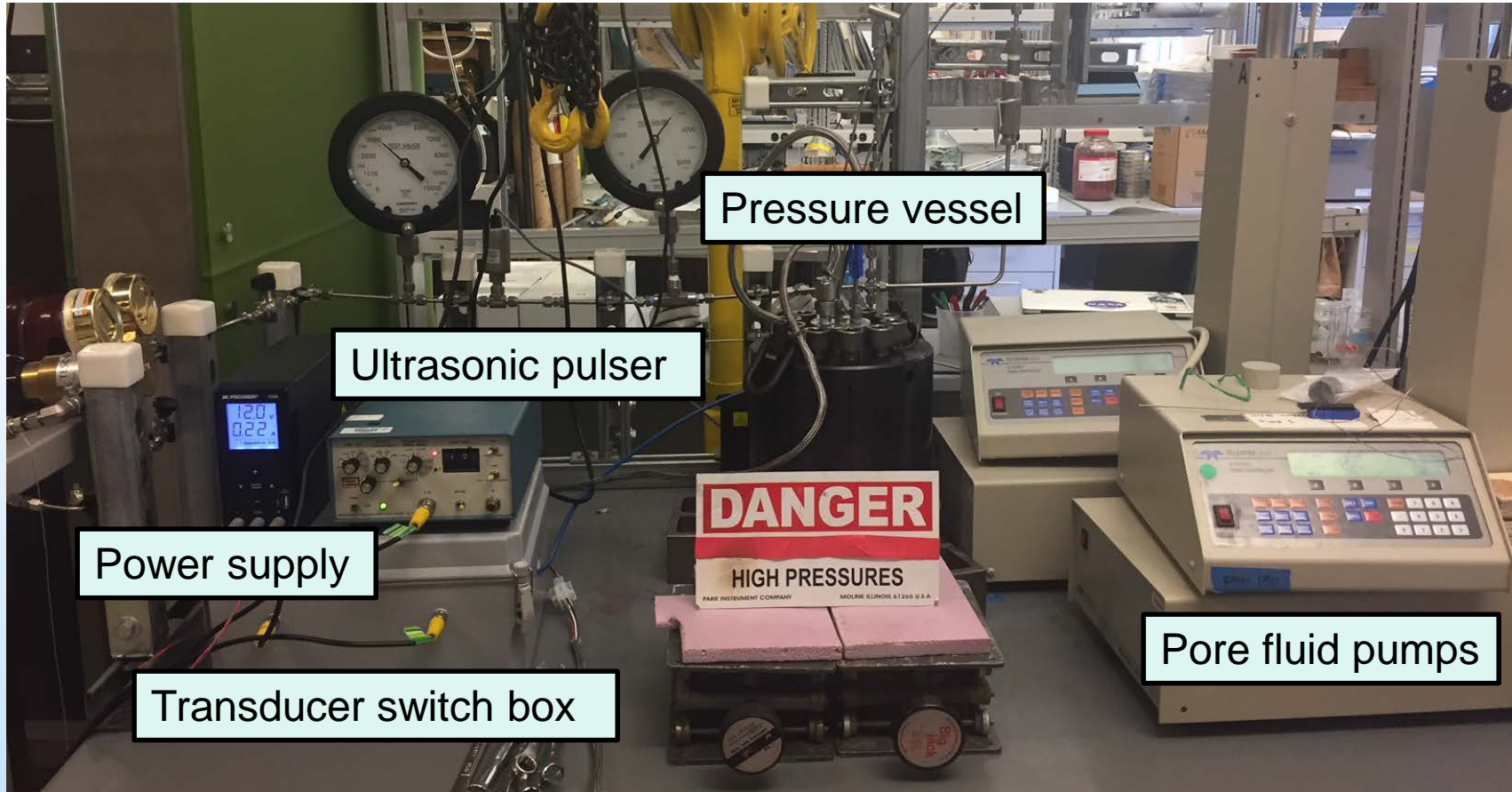
We have pushed our measurements capabilities down to 10mHz

Comparison of intact, naturally fractured and tensile fractured Duperow @ 8Hz



Natural fracture has lower and less pressure dependent modulus than induced tensile fracture, and shows greater attenuation at low normal stress.

Operational high pressure, flow-through vessel with ultrasonic measurement



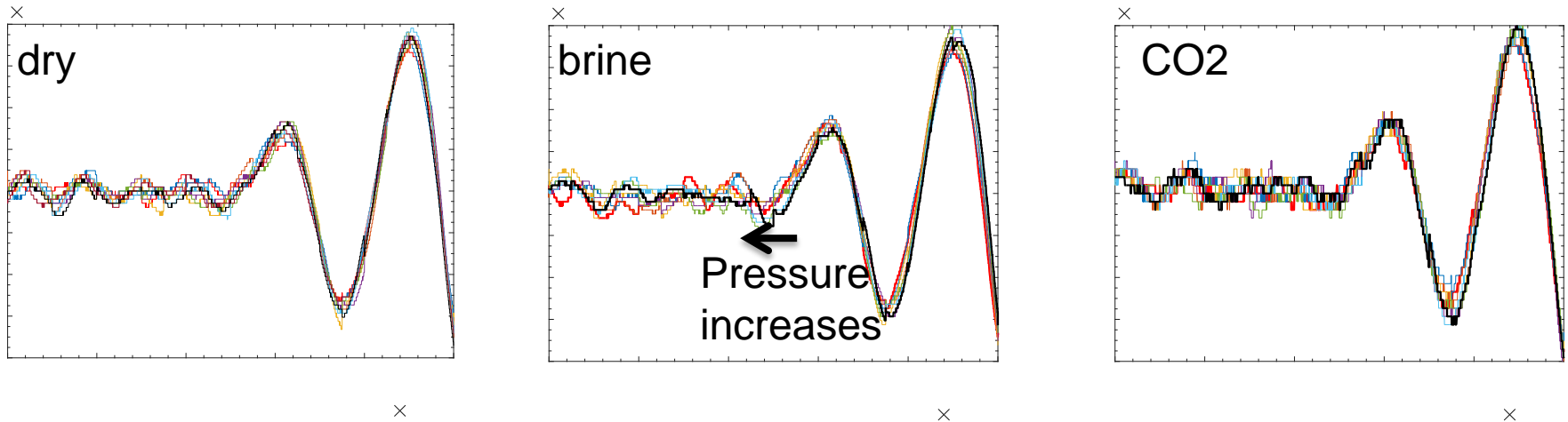
Repairs and slight redesign allows for ultrasonic characterization of fluid replacement and pressure dependence of acoustic velocities at in-situ conditions

Initial ultrasonic results, Danielson Core (~3379 ft)



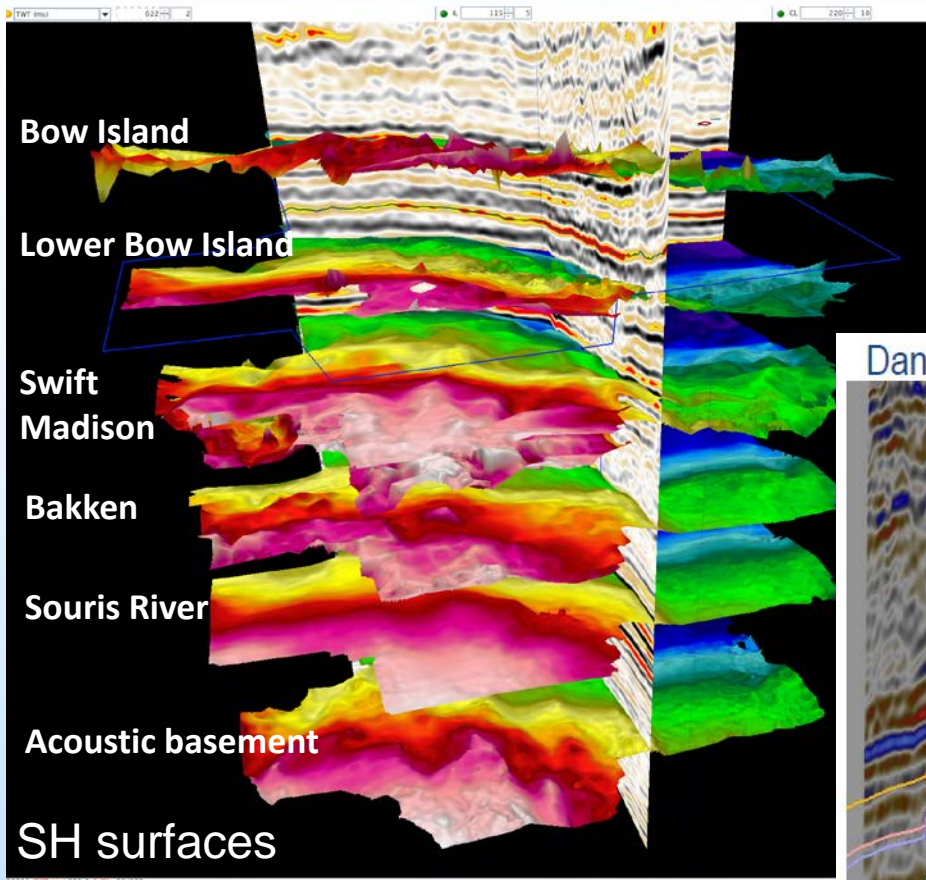
P-waves

$P_p = 1500$ psi, $C_p = 1550 - 4000$ psi



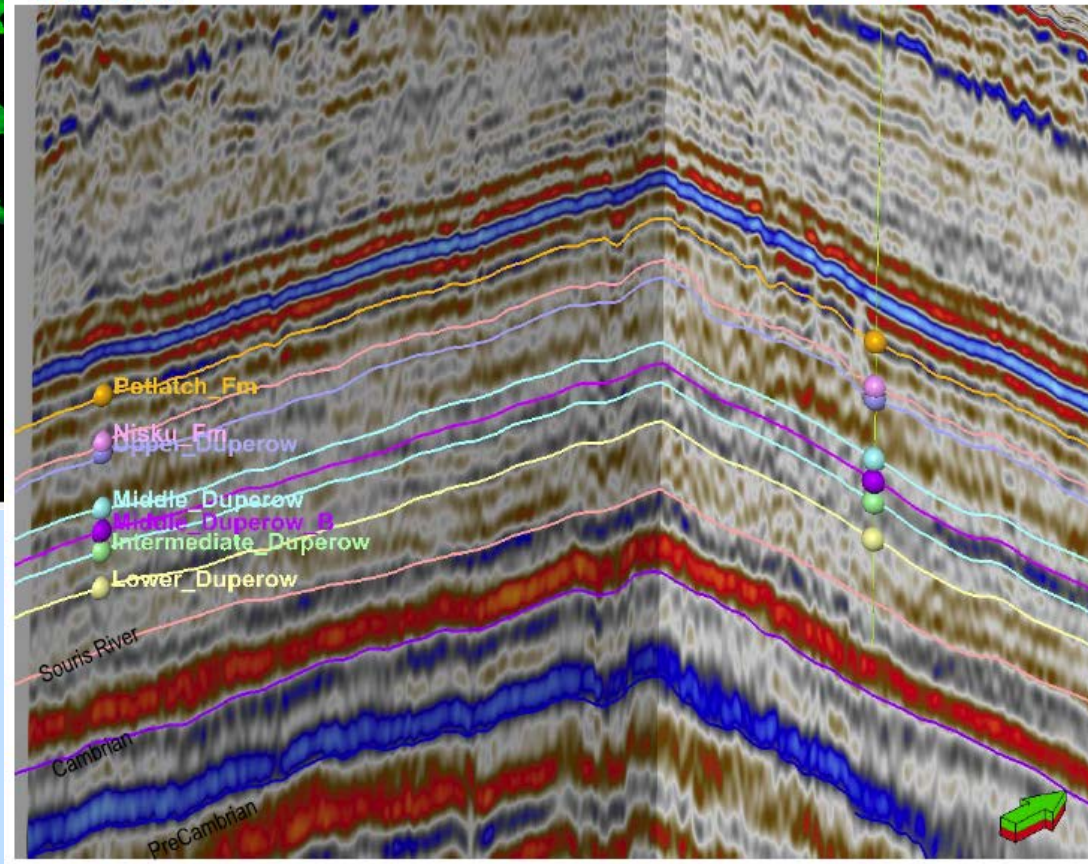
- Well-mated fracture in Duperow dolomite from Danielson well shows surprisingly little pressure dependence in the ultrasonic range; substitution of liquid CO₂ for brine reduces the pressure dependence to negligible.
- Results show smaller dependence than low F torsional shear measurements – potentially due to dominance of single stiff asperities in ultrasonic tests.
- Results show the challenge of seismic monitoring stiff formations with low porosity – fracture response may be greater at lower F and for sheared fractures.

Processing 3D, 9C seismic Seismic

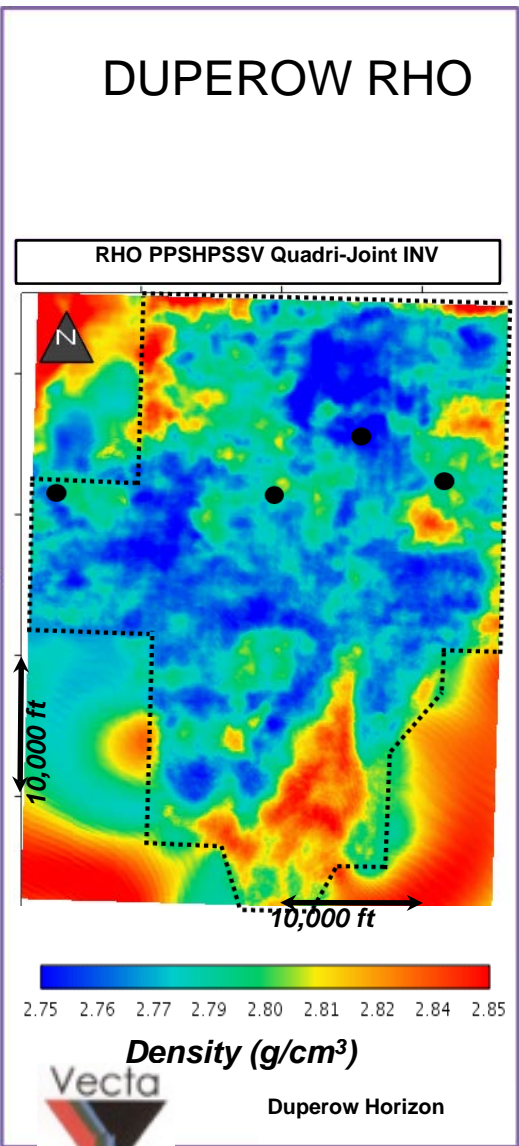
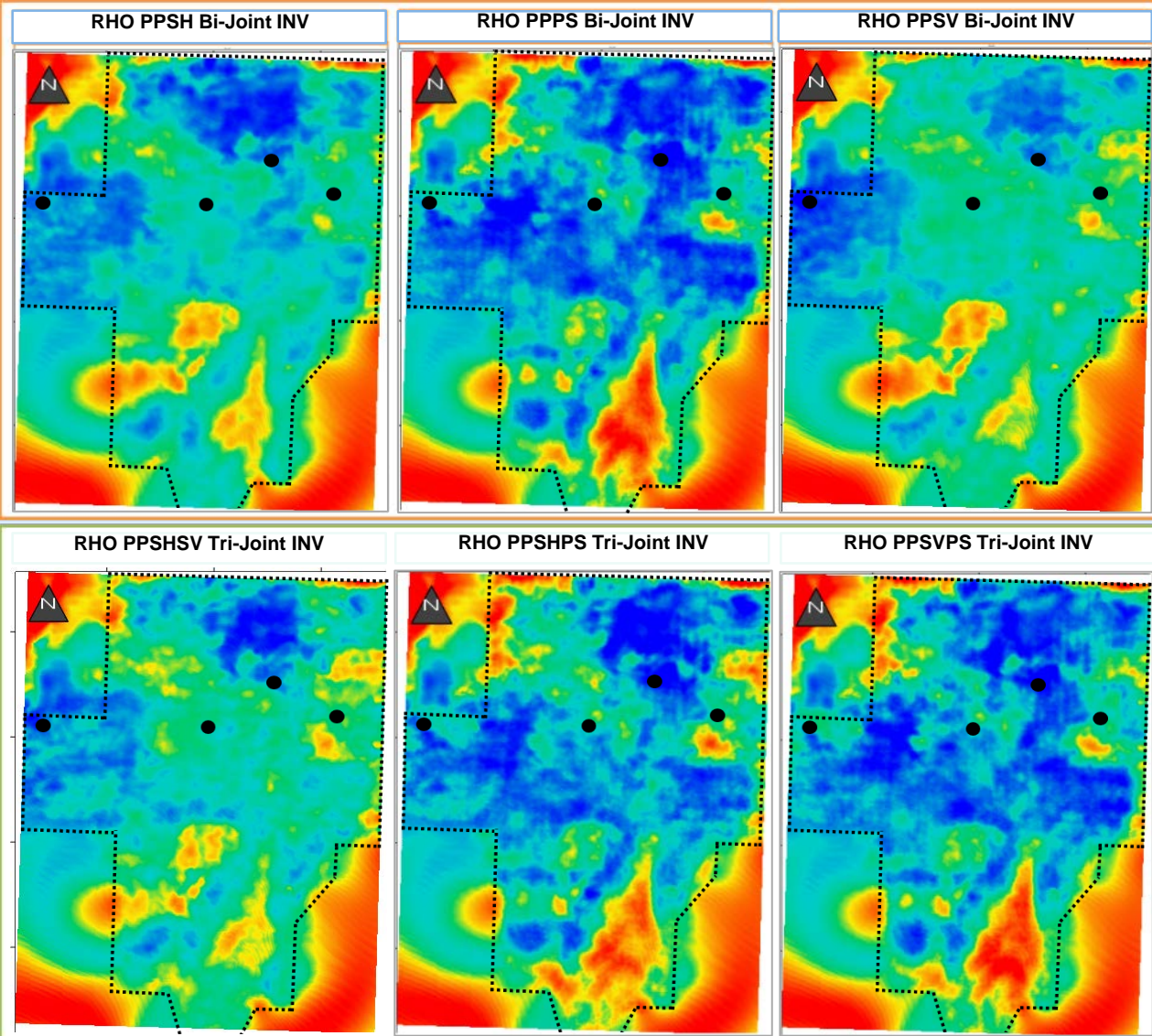


Danielson

Wallewein

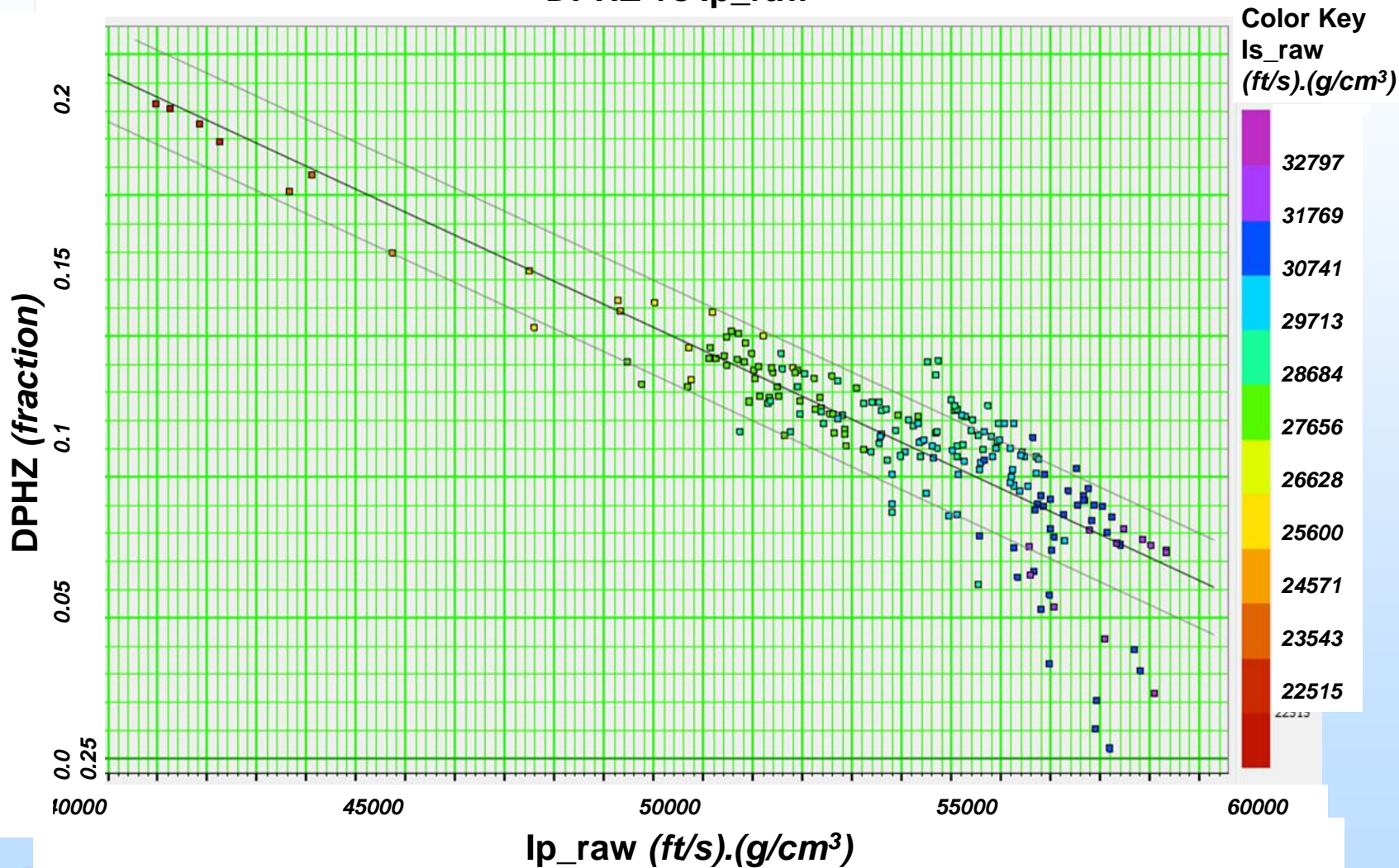


Comparison at mid-Duperow horizon of the inverted density parameter obtained with different kinds of wavefields. bi-joint inversion (3 images at the top), tri-joint (3 images at the bottom) and quadri-joint inversion (right). bi-joint *PP-PS* inversion is very similar to the final **quadri-joint inversion** (right).

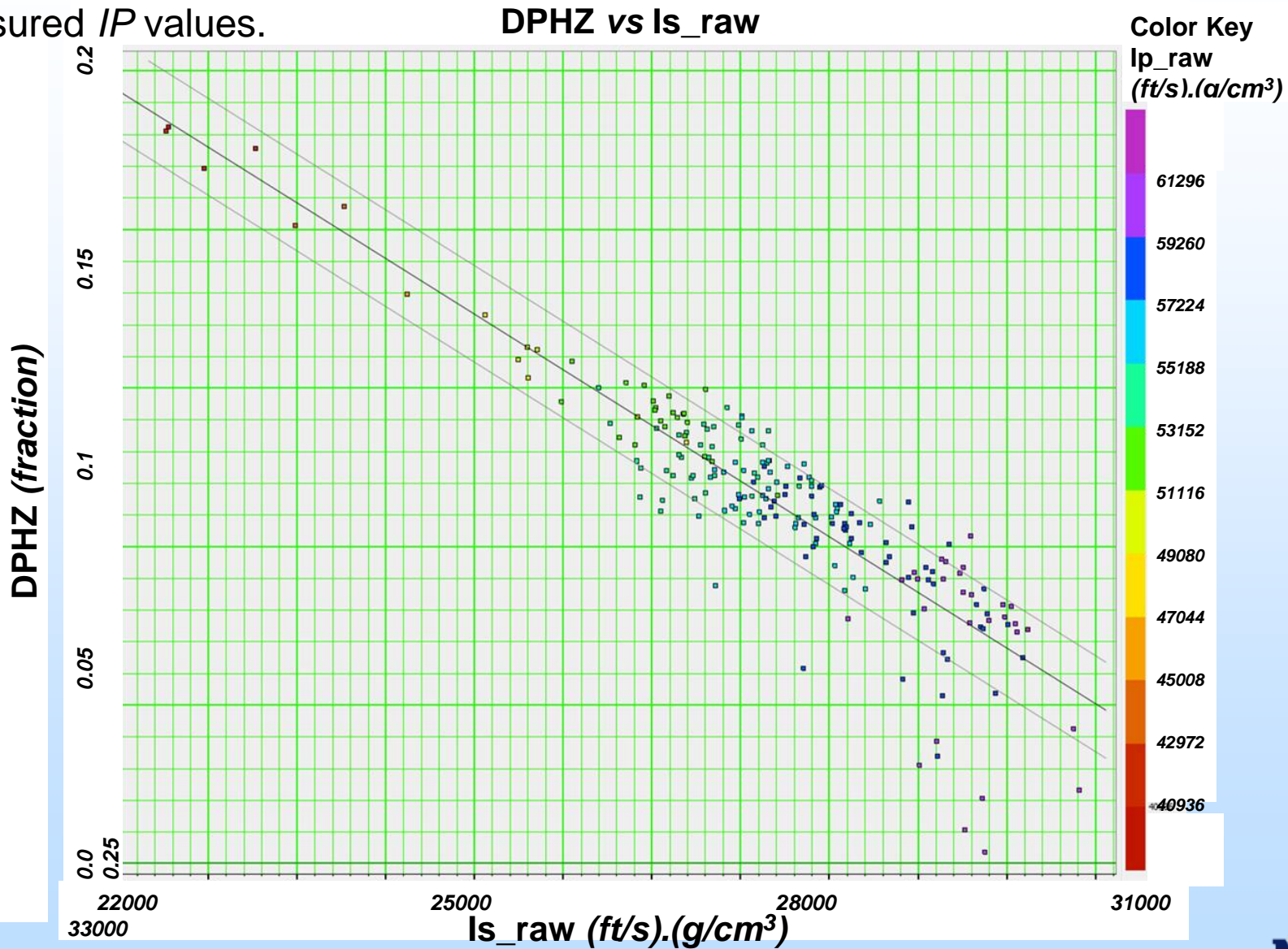


Crossplot between density porosity and computed P -wave impedance (IP) from the Wallewein 22-1 well over the Middle Duperow porosity interval. Note the good correlation observed between the two quantities. The correlation coefficient between the two quantities is 0.87. Colored values are measured IS values.

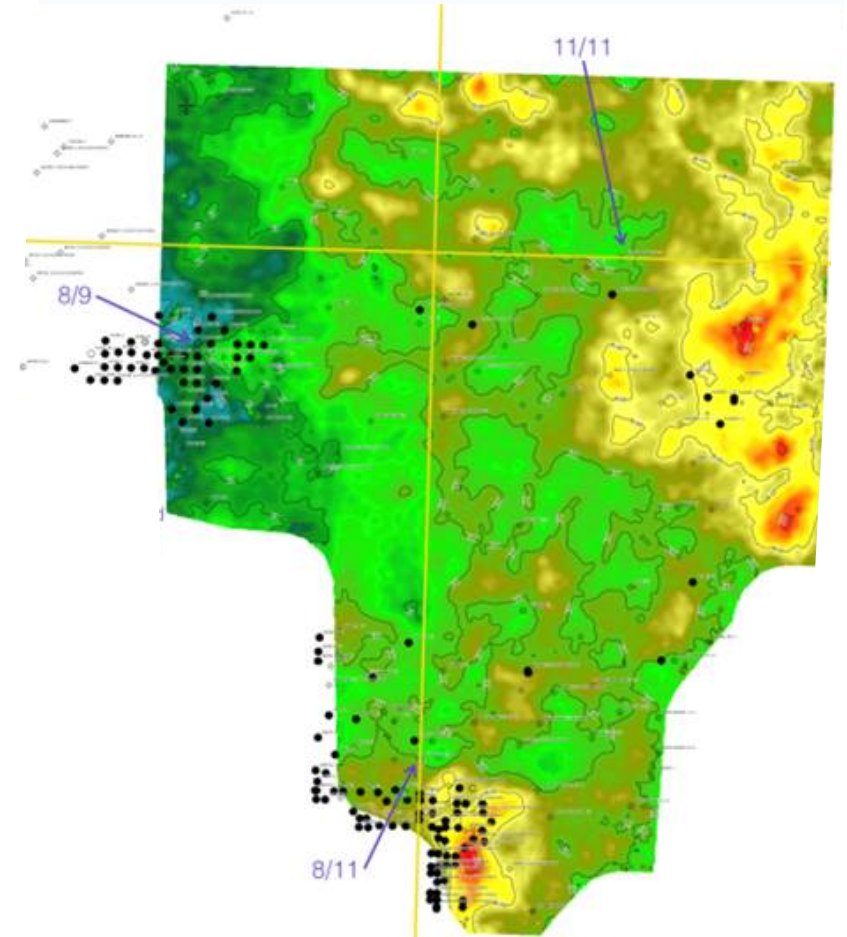
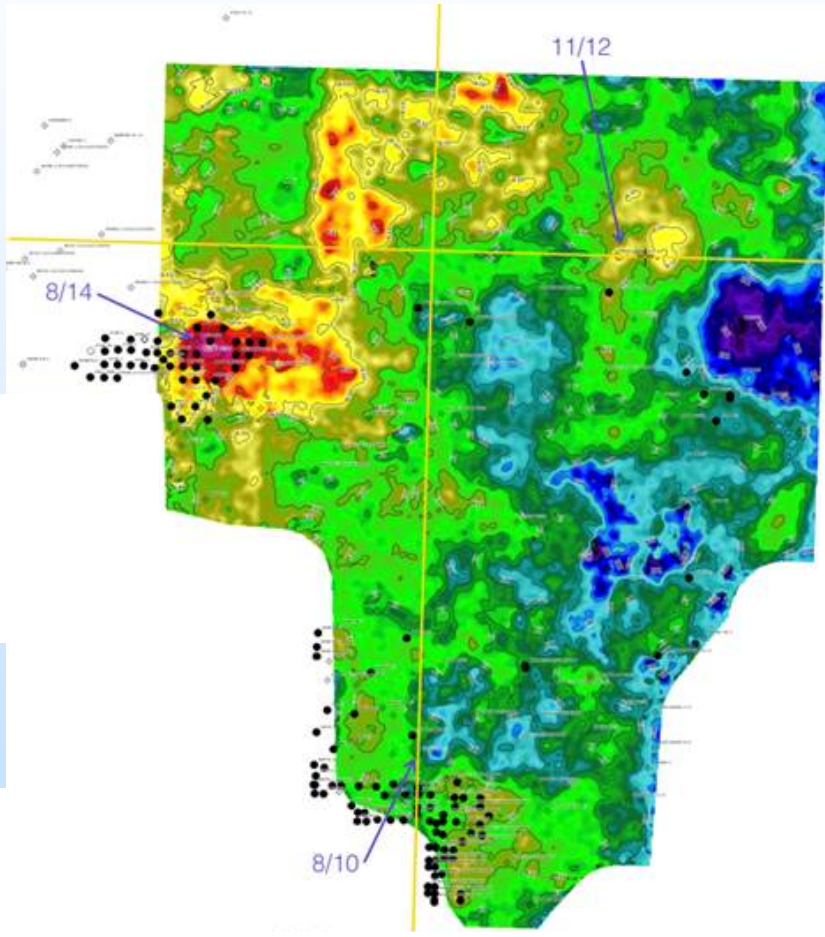
DPHZ vs Ip_{raw}



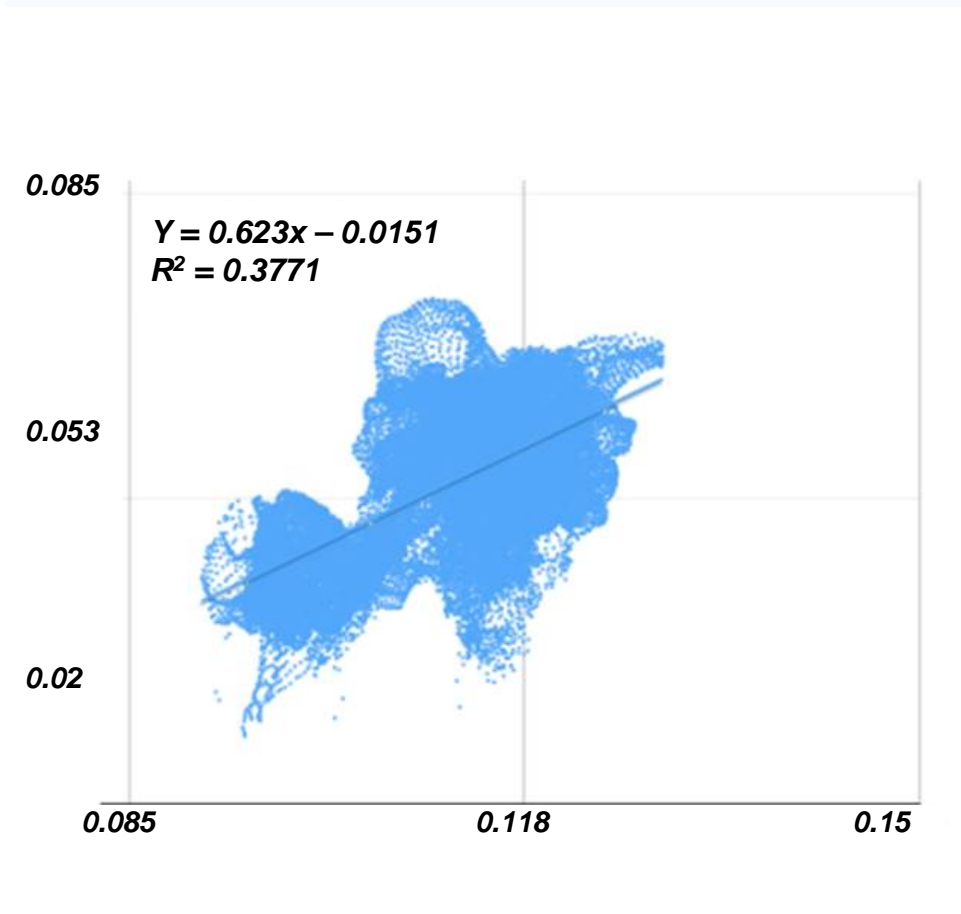
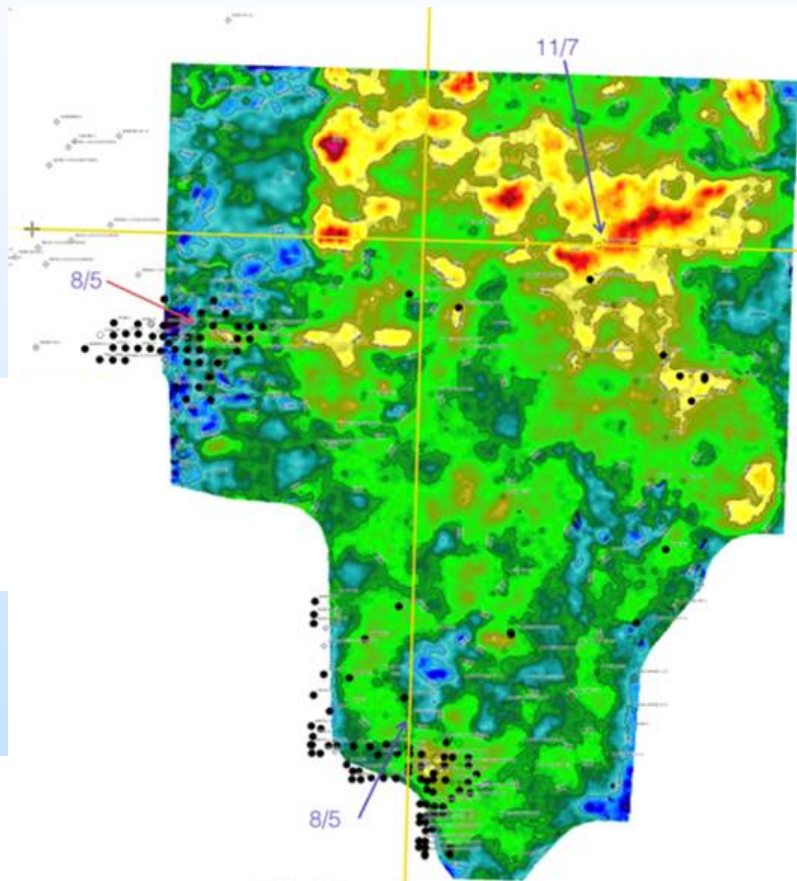
Crossplot of measured density porosity and S-wave impedance (*I*S) in Wallewein 22-1 well in mid-Duperow porosity zone. Note excellent agreement between measured two quantities with correlation coefficient of 0.89. Colored values are measured *I*P values.



Transforms derived from porosity-impedance regressions using *IS* (left) and *IP* (right) maps for the Middle Duperow porosity zone with well locations annotated and well derived values for porosity annotated with values derived from each map at well locations.

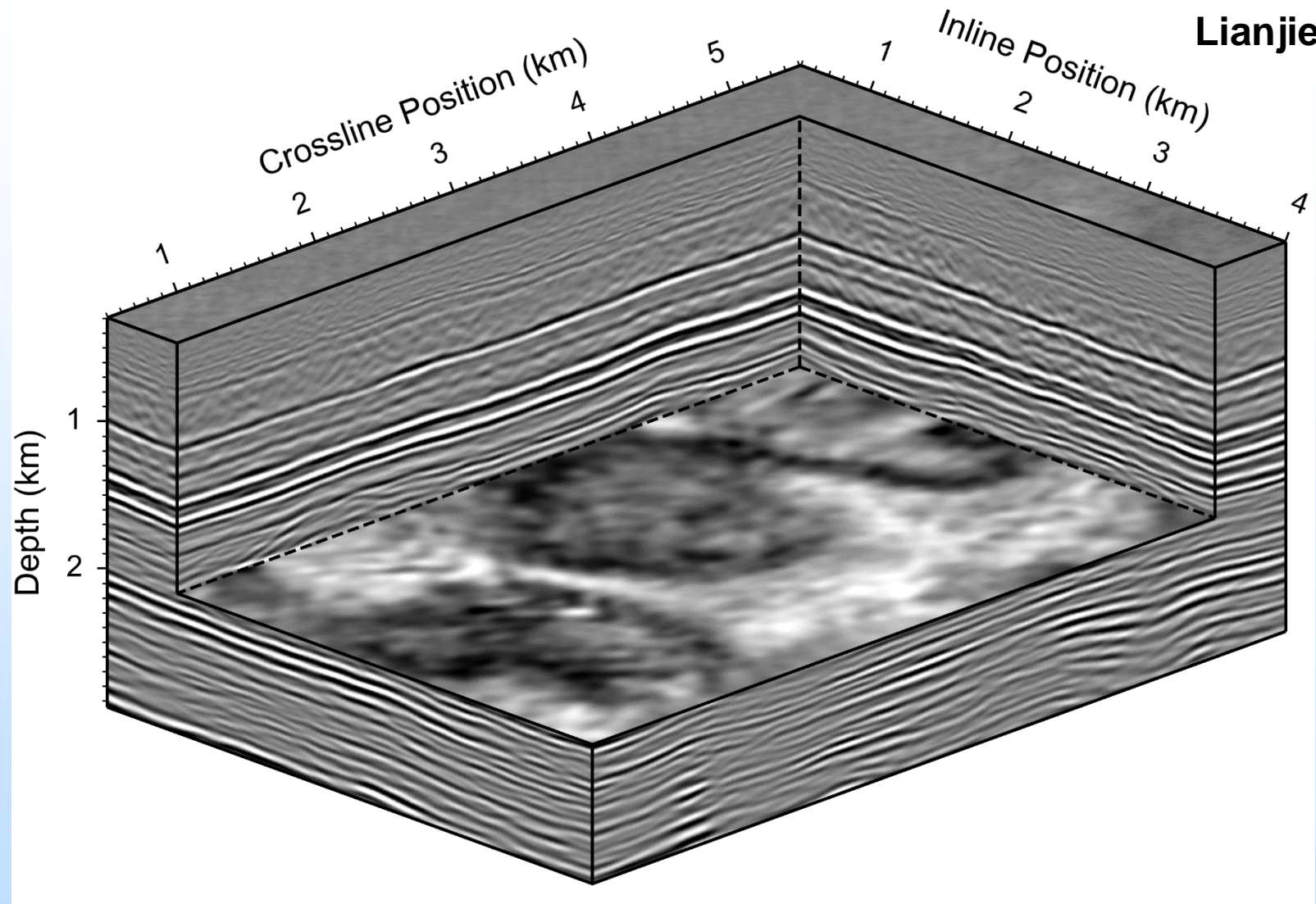


Mid-Duperow porosity derived from average density values from quadri-joint inversion converted to porosity using a dolomite matrix (left) and cross plot of this map with values derived from *IP*-based regression shown in Figure 14. Note the poorer agreement with well values for the density-derived estimate but generally smaller amount of absolute variation than for that derived from the *IP* regression.

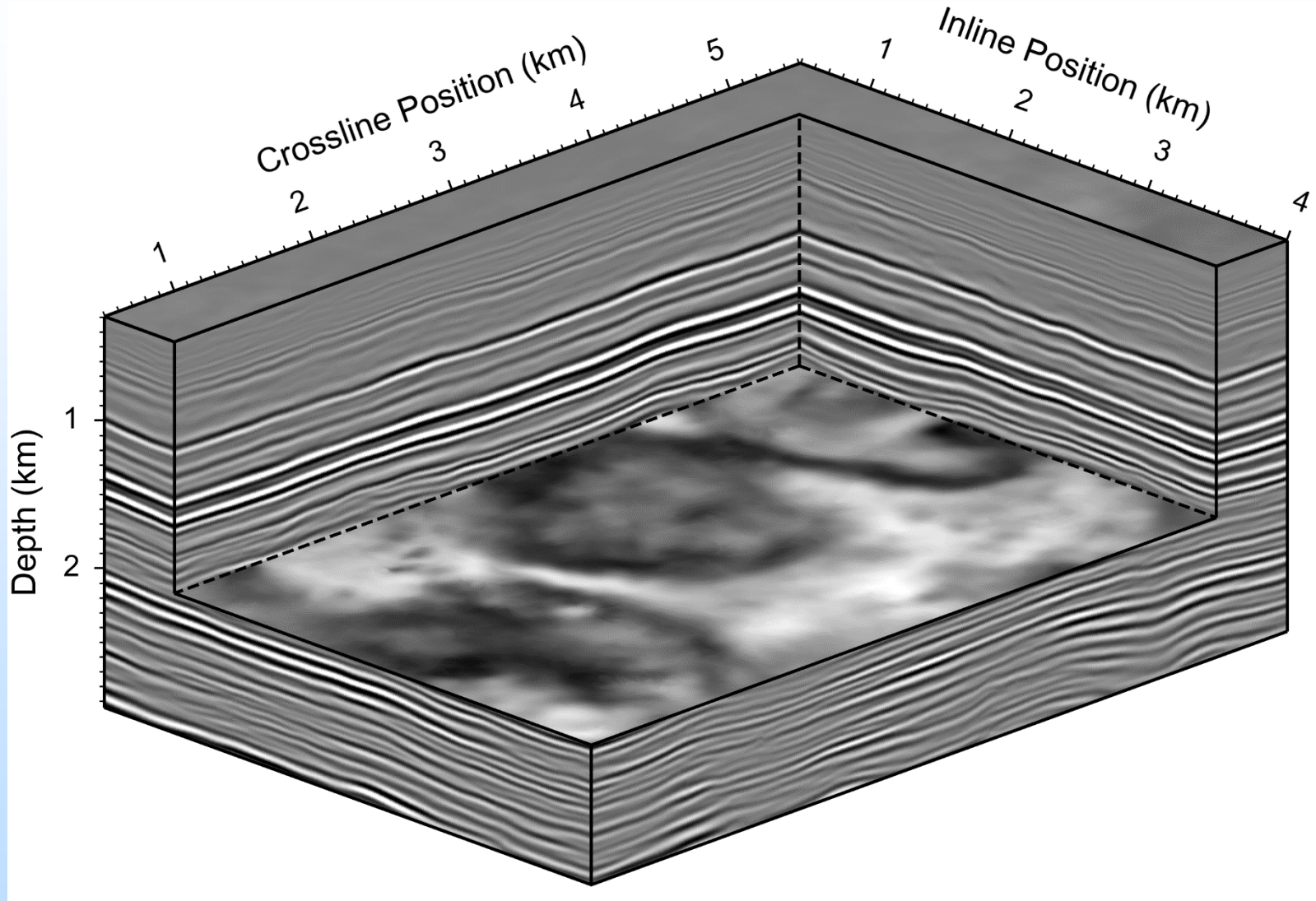


LANL's 3D Reverse-Time Migration Image of 3D Kevin Dome Seismic Data

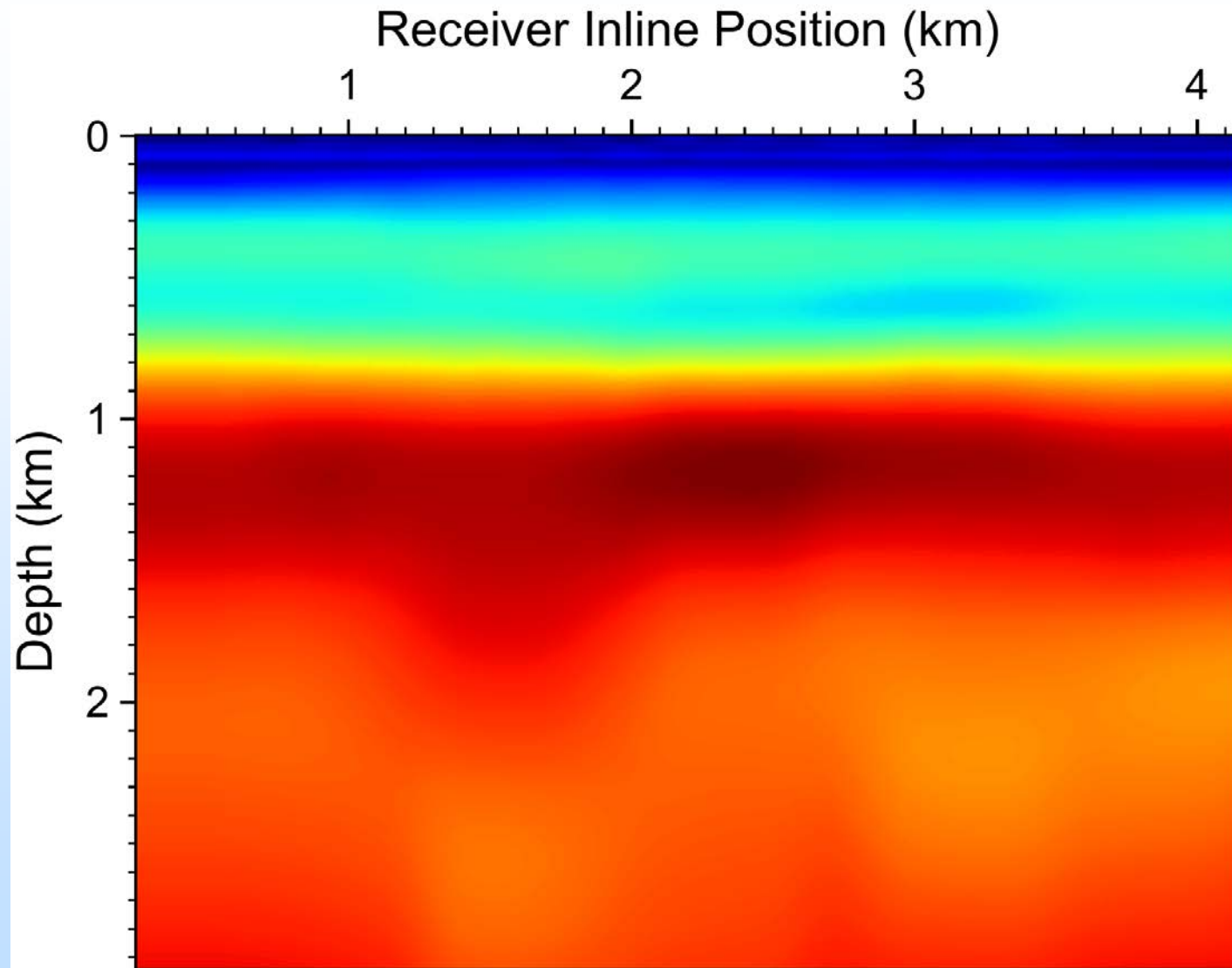
Lianjie Huang



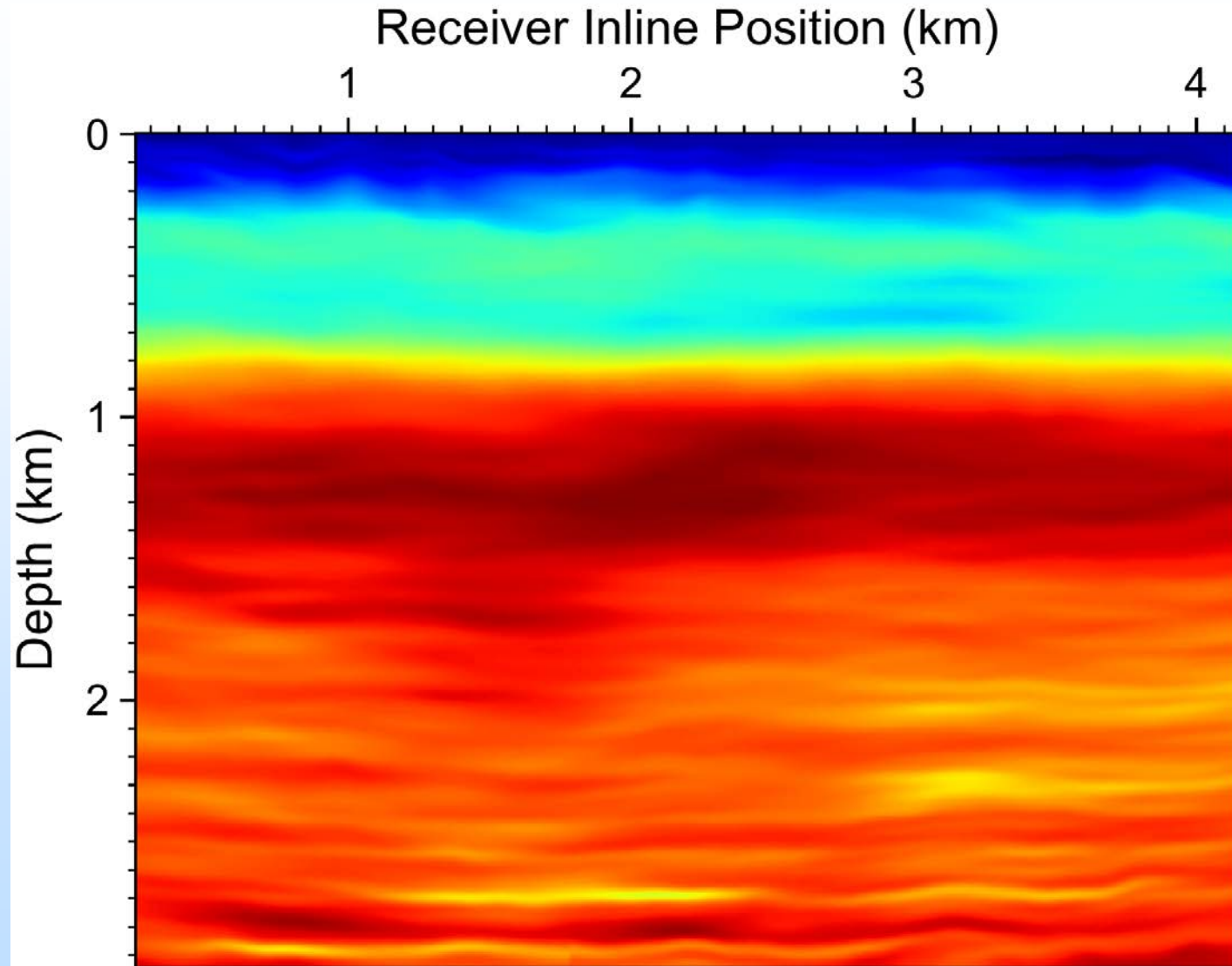
LANL's 3D Structure-Enhanced Least-Squares Reverse-Time Migration Image of 3D Kevin Dome Seismic Data (Further Improved Result)



2D slice of initial low-resolution subsurface velocity model for the Kevin Dome site



2D slice of LANL's high-resolution subsurface velocity model for the Kevin Dome site obtained using full-waveform inversion





Modeling of the Instrumented CO₂ Production Test at the Danielson 33-17 Well (Dec. 26-28, 2014)

Lehua Pan, Curtis M. Oldenburg, and Quanlin Zhou
Energy Geosciences Division
Lawrence Berkeley National Laboratory

July 26, 2018

Modeling of the Instrumented CO₂ Production Test at the Danielson 33-17 Well (Dec. 26-28, 2014)



Lehua Pan, Curtis M. Oldenburg, and Quanlin Zhou

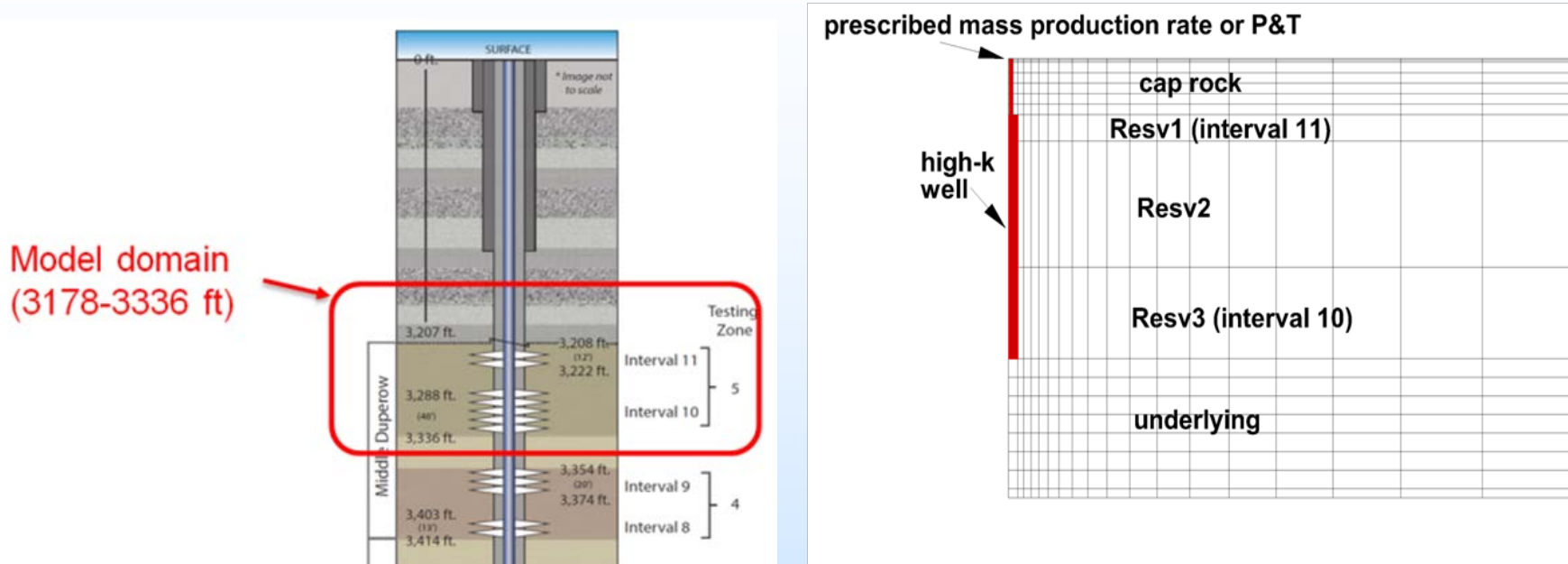
- The CO₂ production test of the Danielson well in 2014 showed very low temperatures in the well and low CO₂ production rate.
- We have simulated this production test to understand the causes of low T and low productivity.
- We use TOUGH2/ECO2M.
- Existing versions of ECO2M had difficulty converging during gas-liquid phase change.
- We developed a new version of ECO2M that solves the convergence problems related to CO₂ phase change.
- TOUGH2/ECO2M retains the lower T limit of 0 °C because the module does not simulate water ice nor hydrate formation.
- We are able to match the production test measurements if we assume a spatially variable permeability field.

Overview



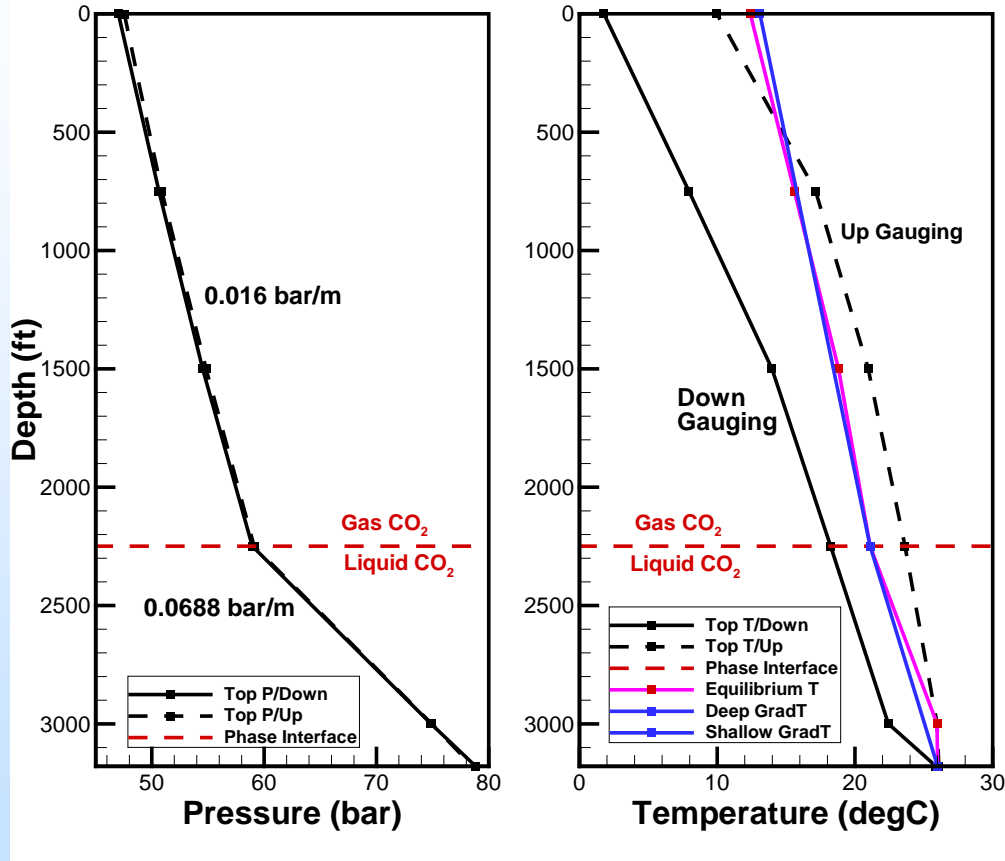
- The CO₂ production test of the Danielson well in 2014 showed very low temperatures in the well and low CO₂ production rate.
- We have simulated this production test to understand the causes of low T and low productivity.
- We use TOUGH2/ECO2M.
- Existing versions of ECO2M had difficulty converging during gas-liquid phase change.
- We developed a new version of ECO2M that solves the convergence problems related to CO₂ phase change.
- TOUGH2/ECO2M retains the lower T limit of 0 °C because the module does not simulate water ice nor hydrate formation.
- We are able to match the production test measurements if we assume a spatially variable permeability field.

Danielson well test interval and model grid



- Radially symmetric grid (dR varies from 0.1 m near well to 100 m at $R = 1$ km).
- 2 7/8" tubing (ID = 0.062 m) and 5 1/2" casing (ID = 0.124 m) are modeled as high-k equivalent porous media with zero capillary pressure and unit porosity.
- All boundaries are closed except for the top of the simulated well which is at the downhole gauge depth.

CO₂ is in liquid phase in the model domain at the start of the production test



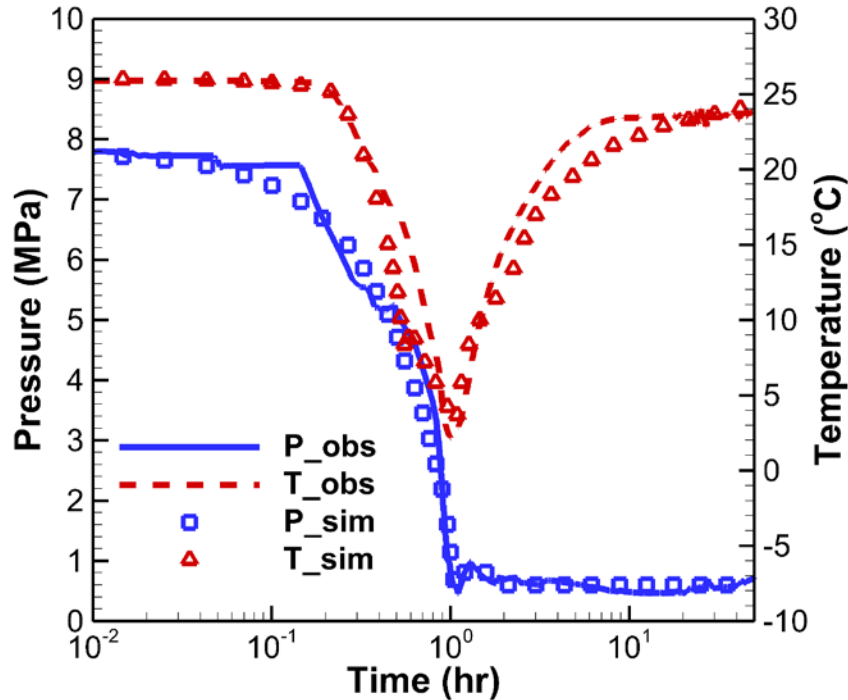
Measured P & T profiles in the entire well before and after the production test (Dec. 26-28, 2014)

- Initial reservoir conditions:
 - Water saturation: 0.2 (< residual saturation)
 - CO₂ is in liquid phase
- This is a very challenging simulation problem because CO₂ production involves expansion of liquid CO₂ during phase transition to gas which causes cooling by both depressurization and latent heat effects.

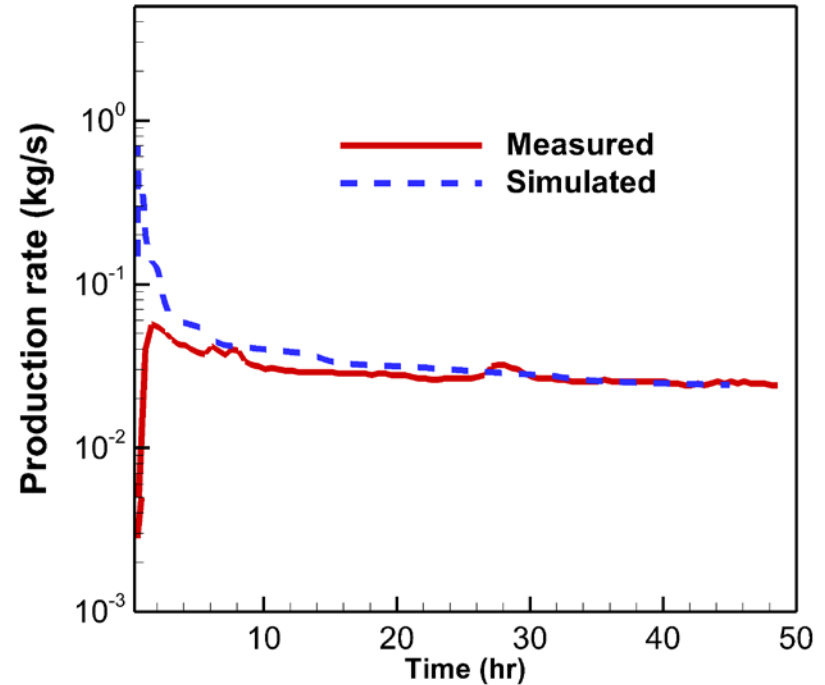
TOUGH2/ECO2M matches field results for the case of a spatially varying permeability field



Known PT@3179'_varK



Known PT@3179'_varK

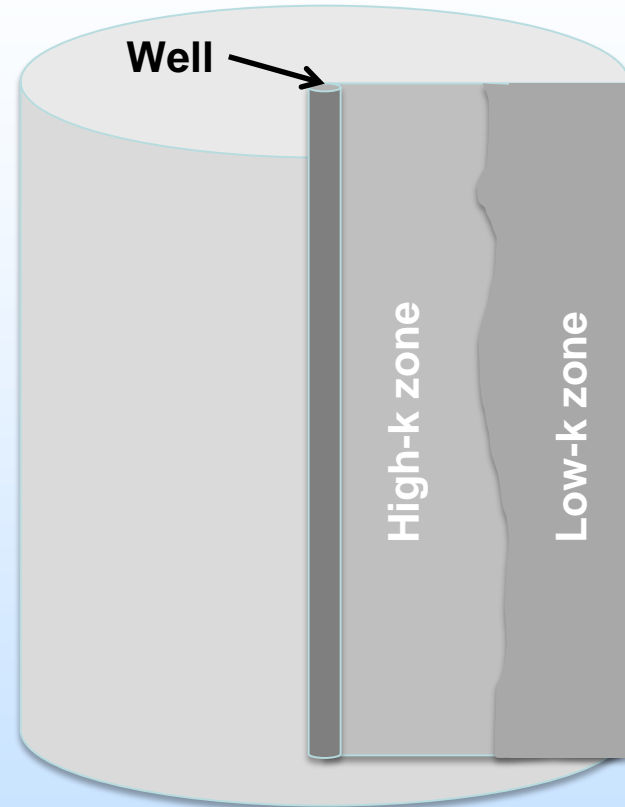


Assumes the core-measured permeability only reflects a small local zone around the well (< 0.522m) which is surrounded by much lower permeability zone

Rock	k (R<0.522m) (10 ⁻¹⁸ m ²)	k (R>0.522m) (10 ⁻¹⁸ m ²)
Resv1	84.4	0.1712
Resv3	4090.0	8.296

Spatially varying permeability

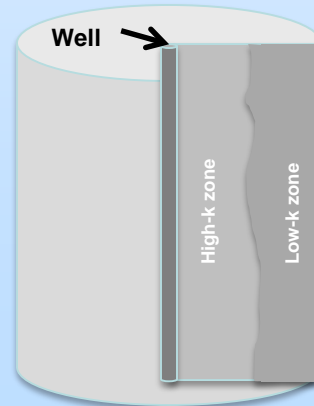
The model assumes the core-measured permeability reflects a small local zone around the well (< 0.522m) that is surrounded by a much lower permeability zone



Rock	k (R<0.522m) (10 ⁻¹⁸ m ²)	k (R>0.522m) (10 ⁻¹⁸ m ²)
Resv1	84.4	0.1712
Resv3	4090.0	8.296

Conclusions

- The 2014 Danielson CO₂ production test is challenging to simulate because of low initial reservoir temperature and significant cooling caused by phase change and decompression.
- One way to match both production rate and temperature data is to assume a spatially varying permeability field in which the near-well region has higher permeability than the far-field region.
- Drilling can induce damage in the formation near the well that could result in such a configuration over these same length scales.
- Another source of low effective k could be formation of hydrate or water ice that plugs pore space.



Subtask R1.5

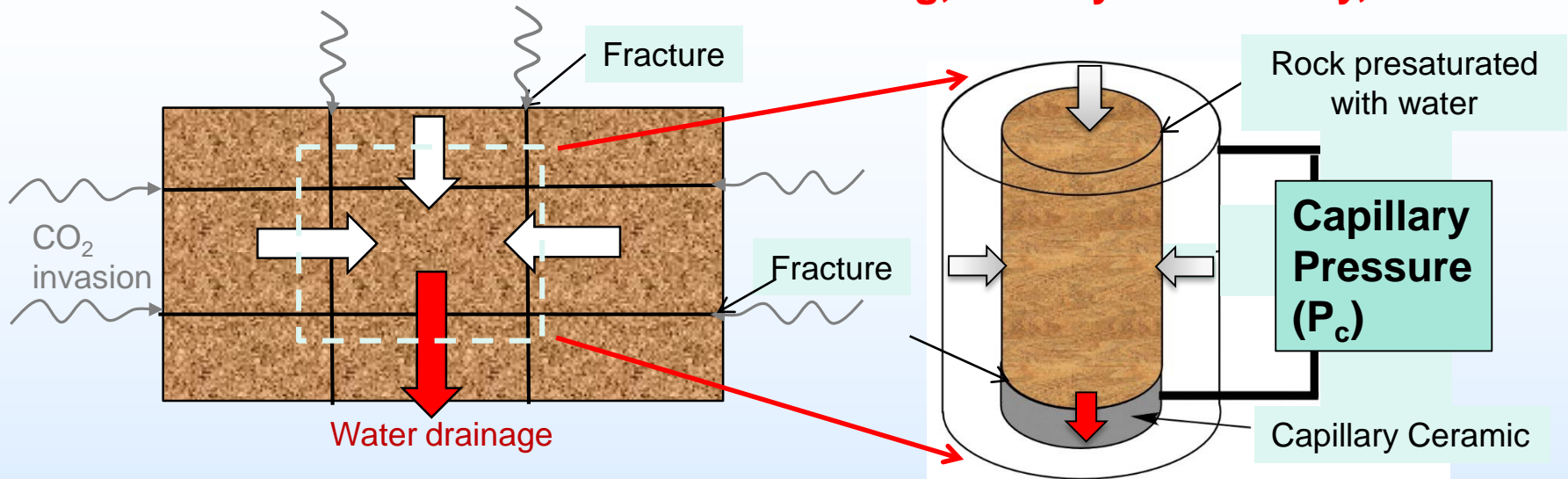
Lab measurements of fracture-matrix flow to help with modeling of two-phase flow in fractured carbonate

Chun Chang, Timothy J. Kneafsey, Quanlin Zhou

Earth and Environmental Sciences Area, Lawrence Berkeley National Laboratory

Subtask R1.5. Lab measurements of fracture-matrix flow to help with modeling of two-phase flow in fractured carbonate

Chun Chang, Timothy J. Kneafsey, Quanlin Zhou



Background:

CO₂ invasion into a fractured system and schematic of laboratory tests

To access CO₂ storage capacity in rock matrix, water must drain through fractures and matrix. Capillary continuity allows drainage across fractures to neighboring matrix blocks and requires quantification.

Laboratory flow tests were conducted to:

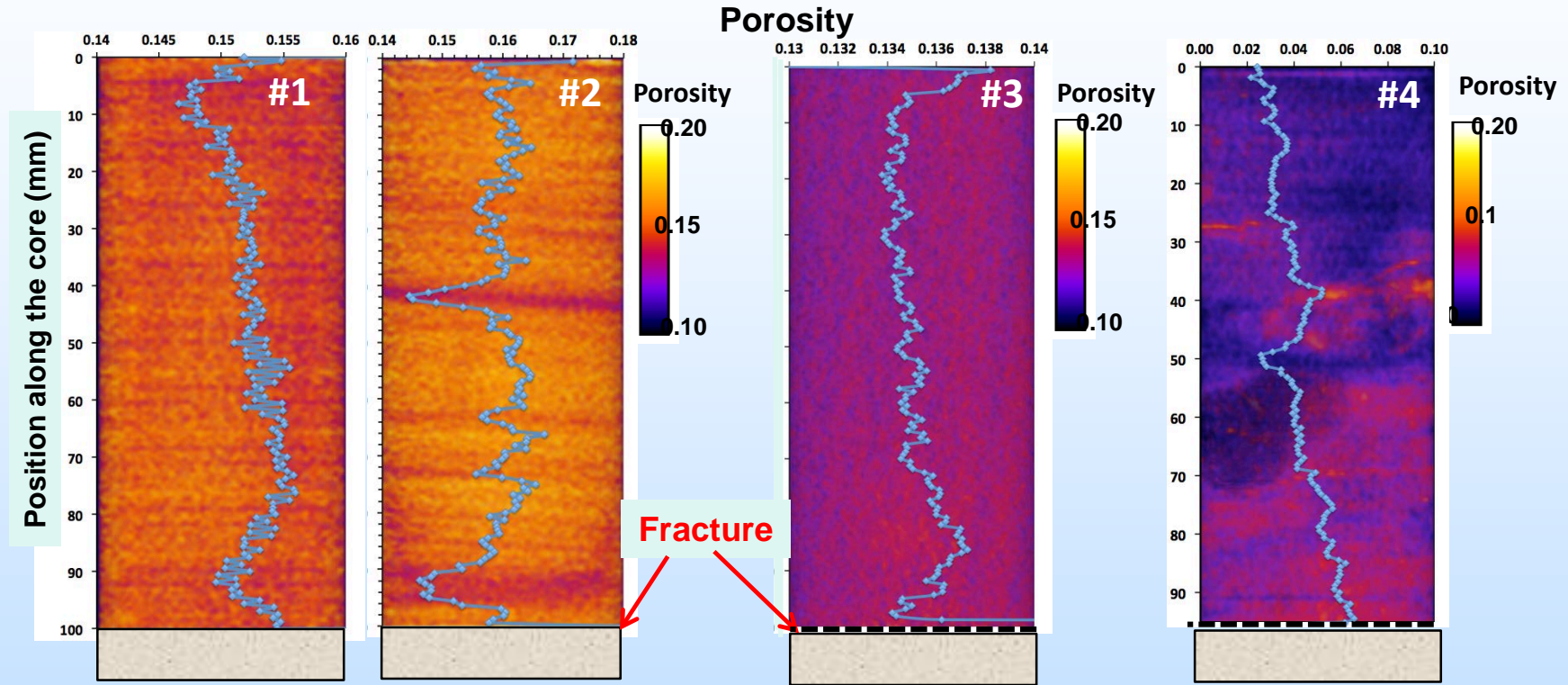
1. investigate the fracture-matrix interactions;
2. visualize processes showing the importance of capillary continuity to geologic carbon storage capacity.

Core samples and fracture types

❖ Two types of capillary continuity of fracture

➤ Good capillary continuity

➤ P_c -dependent capillary continuity



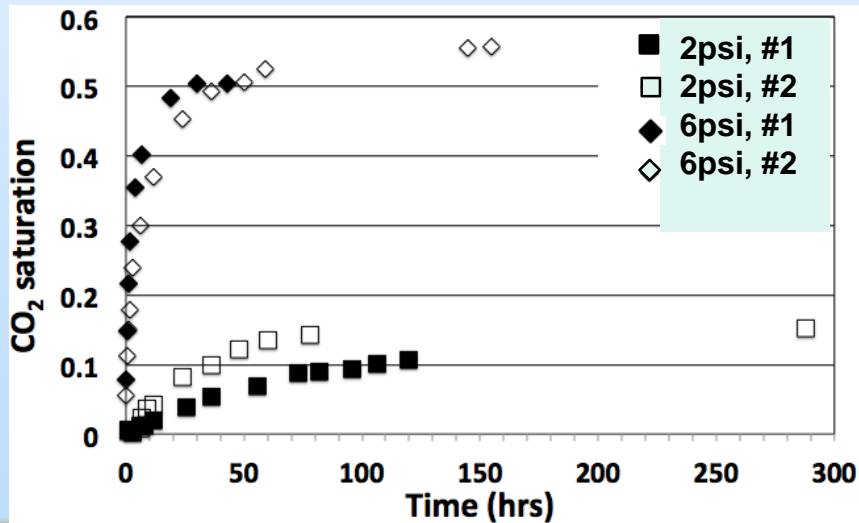
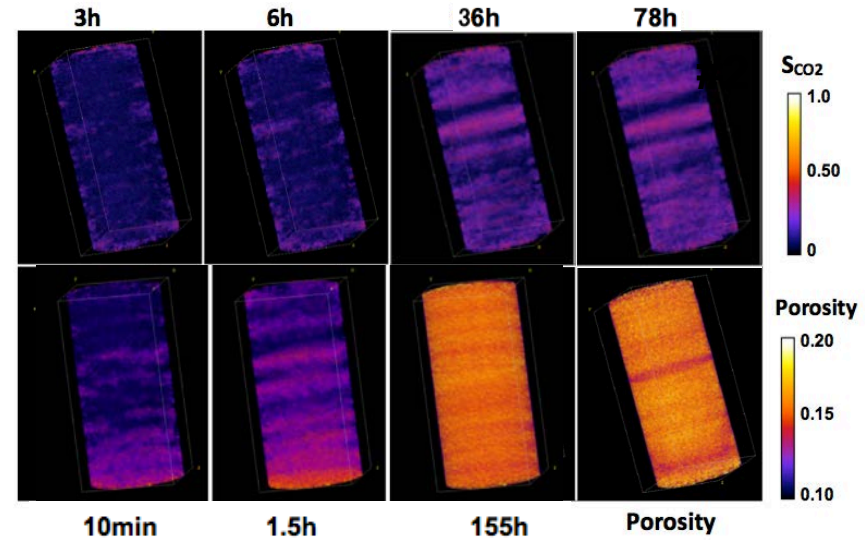
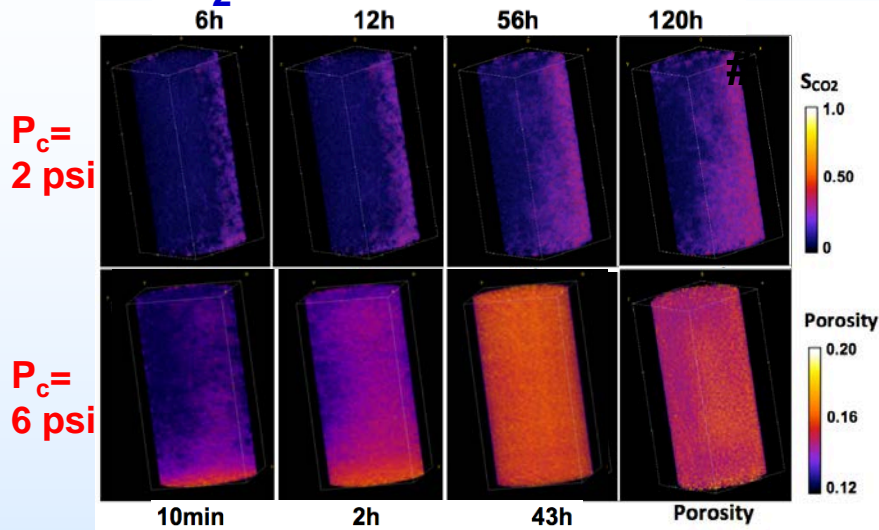
➤ Sample #1: **Homogeneous** sandstone core, Brine permeability: ~10mD, Porosity: 0.153

➤ Sample #2: **Layered** sandstone core, Brine permeability: ~10mD, Porosity: 0.158

➤ Sample #3: **Low-permeability** sandstone core, Brine permeability: ~1mD, Porosity: 0.135

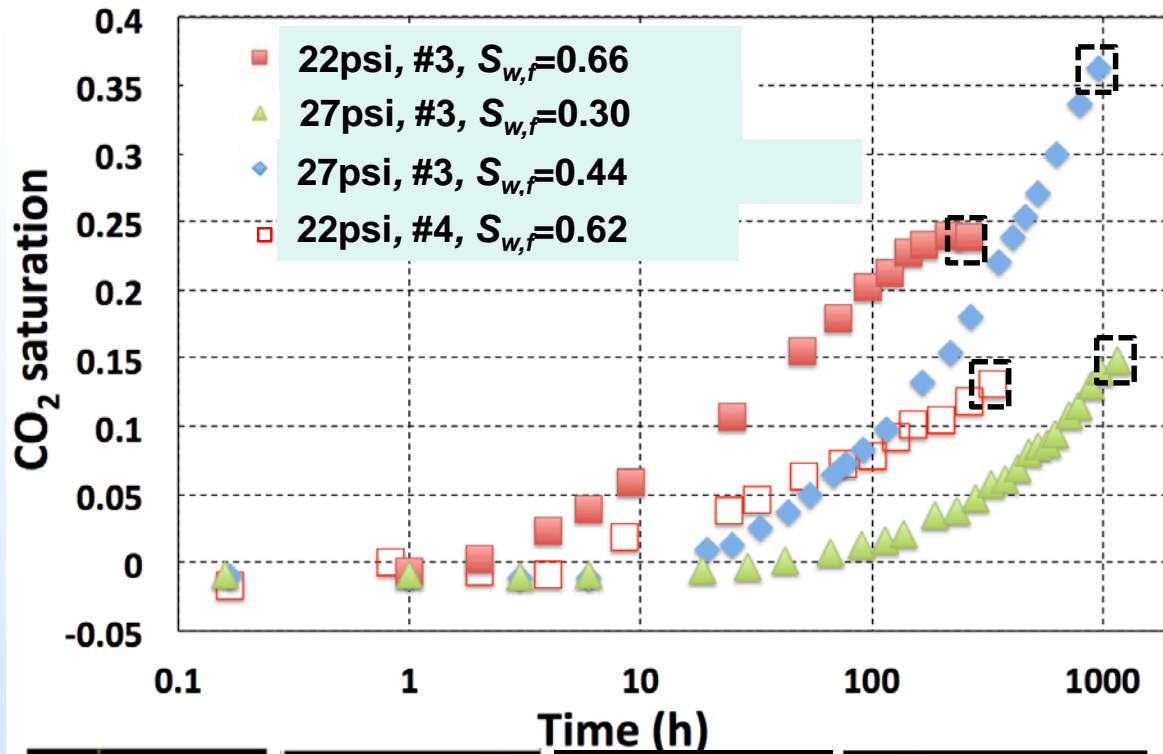
➤ Sample #4: **Heterogeneous** Duperow core (Wallewein 22-1, depth: 4129 feet), Brine permeability: ~1mD, Porosity: 0.042

❖ CO₂ distribution and saturation vs. time in rock matrix

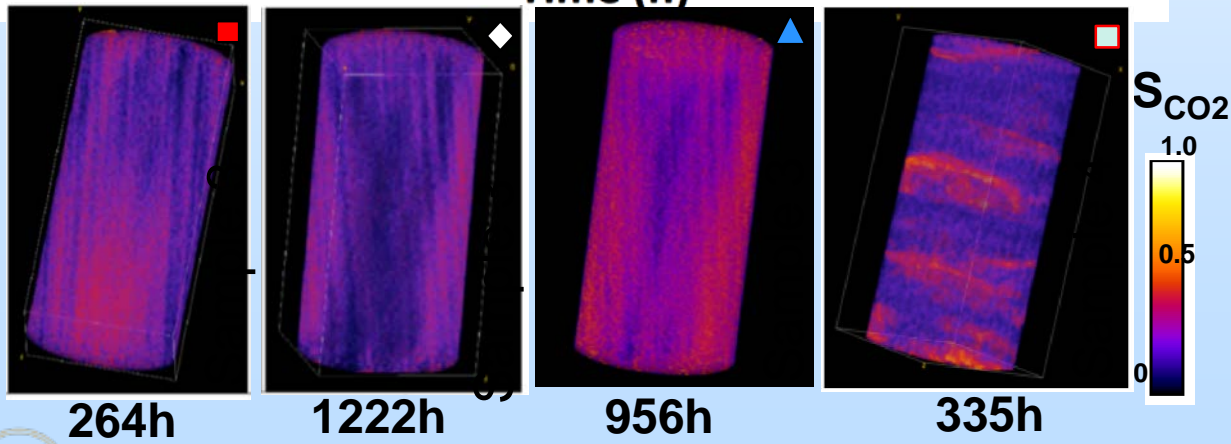


- Water saturations in fracture ($S_{w,f}$) range from **0.73 to 0.94** for both Sample #1 and #2 under $P_c=2$ and 6psi;
- Higher applied P_c results in higher CO₂ saturation at steady state;
- At $P_c=6$ psi, CO₂ invasion in Sample #1 is faster than in Sample #2 (bedding perpendicular to water drainage direction).

CO₂-water flow with P_c-dependent capillary continuity of fracture



- ❖ High capillary pressure causes CO₂ to invade the fracture and lower continuity;
- ❖ Lower $S_{w,f}$ yields slower CO₂ invasion and water drainage;
- ❖ Matrix anisotropy perpendicular to water flow direction (sample #4) results in slower CO₂ invasion than in sample #3 under similar P_c and $S_{w,f}$.



Conclusions

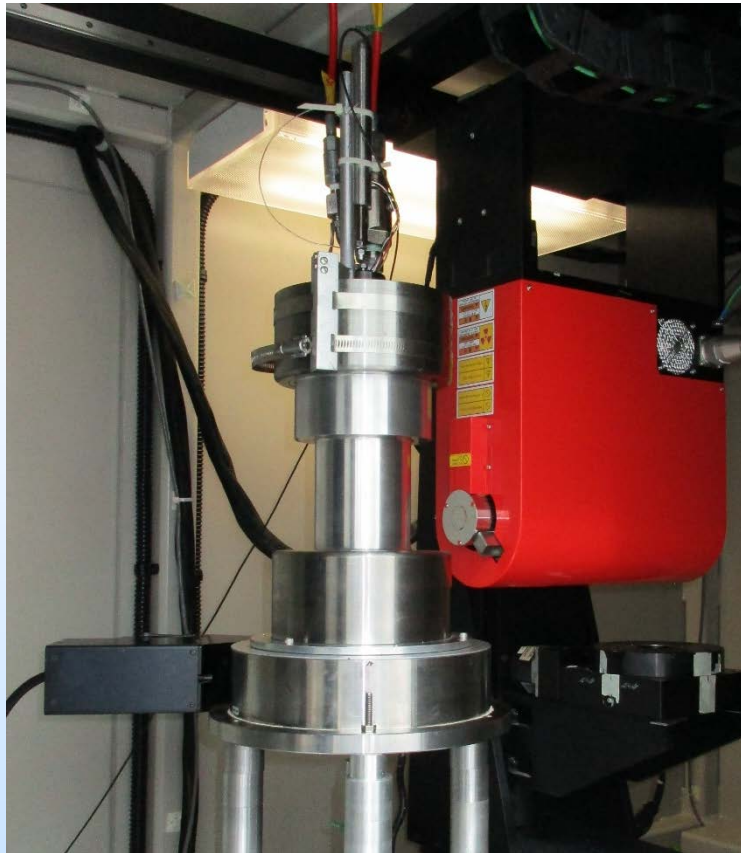
- ❖ The capillary continuity across fractures considerably affects the CO₂-water displacement rate and efficiency within the observed time scale;
- ❖ The capillary continuity across fractures is P_c -dependent and can be expressed in terms of fracture water saturation ($S_{w,f}$);
- ❖ The displacement of water by CO₂ across a matrix-fracture system is also affected by the matrix anisotropy.

Task R1. Core Studies: Motivation

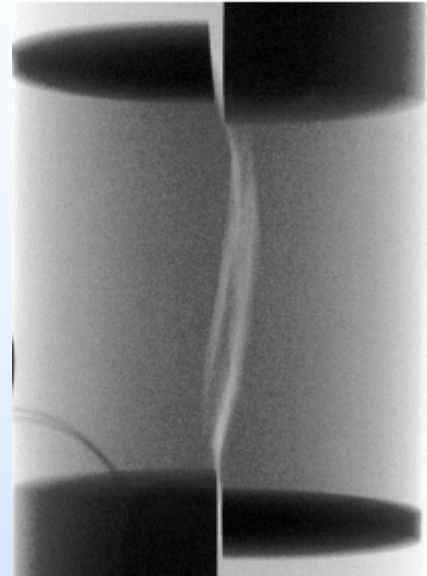


- Assess caprock geomechanical properties and suitability
- Analyze fracture-permeability relations to inform caprock damage and leakage scenarios
- Determine relationship of stress conditions and fracture reactivation on permeability
- Provide input to induced seismicity hazard assessment

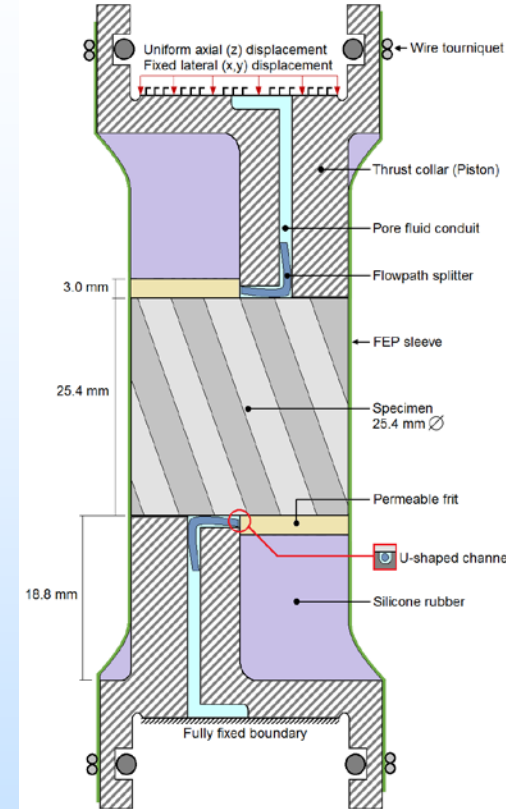
Approach: Triaxial Direct-Shear Coreflood with Simultaneous X-ray radiography/tomography



In situ radiography



Direct-shear device



Creation of shear fractures at reservoir conditions coupled with permeability measurements and x-ray observations

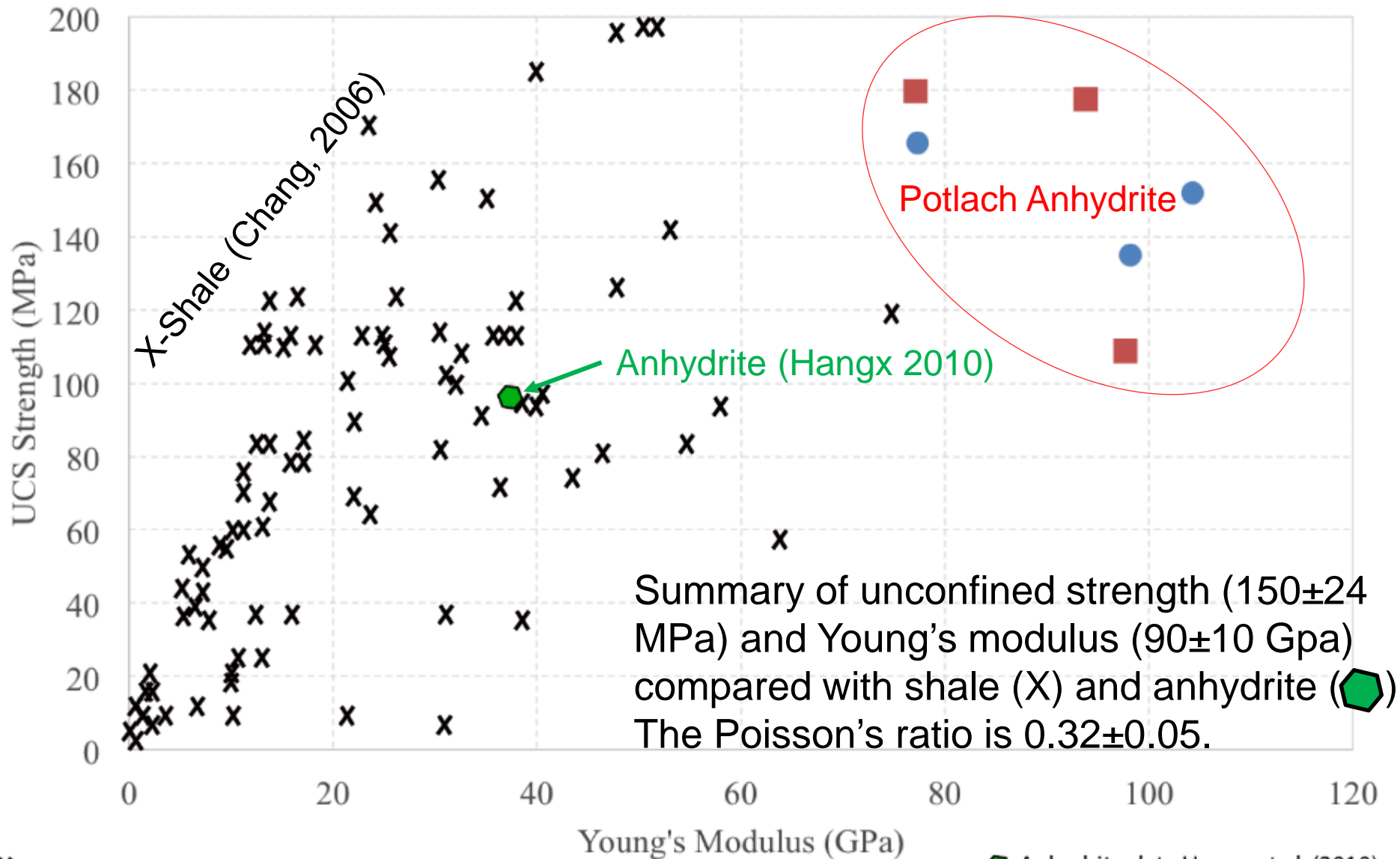
Carey et al., J. Unconv. O&G Res., 2015; Frash et al. (2016) JGR; Frash et al. (2017) IJGGC

Materials

- Potlatch anhydrite—caprock at Kevin Dome, Montana
 - With minor dolomite (Carey et al. 2017; ARMA)
- Upper Duperow dolomite—caprock at Kevin Dome, Montana
 - With minor anhydrite (Frash et al. 2018; ARMA)



Caprock Geomechanical Tests



X Shale data Chang et al. (2006)

◡ Anhydrite data Hangx et al. (2010)

● BA01 - Vertical - 3687 ft

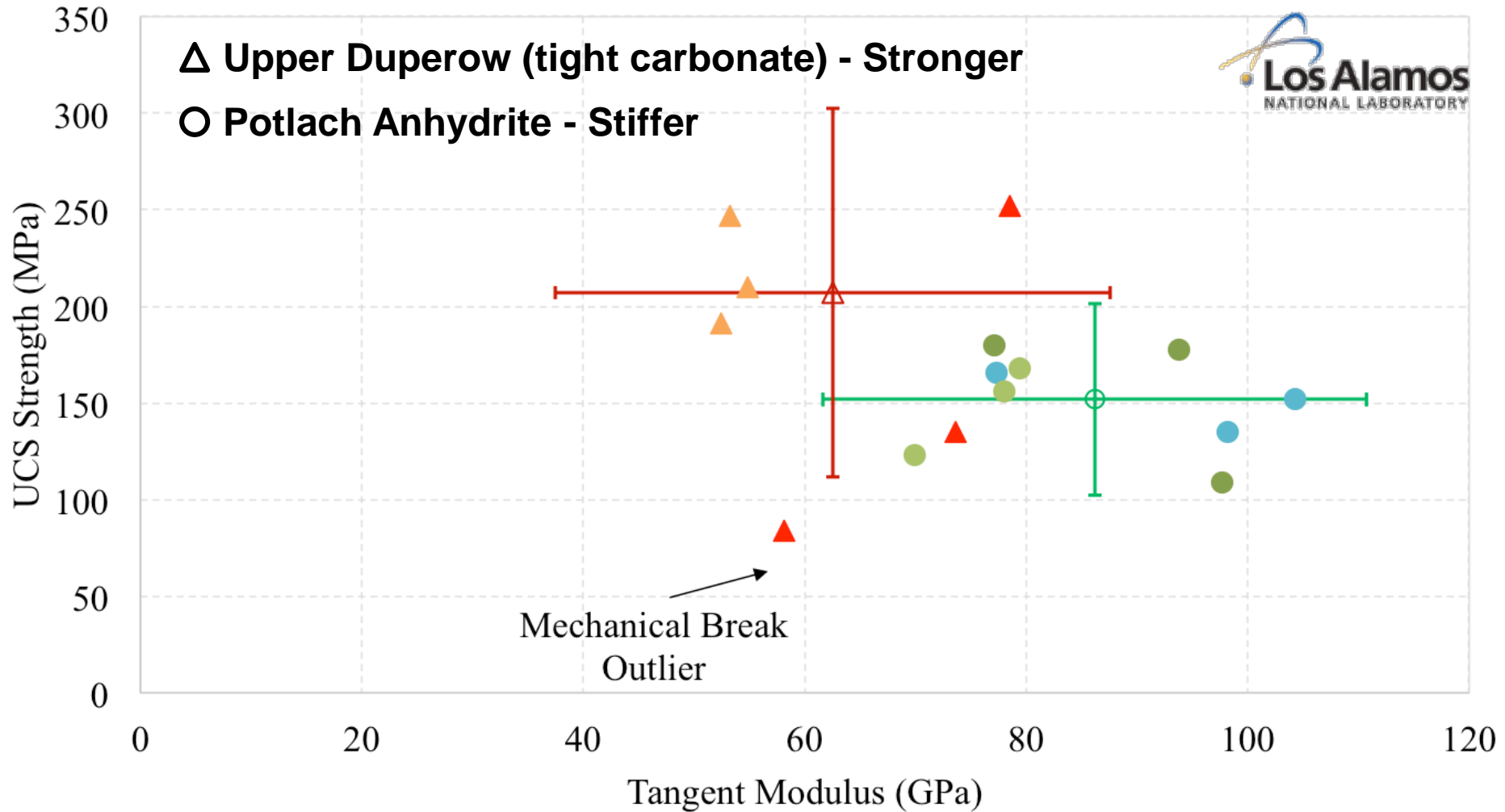
■ BA02 - Horizontal - 3687 ft

Caprock Geomechanical Analysis



△ Upper Duperow (tight carbonate) - Stronger

○ Potlach Anhydrite - Stiffer



● BA01 - Vertical - 3687 ft

● BA02 - Horizontal - 3687 ft

● BA03 - Vertical - 3689 ft

○ BA Mean

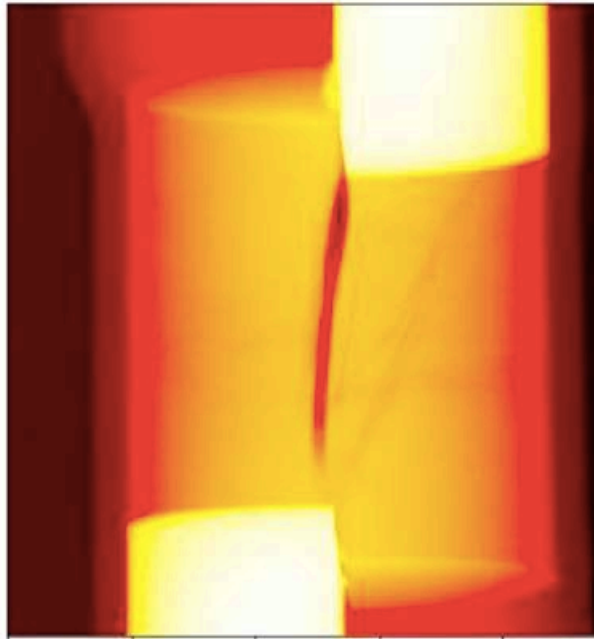
▲ BD01 - Horizontal - 3940 ft

▲ BD02 - Vertical - 3940 ft

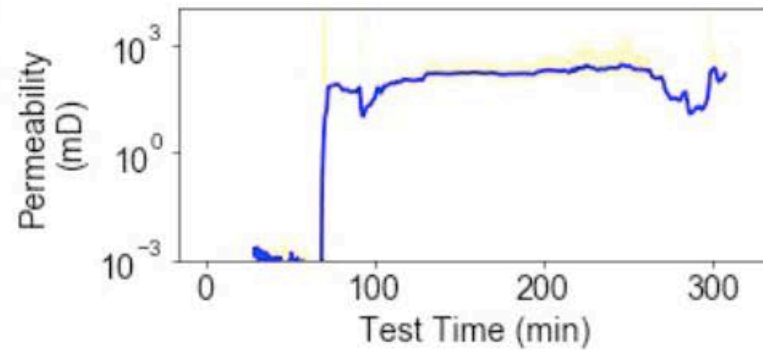
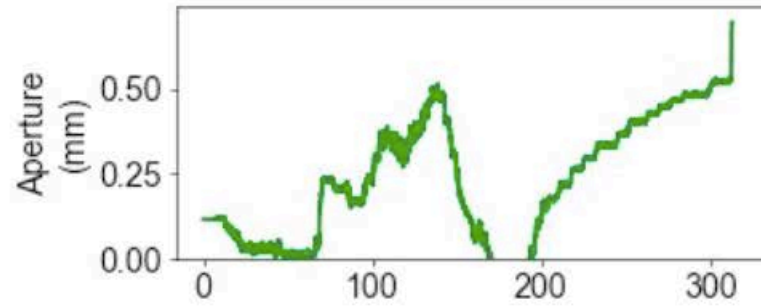
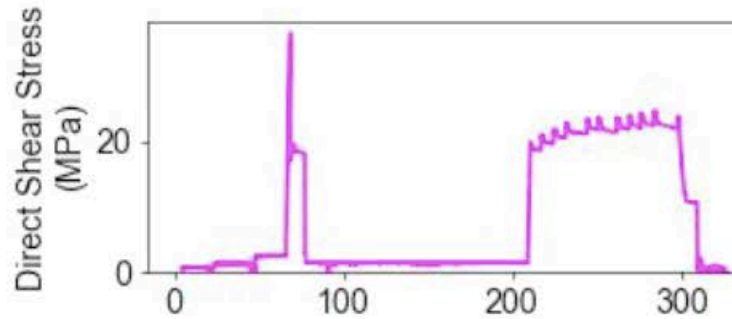
△ BD Mean

Potlatch Anhydrite at 10 MPa

BA05-05:
0.1 MPa Effective Confining

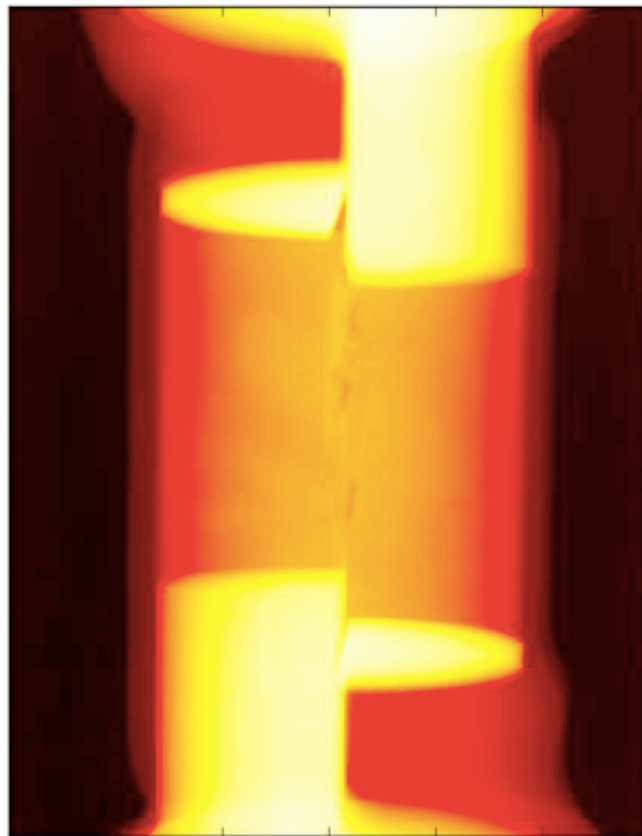


320.00 min

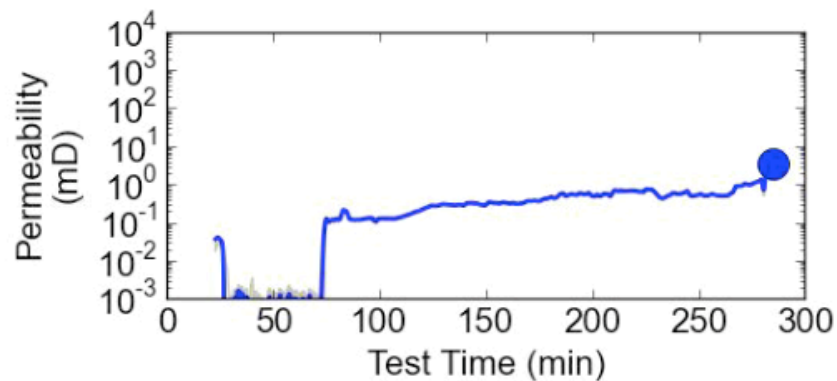
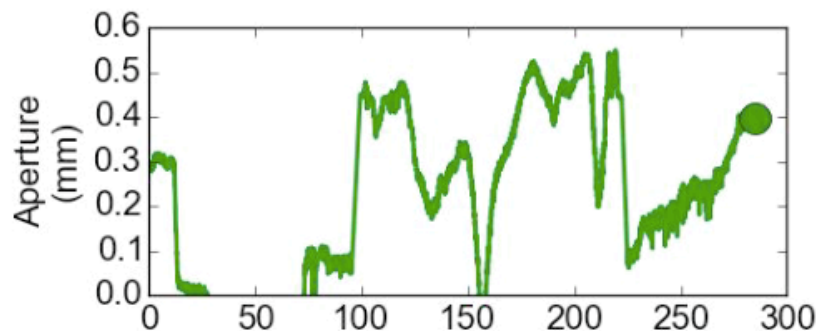
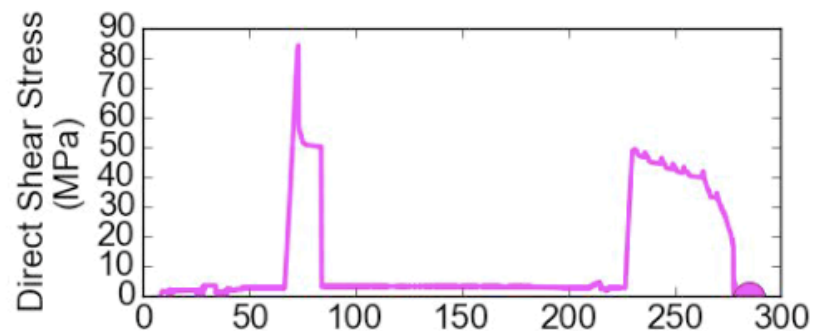


Upper Duperow Dolomite at 30 MPa

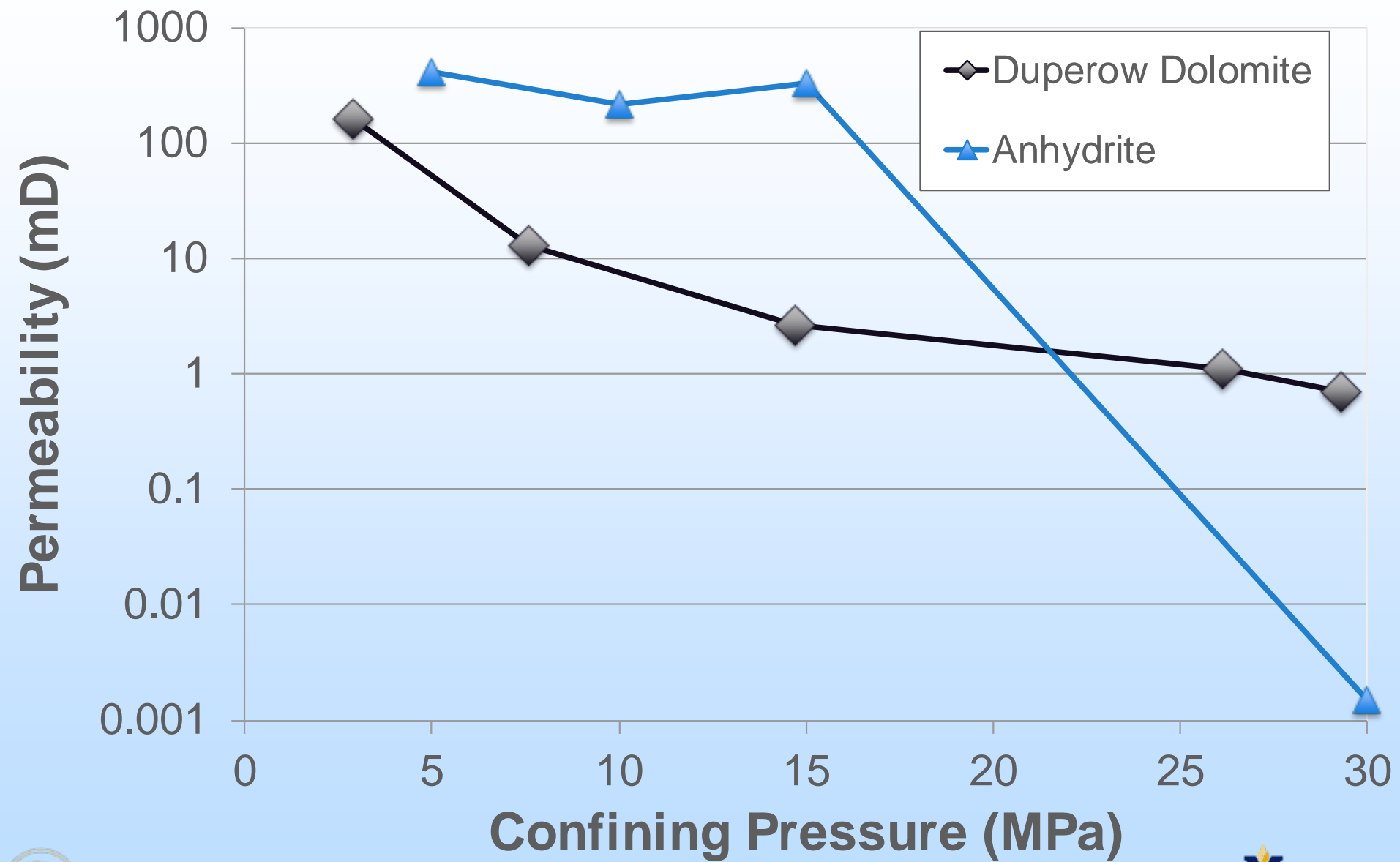
ANS01-04:
2.8 MPa Effective Confining



285.00 min



Summary Permeability-Stress Relations



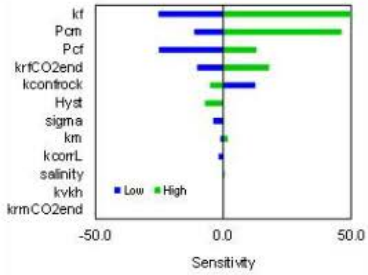
Risk Assessment – 1st paper submitted

Tsubasa Onishi, Minh Nguyen, Phil Stauffer

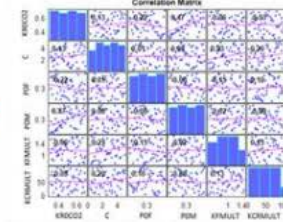
OVERVIEW

- Adopted the NRAP-IAM workflow from injection reservoir simulation to risk assessment of potential leakage
- Did not incorporate seismic interpretation into building the injection reservoir property models to characterize heterogeneity
- Focused on potential CO₂/brine leakage through legacy wells

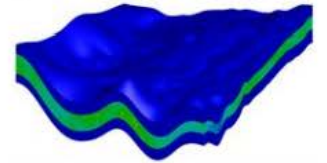
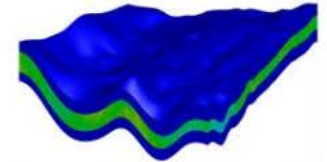
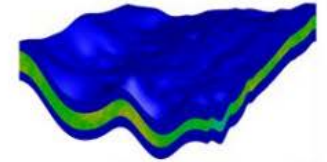
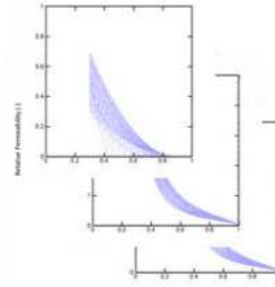
Risk Assessment – 1st paper submitted



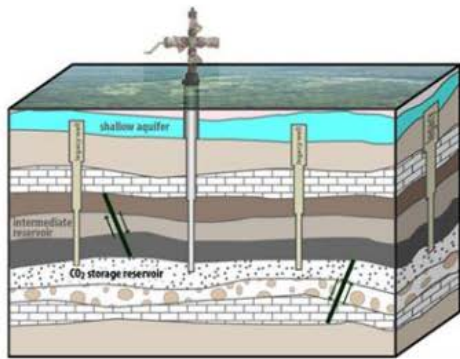
Identify Sensitive Parameters



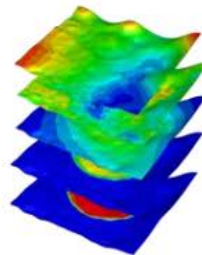
Latin Hypercube Sampling



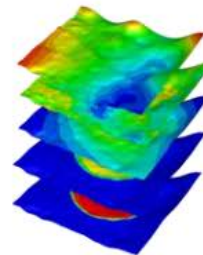
Reservoir Simulation



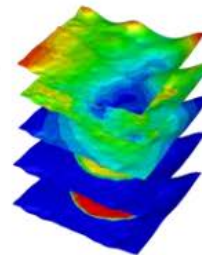
NRAP-IAM



ROM#1



ROM#2

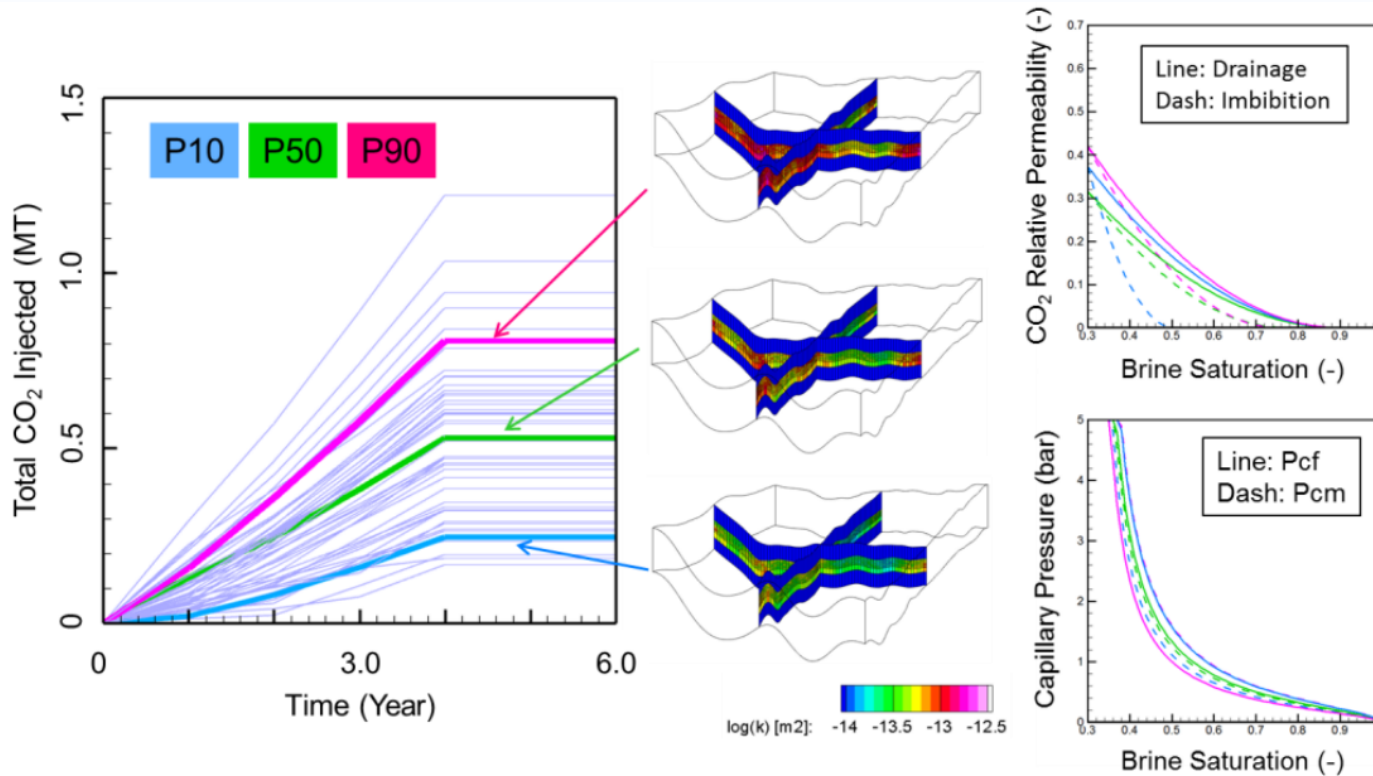


ROM#3

RROM-Gen

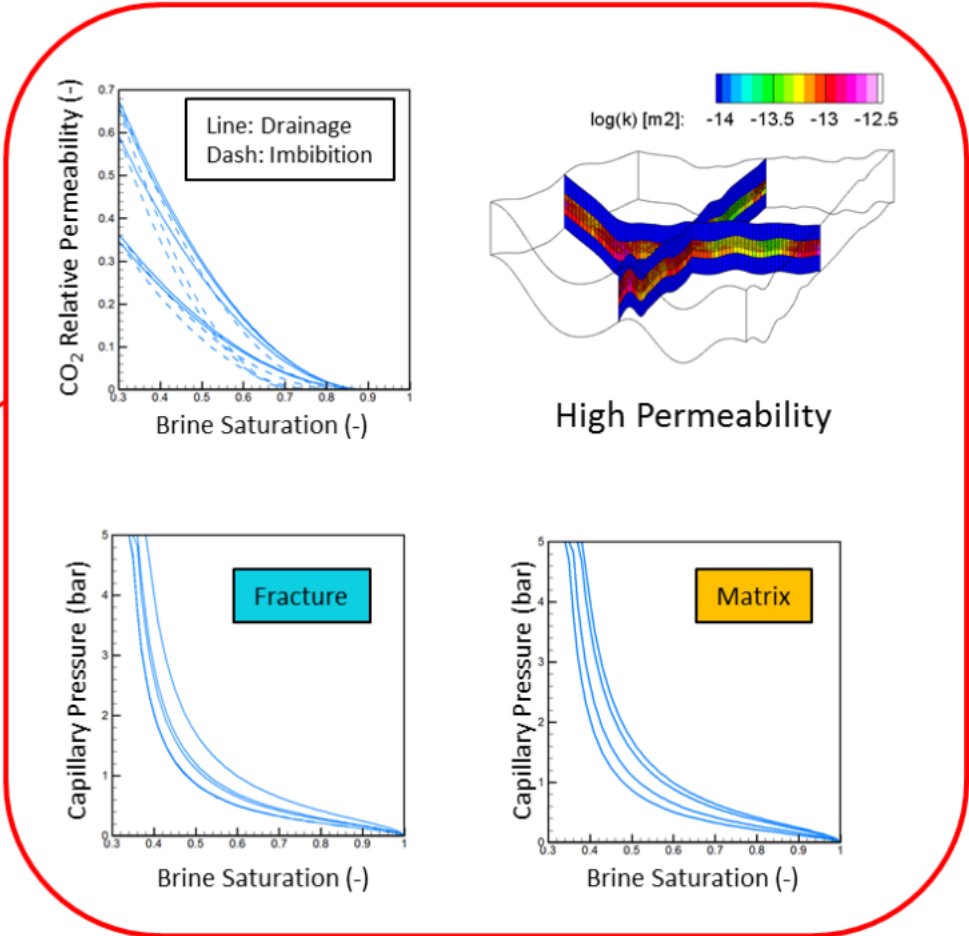
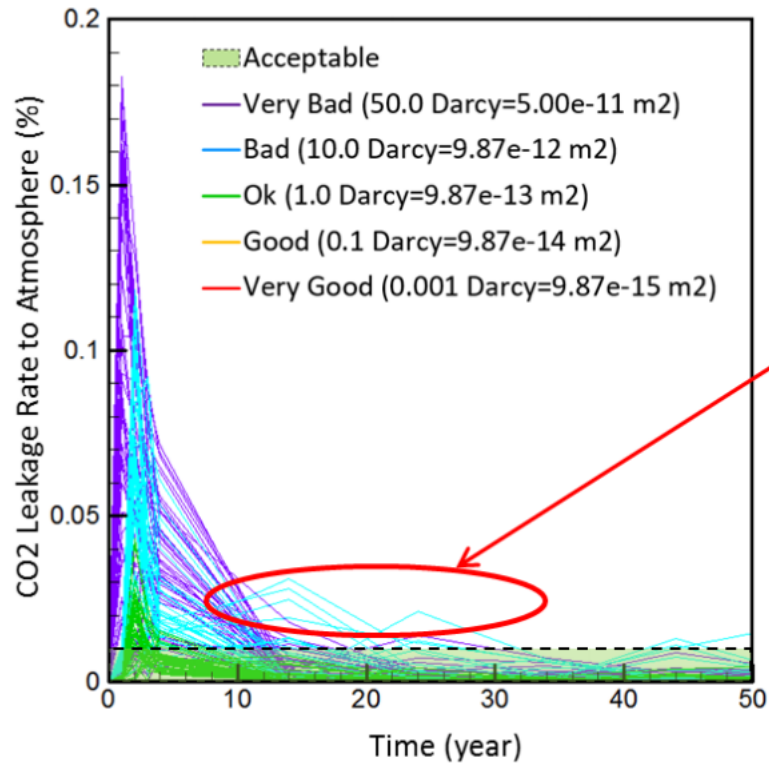
The risk assessment workflow using the reservoir simulation, RROM-Gen and NRAP-IAM

Risk Assessment – 1st paper submitted



Reservoir simulation results: total amount of CO₂ injected delineated with P10, P50 and P90 probability ranges. Different colors in right-hand figures correspond to P10, P50, and P90 in the left-hand figure.

Risk Assessment – 1st paper submitted



Reservoir simulation results including total amount of CO₂ injected and parameters for P10, P50 and P90. The dashed line shows a 0.01% leakage rate. Right-hand figures illustrate parameters of realizations that showed unacceptable leakage.

NRAP simulation results show that unless the quality of wellbore cement is extremely poor, it is unlikely that there will be CO₂ leakage to the atmosphere.

SUMMARY AND CONCLUSIONS

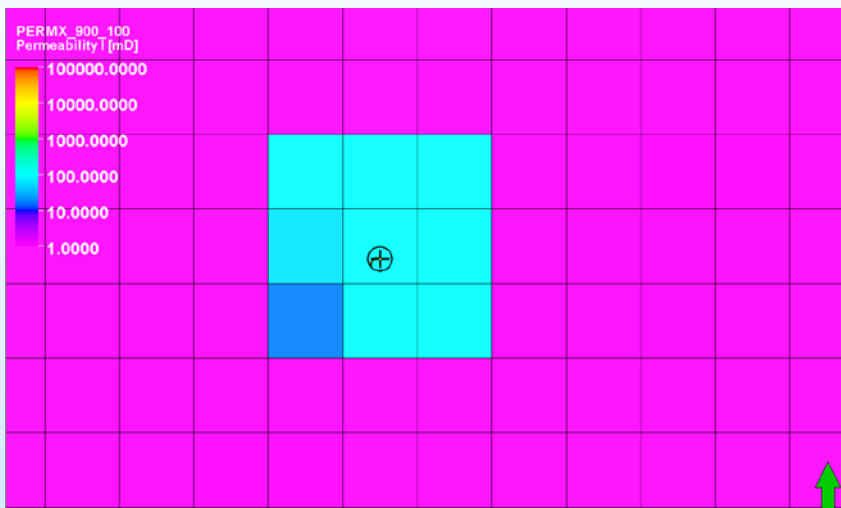
- The maximum total mass of injected CO₂ is predicted to be lower than that of previous work due to different parameter uncertainties
- The potential amount of CO₂ and brine leakage is most sensitive to values of fracture permeability, capillary pressure in both the fracture and matrix, end-point fracture CO₂ relative permeability, permeability of confining rocks, and hysteresis in the CO₂ relative permeability.
- Carbon storage in the Kevin Dome has little risk of CO₂ leakage to the atmosphere unless the quality of the legacy wells is extremely poor.

OVERVIEW

- Using seismic-driven property extrapolation to improve the injection reservoir model heterogeneity
- Incorporating a Discrete Fracture Network (DFN) model to characterize fractures in the Middle Duperow formation
- Focusing on potential leakage through hypothetical faults using NRAP-IAM

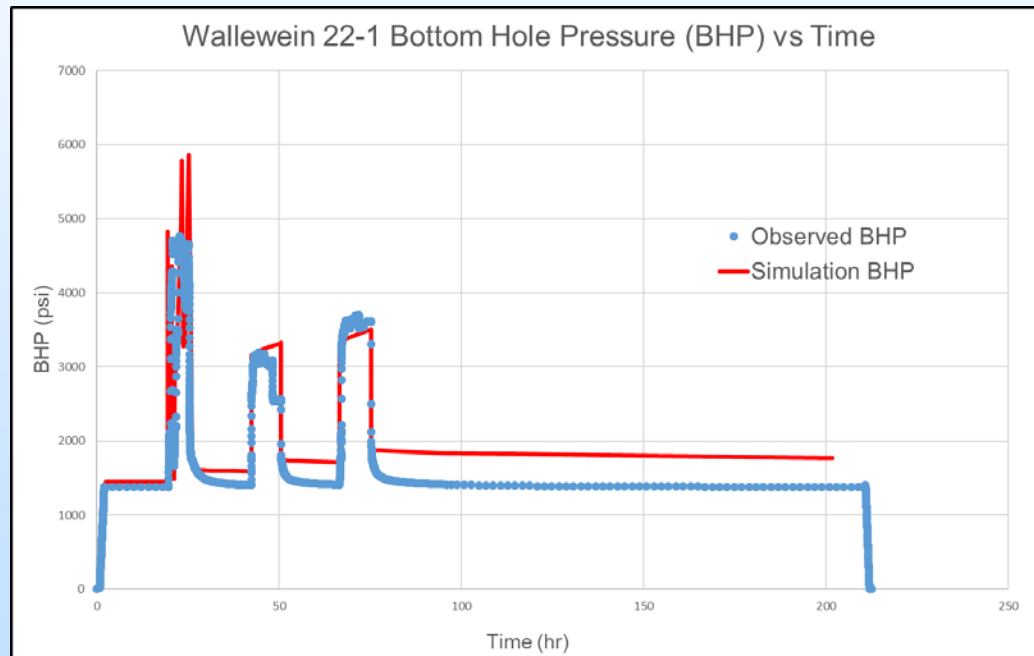
Grid Upscaling for Simulation

Cell Dimensions (ft)	Total Number of Cells	Note
200 x 200 (Original)	5,193,900	
330 x 330	1,940,449	
660 x 660	480,249	Most Optimal



Grid upscaling is done to ensure the overall number of grid cells is not computationally expensive for simulation. Permeability around Wallewein 22-1 is calibrated to the injection well test. Since the injection interval is smaller than the total thickness of Middle Duperow, vertical permeability is important in explaining the bottomhole pressure behavior during well test. It is more important to match the pressure behavior during the beginning of well test at Wallewein 22-1.

BHP Match with Well Test (Wallewein 22-1)



Radius around Wallewein 22-1	K Multiplier	Kv/Kh	Perforation Interval
3200	30	1	4040-4057
ft	Dimensionless	Dimensionless	ft

PRELIMINARY RESULTS

- Well test results suggest that the radius of investigation is relatively small due to short duration and vertical permeability is important in explaining pressure response at the wellbore.
- DFN modeling shows fracture aperture and the fracture intensity have a significant impact on the calculated fracture permeability while fracture length has a relatively minor impact.
- CO₂ injection simulation results indicate it is unlikely that Big Sky could meet its target of 1 million tons of CO₂ stored in the Middle Duperow formation, with a lower estimated probability of success compared to previous estimates based on regional parameters.

US-EPA Class IV Requirements

Project Re-Scope: Underground Source of Drinking Water (USDW) Definition

- (40 CFR) Section 144.3 is an aquifer or part of an aquifer which:
 - a. supplies any public water system, or contains a sufficient quantity of ground water to supply a public water system and currently supplies drinking water for human consumption or contains fewer than **10,000 milligrams/liter of Total Dissolved Solids (TDS)**; and
 - b. is not an exempted aquifer.
- An "exempted aquifer" is part or all of an aquifer which meets the definition of a USDW but which has been exempted according to criteria in 40 CFR Section 146.4:
 1. It is mineral, hydrocarbon or geothermal energy producing, or can be demonstrated by a permit applicant as part of a permit application for a Class II or III operation to contain minerals or hydrocarbons that considering their quantity and location are expected to be commercially producible;
 2. It is situated at a depth or location which makes recovery of water for drinking water purposes economically or technologically impractical;
 3. It is so contaminated that it would be economically or technologically impractical to render that water fit for human consumption;
 4. It is located over a Class III well mining area subject to subsidence or catastrophic collapse;
 5. The total dissolved solids content of the ground water is more than 3,000 and less than 10,000 milligrams/liter and it is not reasonably expected to supply a public water system.

Not allowed under Class IV, but allowed under Class II

US-EPA Class IV Requirements

USDW under Class II, but not Class VI

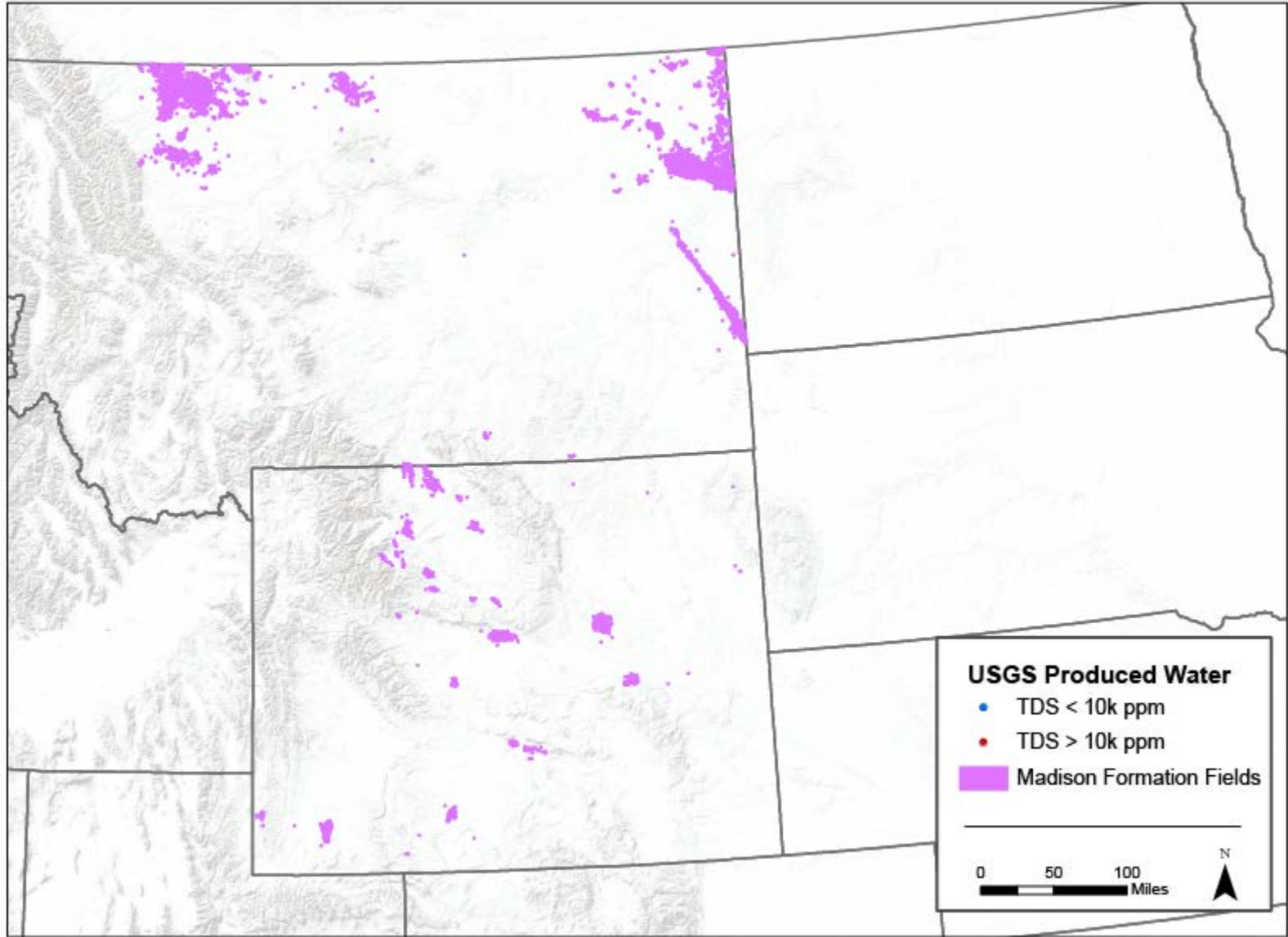
If the target reservoir (the Duperow) had high enough salinity, the lower most USDW by UIC Class VI regulations would be the Madison (~5000 ppm TDS).

The Madison is oil producing and so is NOT a USDW under Class II because of exemptions

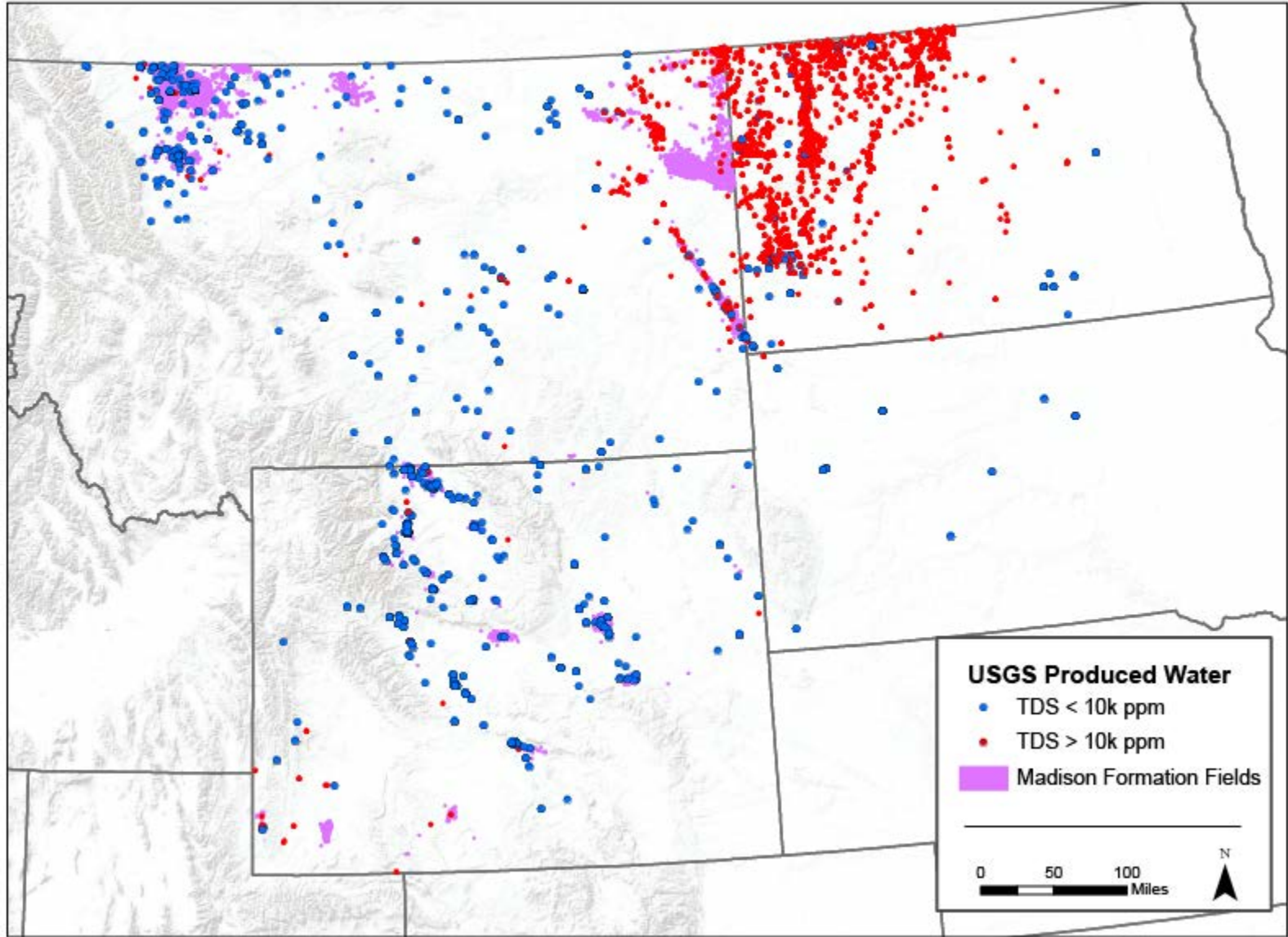
Yet to store in the Duperow beneath the Madison, the CO₂ storage project would have to treat the Madison as a USDW. This would mean:

- Setting surface casing through the Madison (which is karsted). The larger diameter borehole would likely have less integrity.
- Wastewater disposal is permitted in the Madison, yet a storage project in the Duperow would have to protect it against any reduction in water quality
- CO₂ EOR *could* be permitted in the Madison, yet a storage project in the Duperow would have to protect the Madison from CO₂ intrusion while others intentionally inject

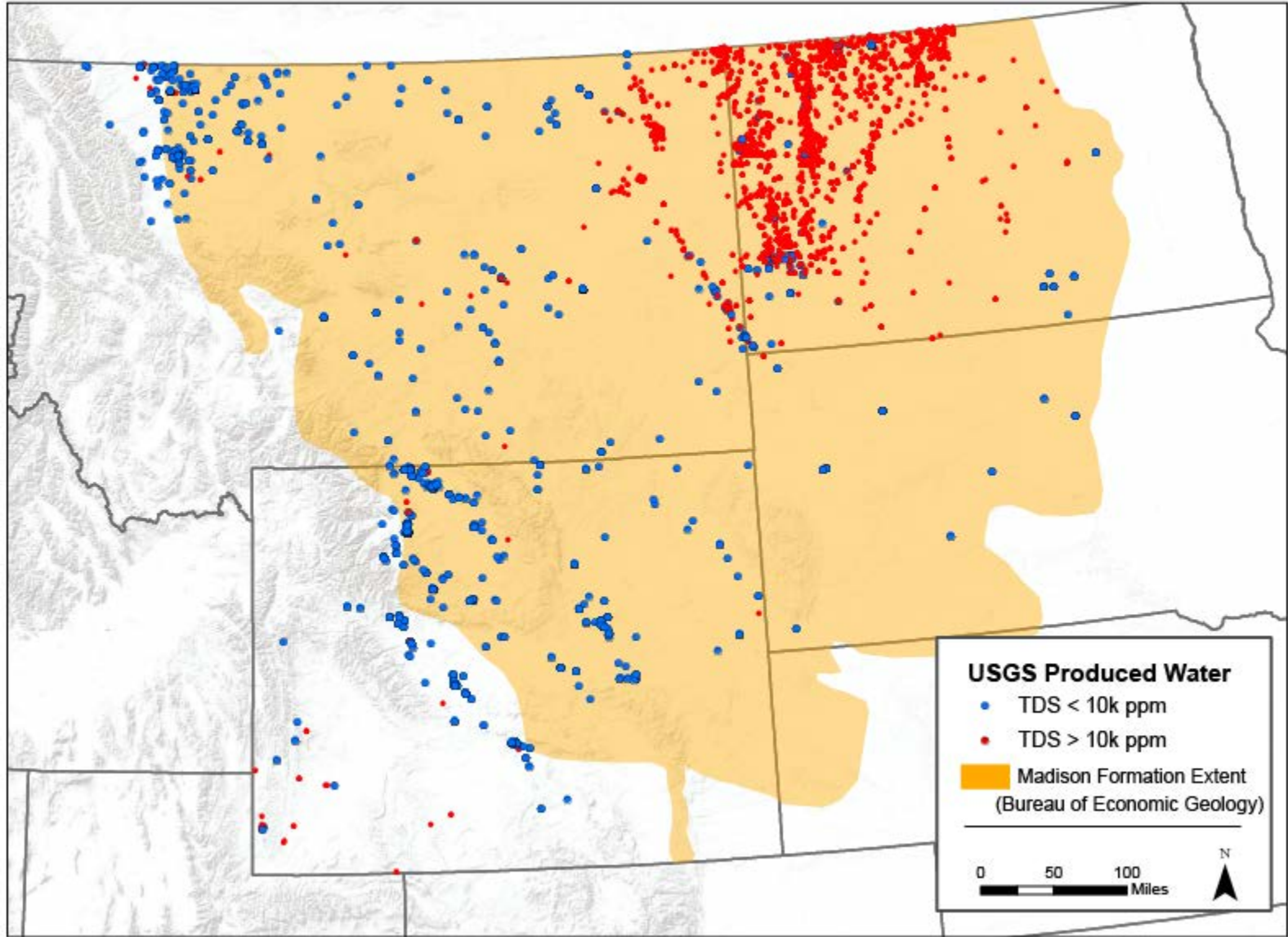
Produced Water and Madison Formation Oil & Gas Fields in and around the BSCSP Region



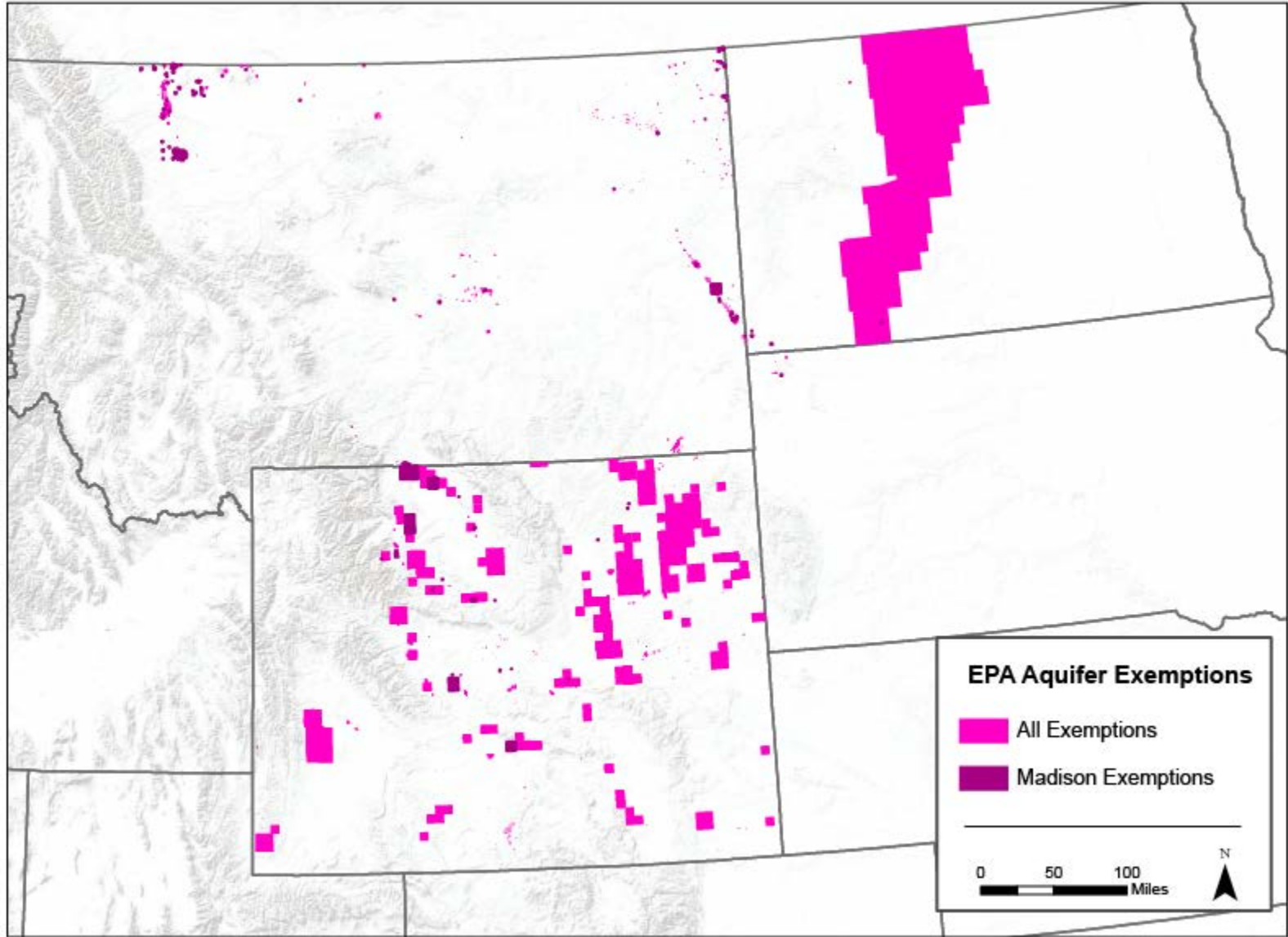
Produced Water and Madison Formation Oil & Gas Fields in and around the BSCSP Region



Produced Water and Madison Formation Continuity in and around the BSCSP Region

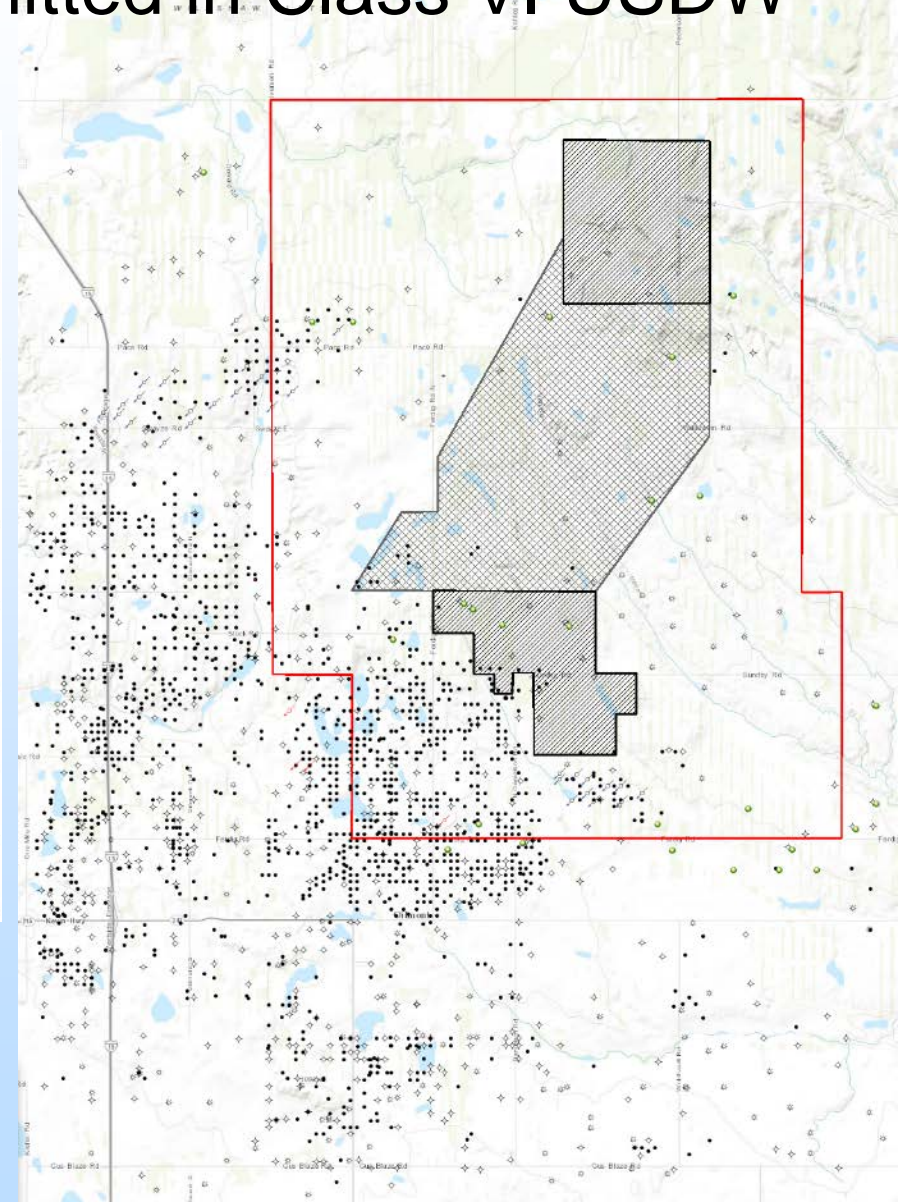
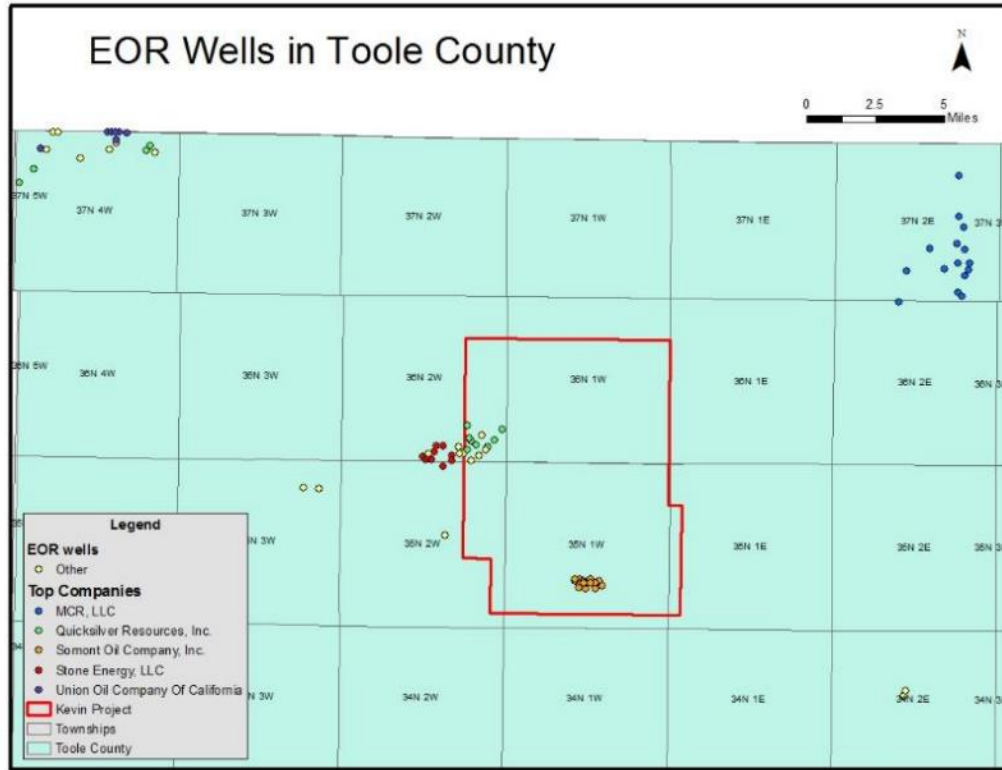


Aquifer Exemptions under EPA Safe Drinking Water Act UIC regulations



US-EPA Class IV Requirements

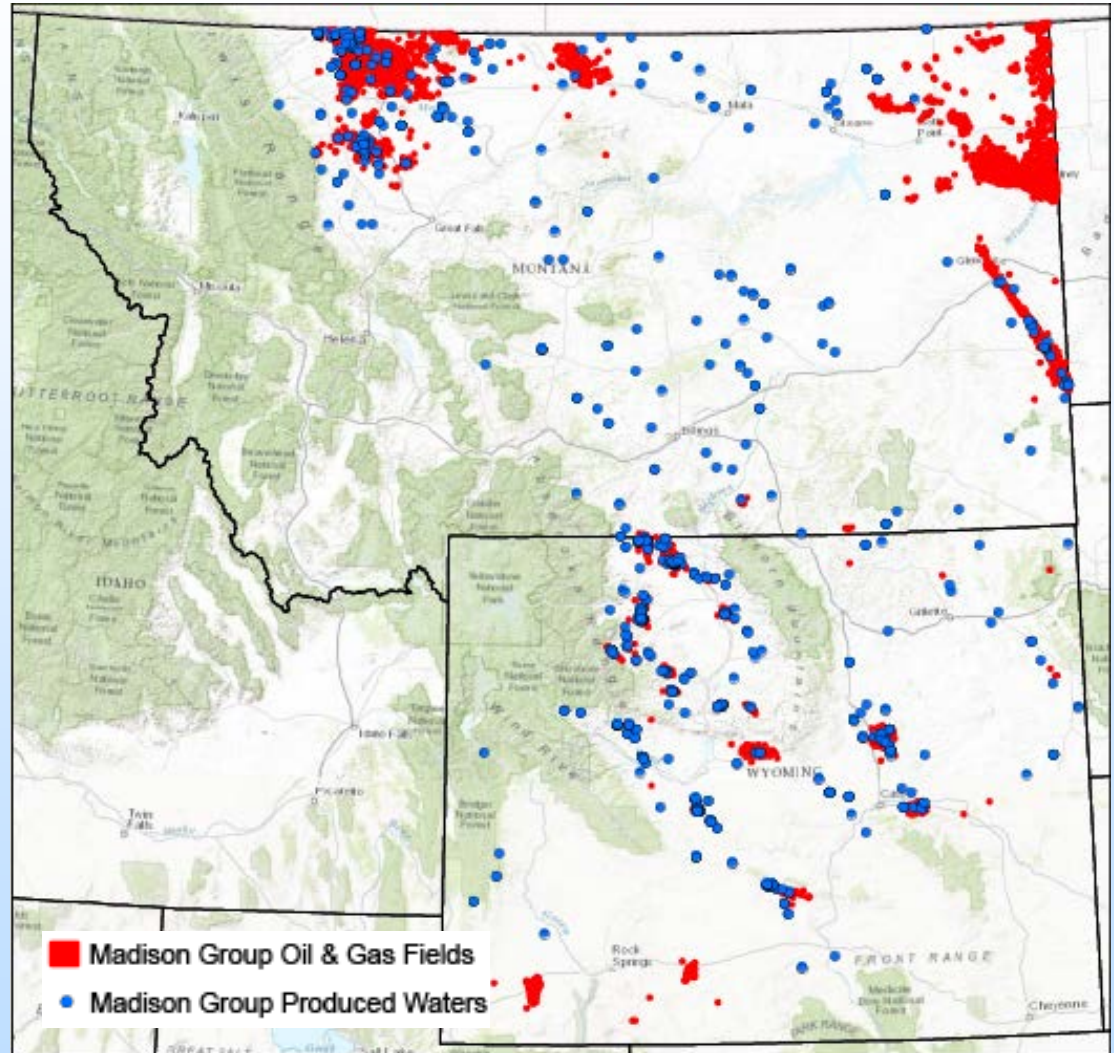
CO₂ EOR in Could be Permitted in Class VI USDW



US-EPA Class IV Requirements

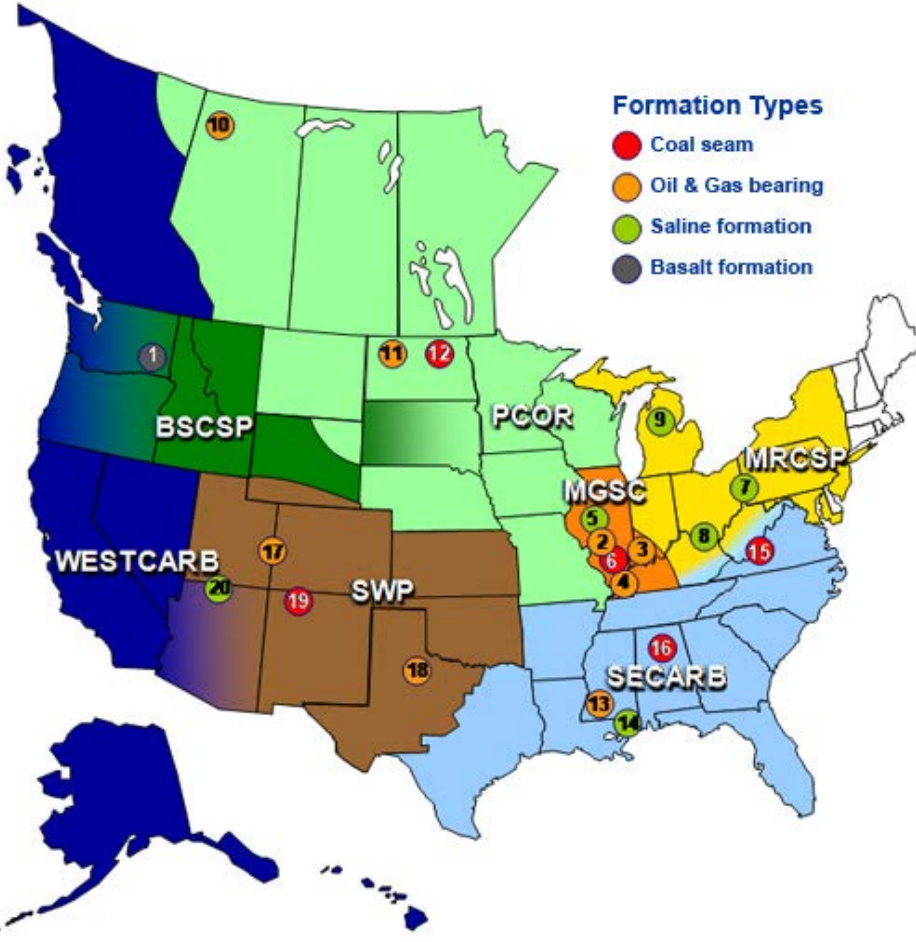
Regional Significance:

Oil fields producing from the Madison (red) and produced water sampled from Madison Group formations less than 10,000 mg/L TDS (blue)



US-EPA Class VI Impact on Research Projects

Class VI Scale and Cost:



DOE Regional Carbon Sequestration Partnership Phase II Program:

- Performed 20 injections
- 100s – 100,000 tonnes
- Wide variety of geologies
- Operated under Class V, Class II
- No extended PISC
- No Financial assurance
- Careful site characterization
- Operational monitoring

How many could have been conducted under Class VI?

Data strongly suggests Class VI requirements are overly stringent for smaller injections.

Restricts valuable research and may incentivize undesirable behavior commercially



Questions?

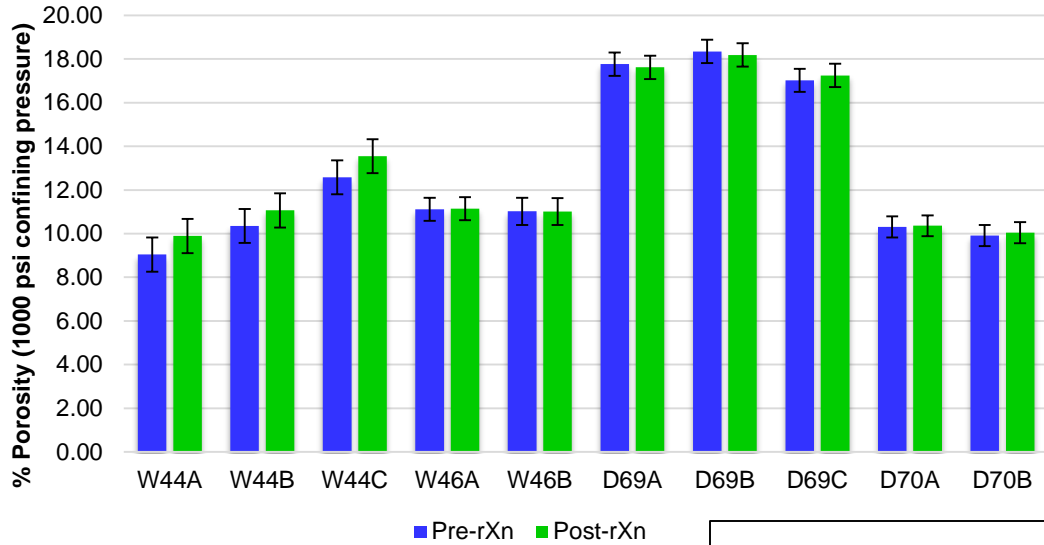


Core Flood Experiments

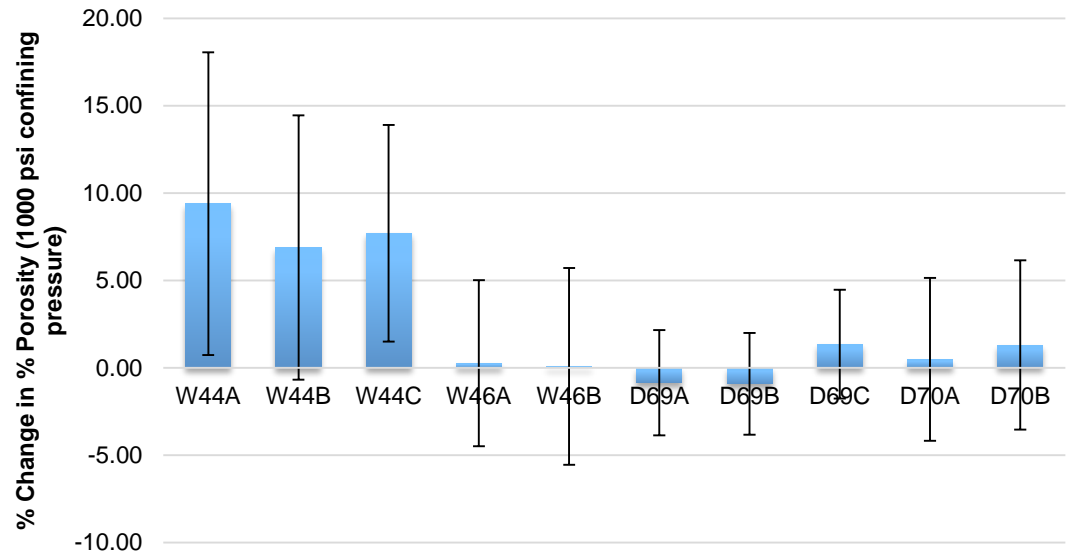
	Sample ID	Avg. pressure (psi)	Temperature (°C)	Brine/DI	Duration of N ₂ exposure (days)	Duration of CO ₂ exposure (days)
Set 1	D69A	1400	60	Brine	5	28
	D69B	1400	60	Brine	5	28
	D69C	1400	60	Brine	33	0
	W44A	1400	60	Brine	5	28
	W44B	1400	60	Brine	5	28
	W44C	1400	60	Brine	33	0
	W46A	1400	60	Brine	5	28
	W46B	1400	60	Brine	5	28
	W46C	1400	60	Brine	33	0
Set 2	D70A	1400	60	DI	5	28
	D70B	1400	60	DI	5	28
	D70C	1400	60	DI	5+28 (not consecutive)	0
	D68A	1400	60	Brine	5	0

Core Flood Experiments

Segments A, B, and C Porosity

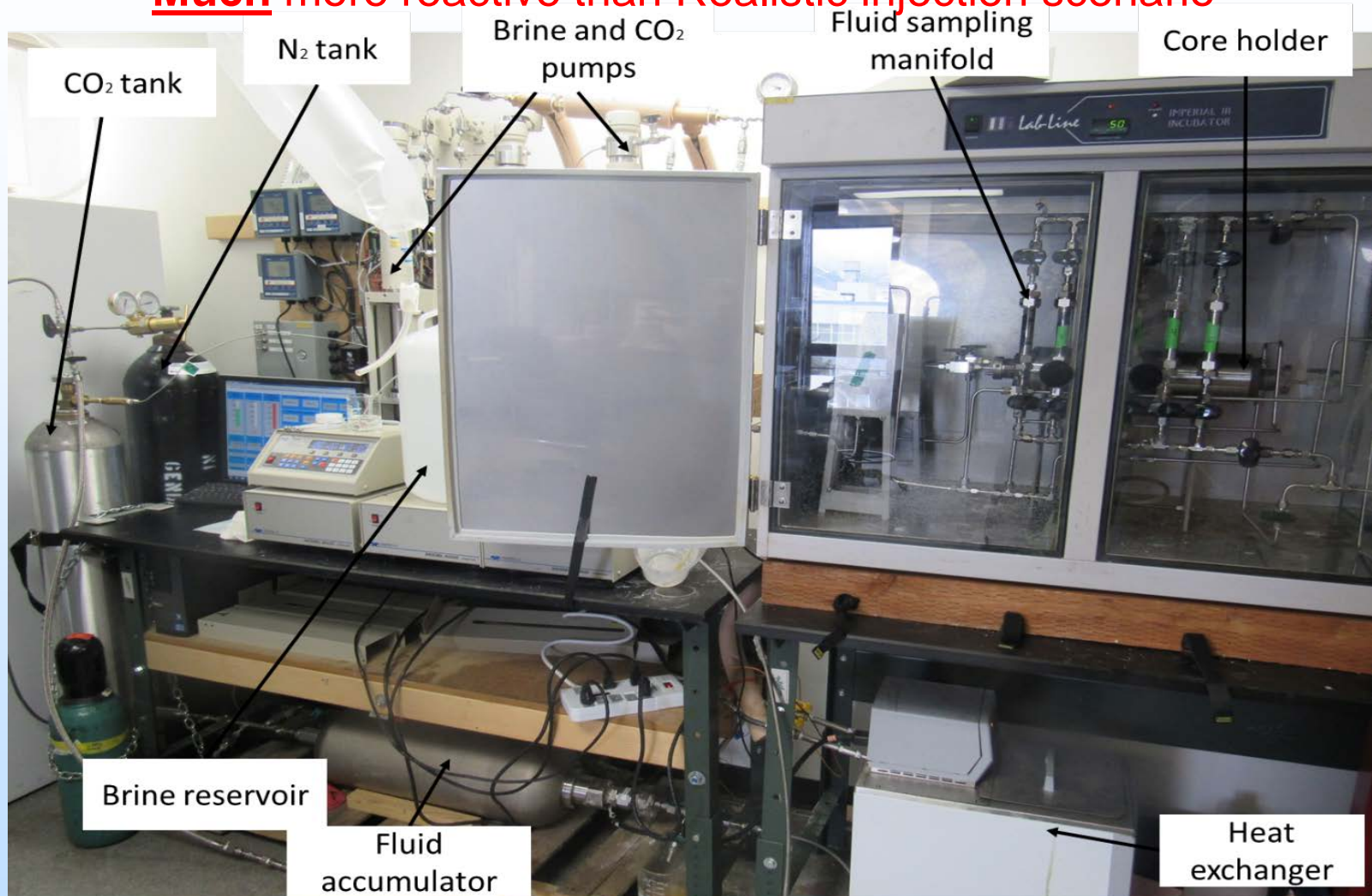


Segments A, B, and C Porosity Change



Methods: CO₂ Core Flow Experiment

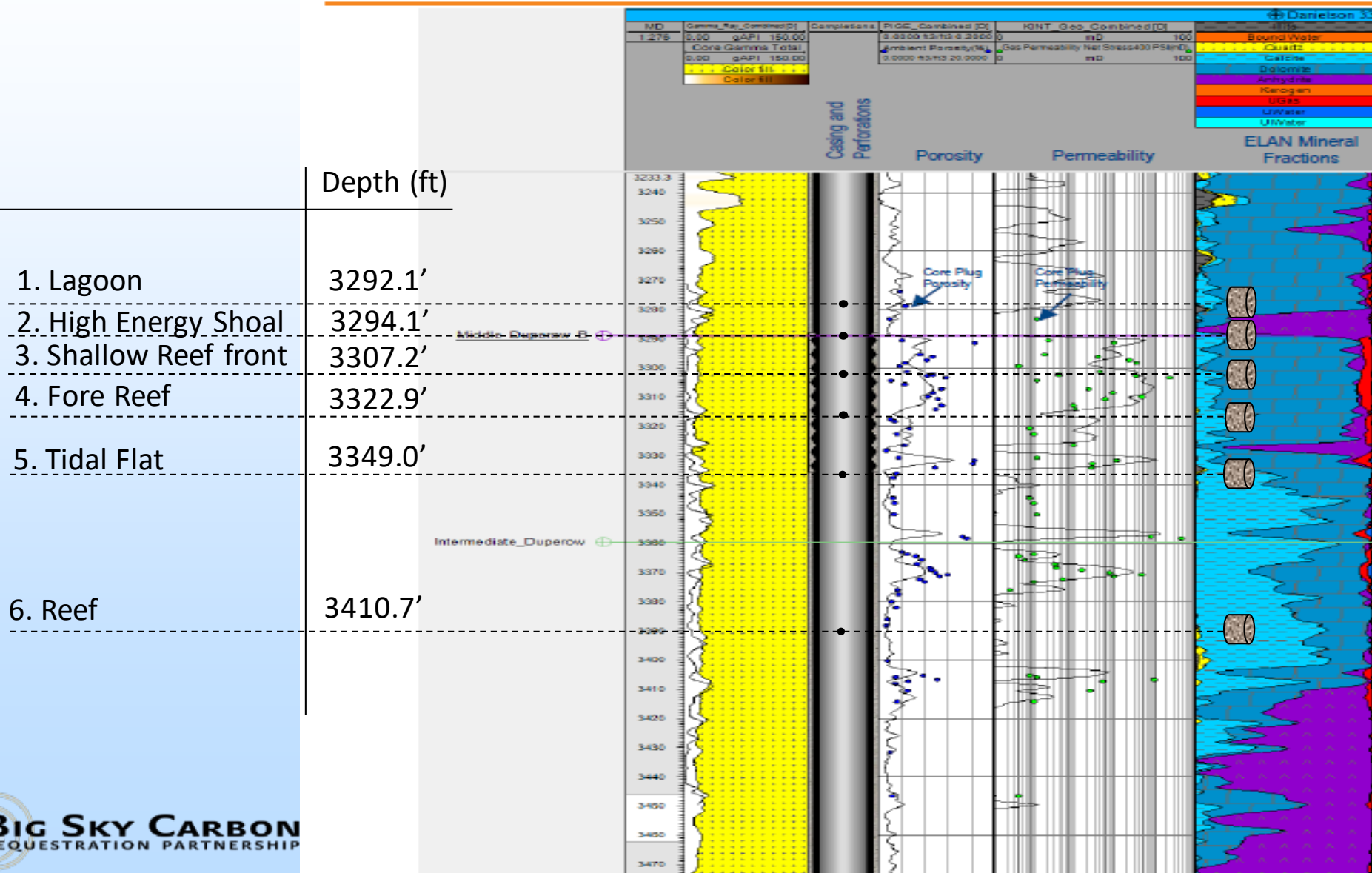
Much more reactive than Realistic injection scenario



- Injection pressure: ~ 1,300 psi
- Temperature: 50°C (122°F)
- Test period: 3 days of pure brine flow + **14 days of brine/scCO₂ flow**

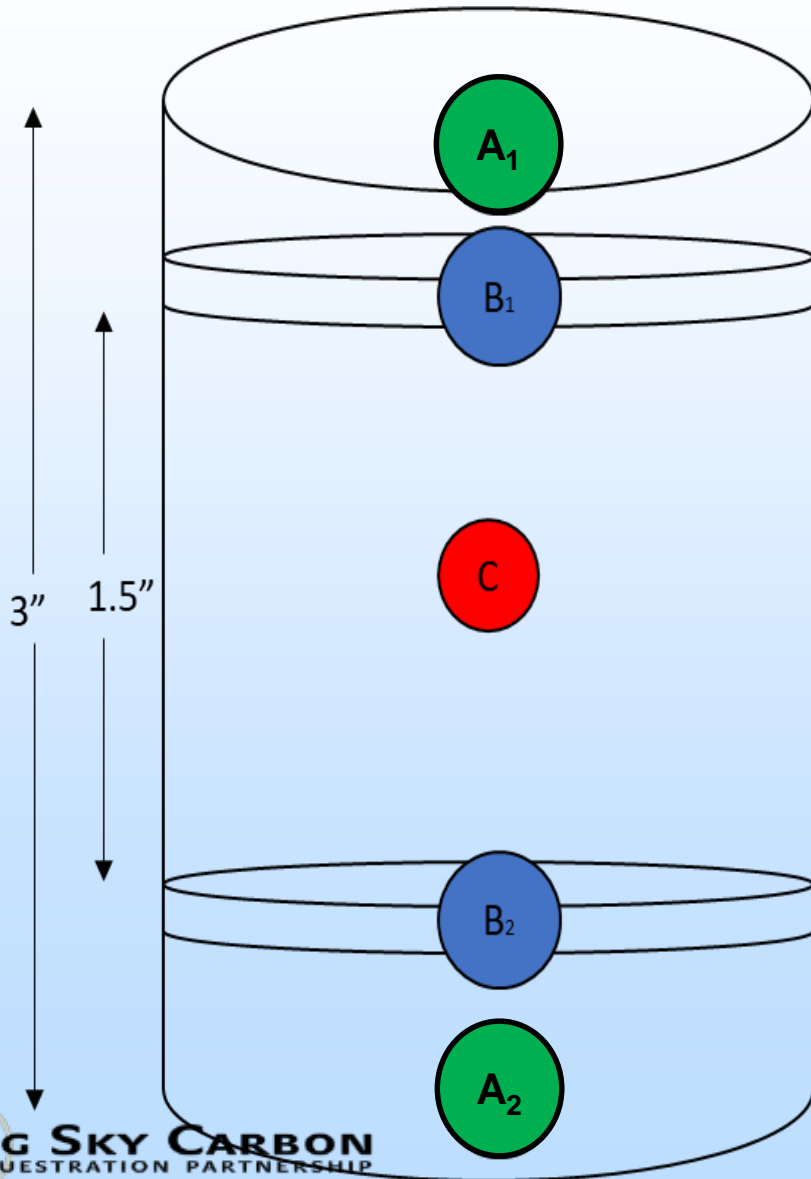
Core Flow: Sampling

Danielson Core Interval (3271-3451 ft MD)



Core Flow Methods: Sub-Sampling



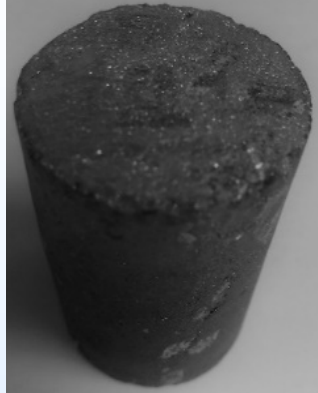
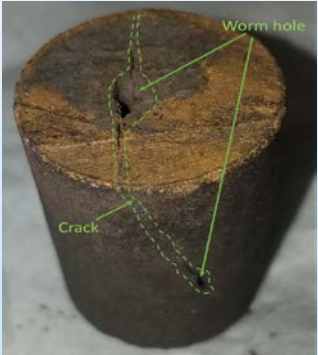

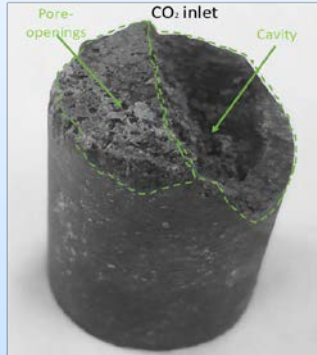
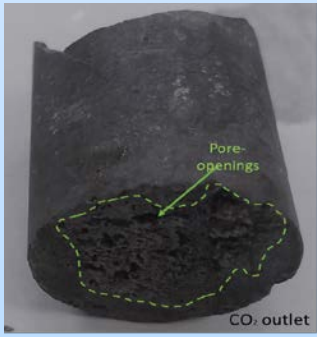

Characterization
Method



- XRD
- XRF
- N₂ adsorption
- SEM-BSE-EDX
- Raman
- Thin section
- Gas ϕ and k
- Micro-CT scan
- NMR (Water ϕ and k)
- Strength
- SEM-BSE-EDX
- Raman
- Thin section
- XRD
- XRF
- N₂ adsorption

Flow Through
CO₂ Challenge

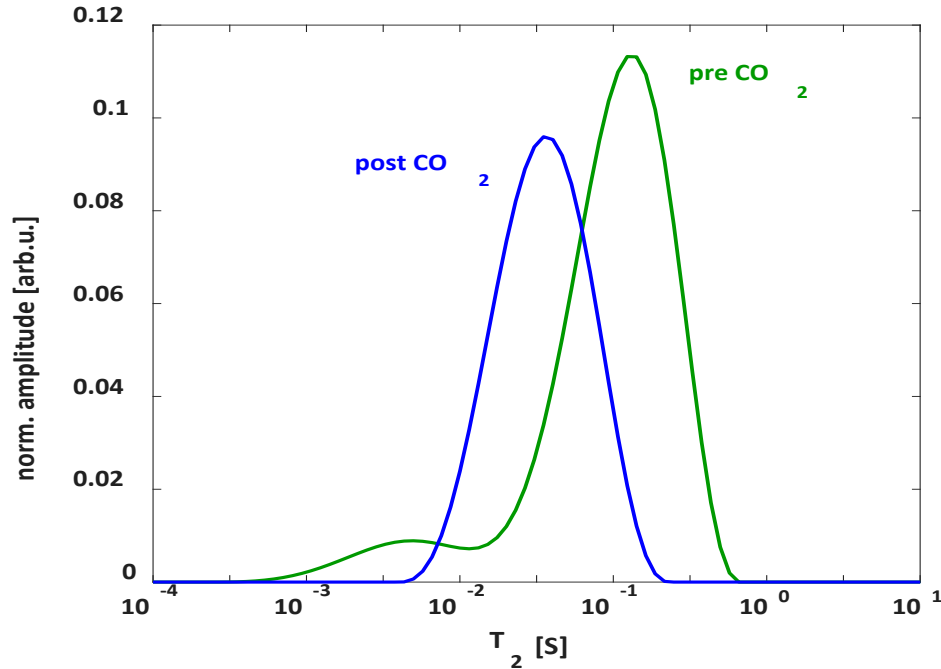
Experimental Results

	High Energy Shoal	Reef	Lagoon	
Before CO ₂ Challenge				<p><i>High Energy Shoal:</i></p> <p>Massive crack and see-through wormhole are visible on the sample, indicating that the presence of scCO₂ initiates chemical reactions leading to mineral dissolution</p>
After CO ₂ Challenge	 	 		<p><i>Reef:</i></p> <p>Severe erosion of the sample and pore opening provide physical evidence of significant changes in pore structure and connectivity</p> <p><i>Lagoon:</i></p> <p>Physical structure remains the same, just some discolorations</p>

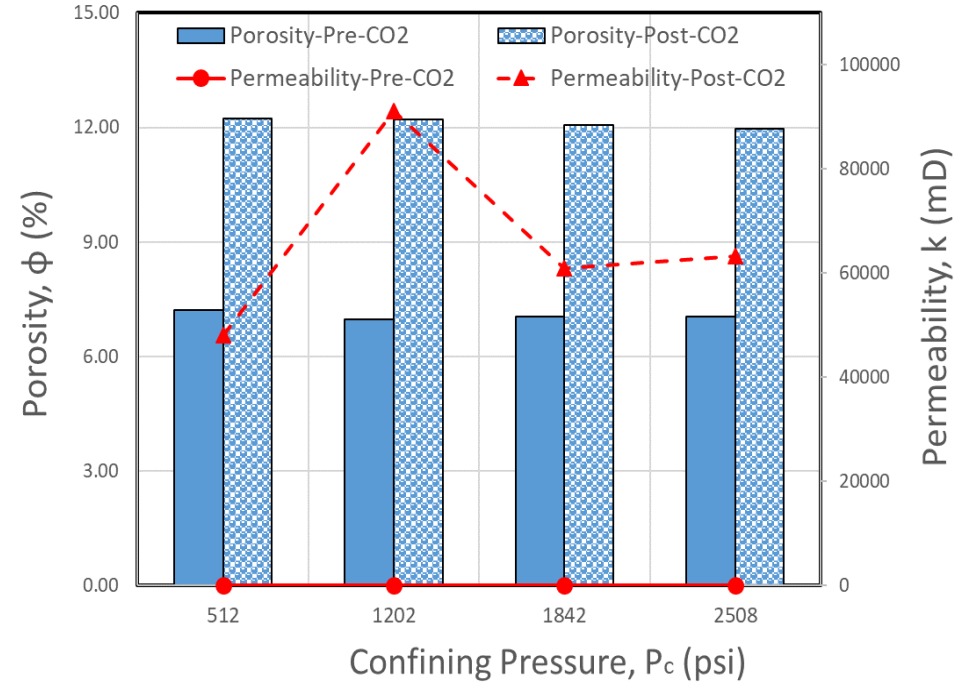
Much more reactive than Realistic injection scenario

NMR: High Energy Shoal

NMR: Fully-saturated core



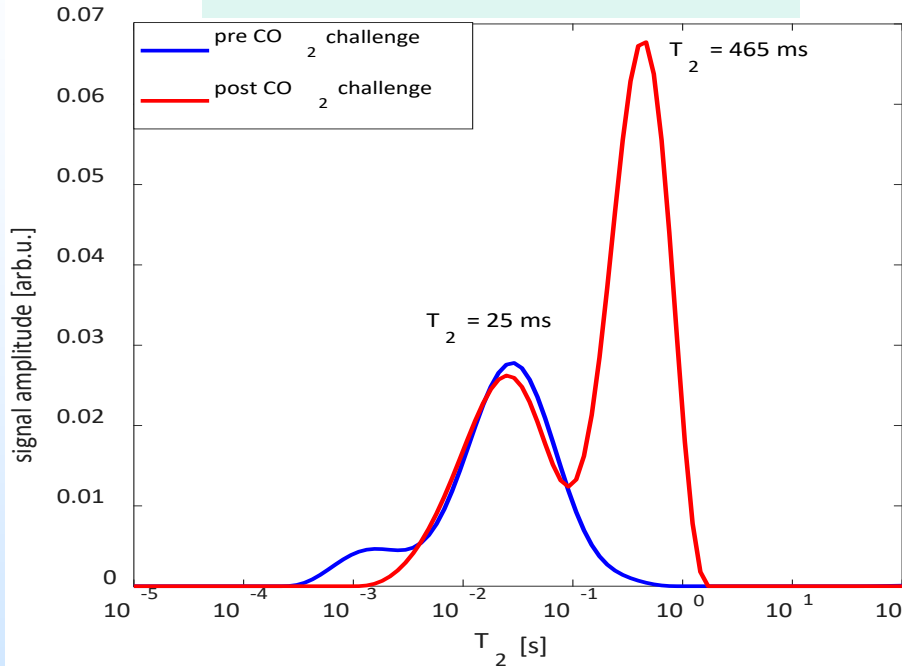
Gas Porosity/Permeability: Dried core



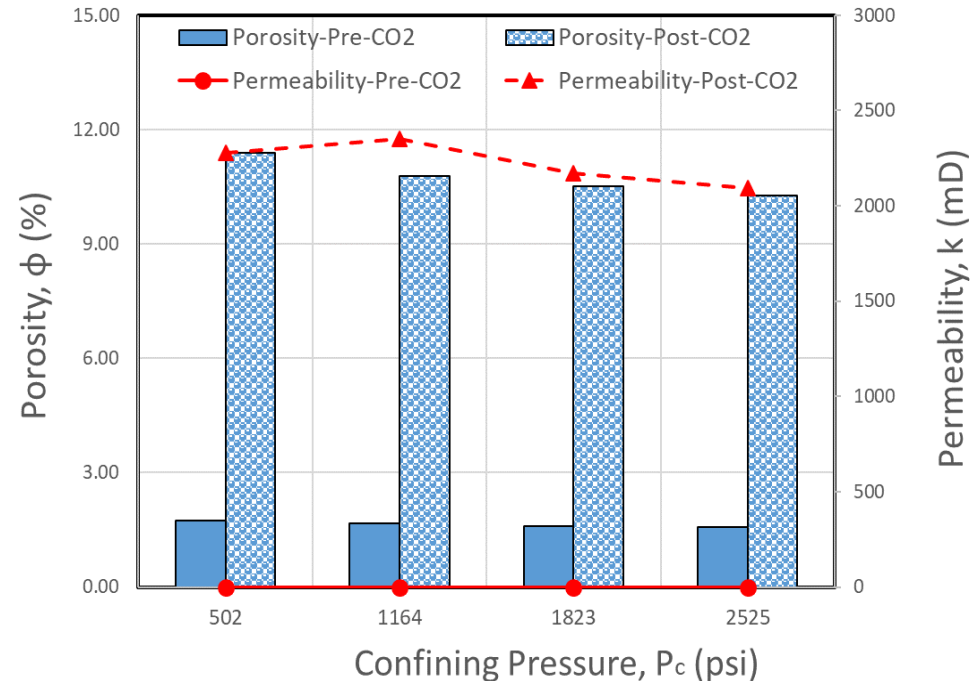
- A shift towards shorter T_2 times indicating either a decrease in the pore size distribution or a change in the mineral composition on the surface of the pores.
- Decrease in pore size distribution is unlikely after a CO₂ challenge unless new mineral is precipitated or CO₂ is trapped in the pores, causing less water to enter the core resulting in an apparent smaller pore size distribution.
- A change in the mineral composition of the surface will affect the surface relaxivity, ρ , and could potentially cause the shift to shorter T_2 times.
- Gas ϕ/k : Significant increase is due to mineral dissolution

NMR: Reef

NMR: Fully-saturated core



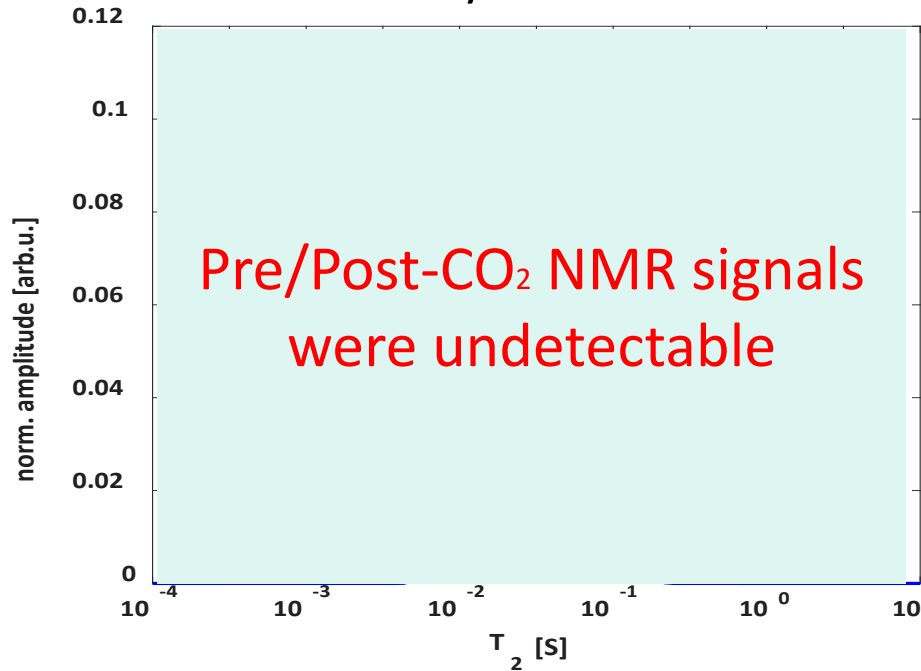
Gas Porosity/Permeability: Dried core



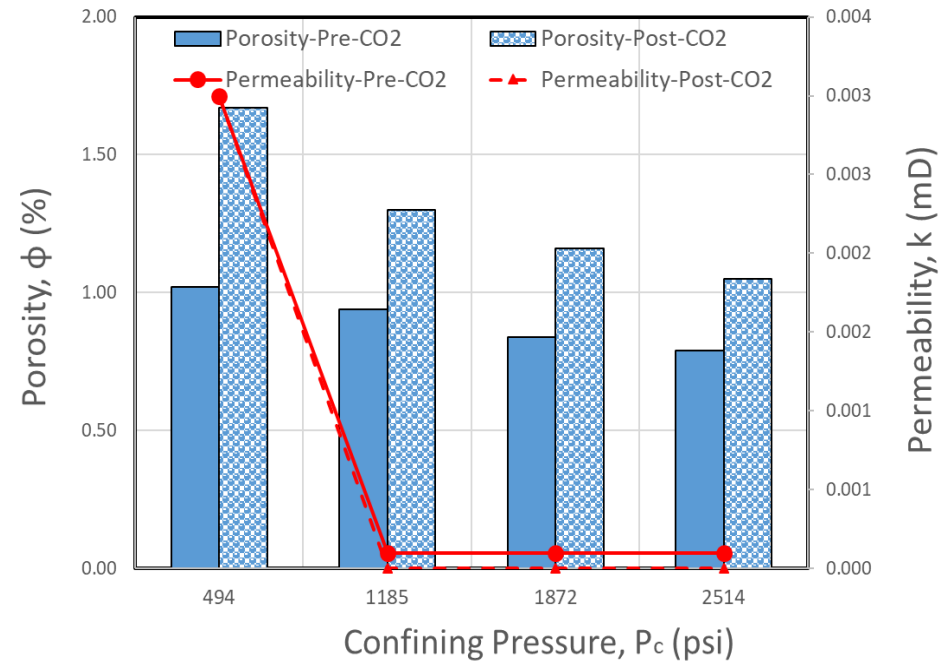
- Shorter T_2 population disappears after CO₂ challenge.
- No significant shift is observed for the longer T_2 population.
- New T_2 population appears after CO₂ challenge, indicates that the CO₂ challenge has potentially created larger void spaces within the core.
- Gas ϕ/k : Significant increase is due to mineral dissolution

NMR: Lagoon

NMR: Fully-saturated core



Gas Porosity/Permeability: Dried core



- NMR signal is undetectable before and after CO₂ experiment because the pores were inaccessible
- No significant change in porosity and permeability

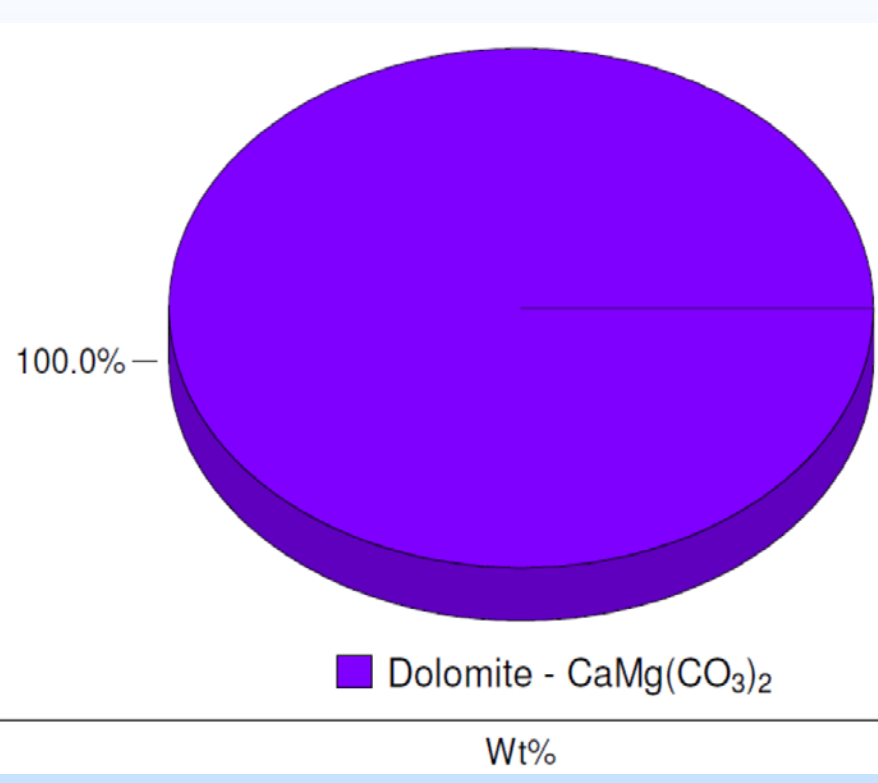
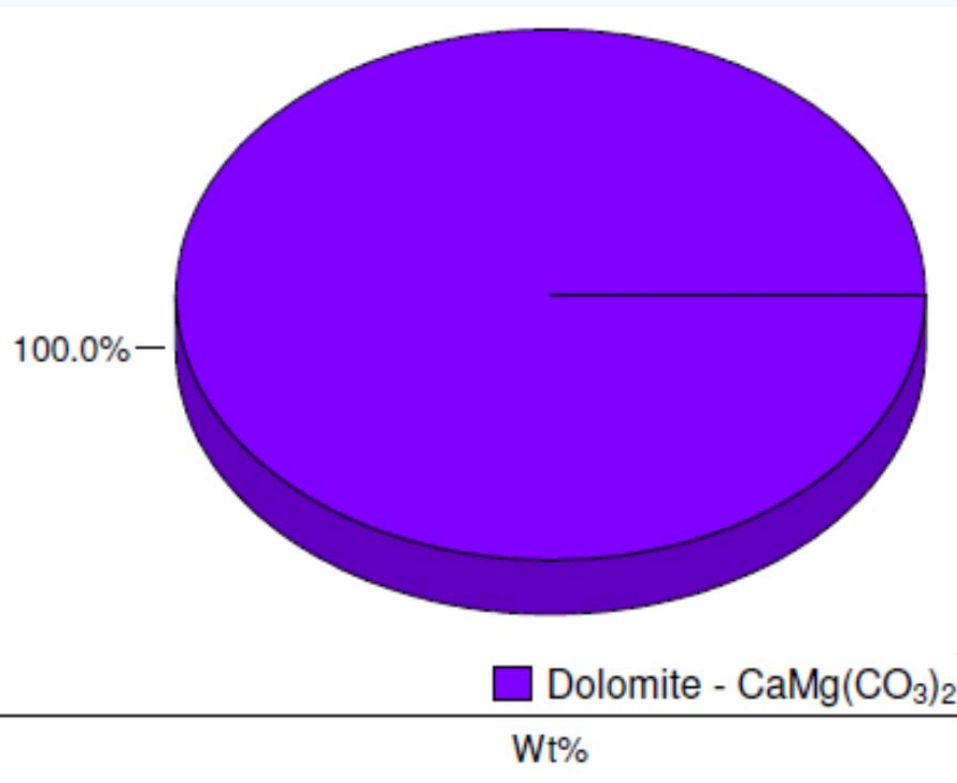
Sample ID	NMR Porosities (%)								Remark
	Pre-CO ₂ Challenge				Post-CO ₂ Challenge				
	Fully saturated	1 st centrifuge (3,000 g)	2 nd centrifuge (6,000 g)	3 rd centrifuge (10,000 g)	Fully saturated	1 st centrifuge (3,000 g)	2 nd centrifuge (6,000 g)	3 rd centrifuge (10,000 g)	
High Energy Shoal (HES 1)	10.6	--	6.2	5.4	7.6	--	--	5.4	
Shallow Reef Front (SR 1)	8.8	4.4	--	3.8	--	--	--	--	Core was destroyed during CO ₂ experiment
Shallow Reef Front (SR 2)	5.3	3.8	--	2.9	**	**	--	--	Replacement core for SR 1
Fore Reef (FR 1)	4.2	3.6	--	3.0	***	***	--	--	
Reef (R 1)	2.5	2.0	--	--	9.0	7.6	--	--	
Tidal Flat (T 1)	1.6	1.4	--	--	*	*	--	--	
Lagoon (EL 2)	No NMR Signal				No NMR Signal				

--	No NMR data	*	NMR experiment is ongoing
**	CO ₂ experiment is ongoing	***	Planned CO ₂ experiment

XRD Mineralogy: High Energy Shoal

Pre-CO₂

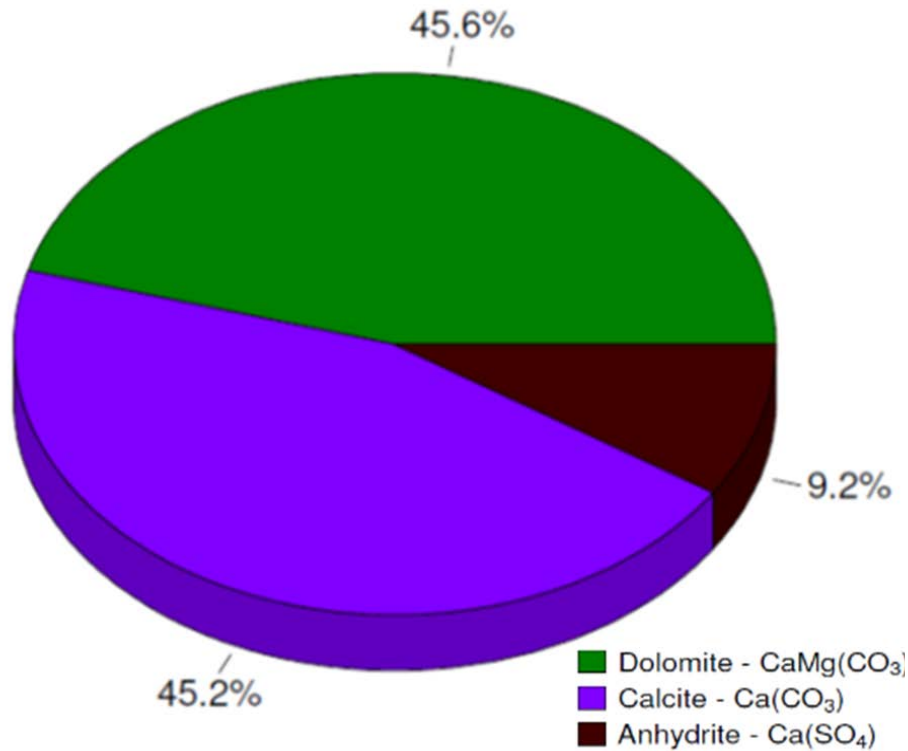
Post-CO₂



- No significant change in mineralogy

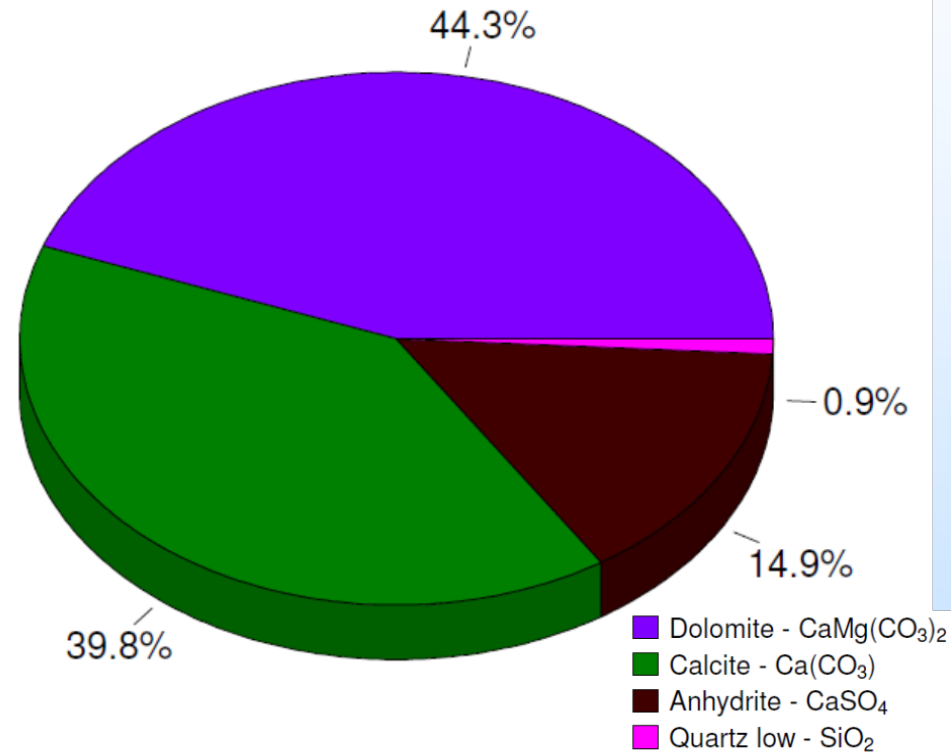
XRD Mineralogy: Reef

Pre-CO₂



Wt%

Post-CO₂



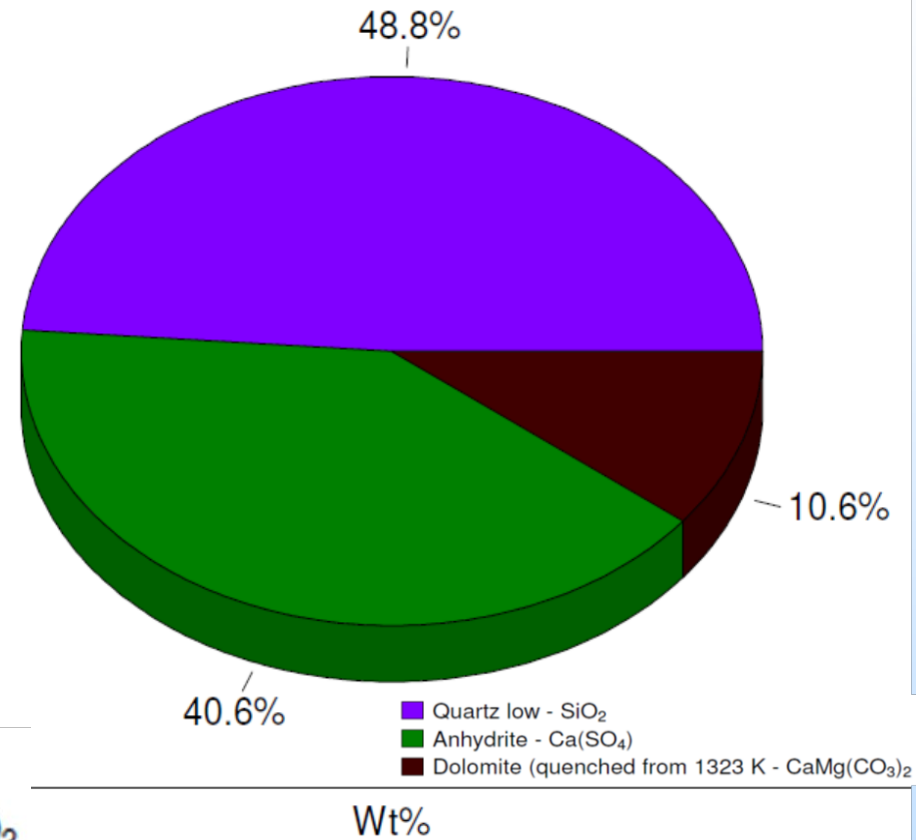
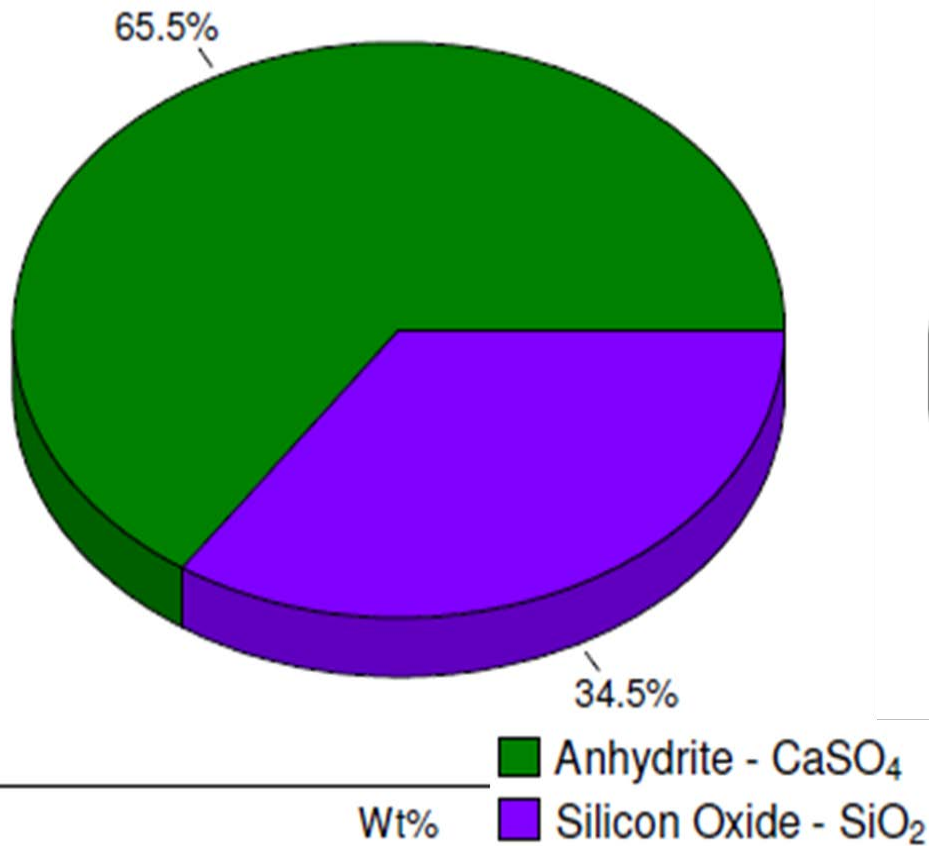
Wt%

- No significant change in mineralogy

XRD Mineralogy: Lagoon

Pre-CO₂

Post-CO₂



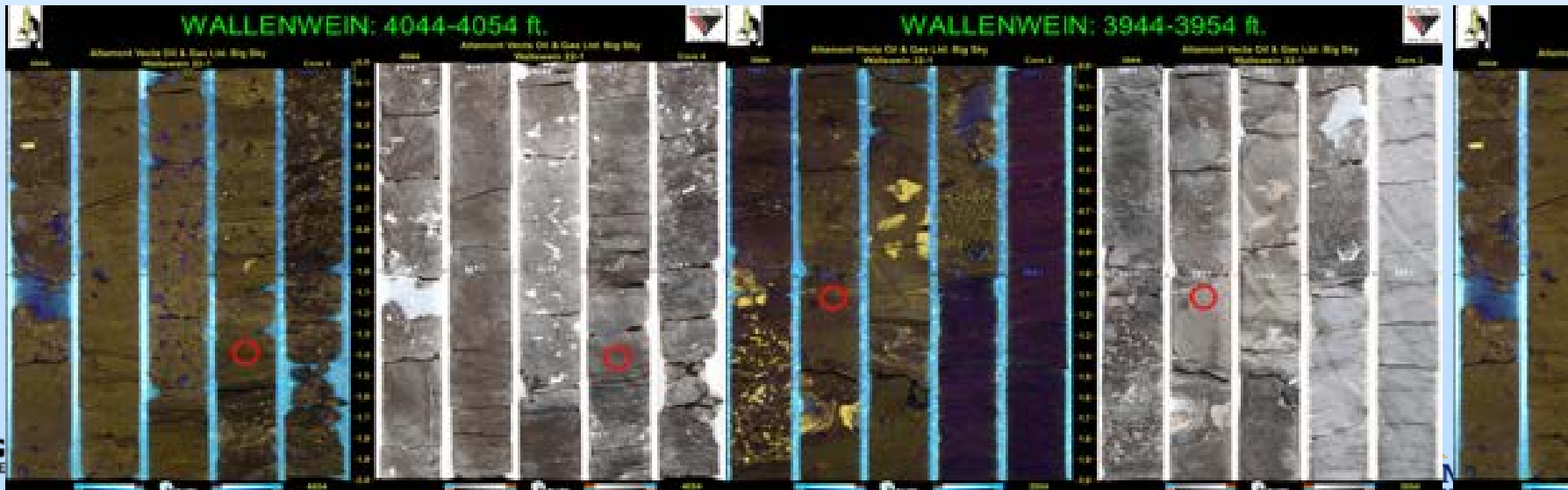
- Dolomite in the post-CO₂ core is likely present before the test as the well log shows

Summary

- High energy shoal, reef, and lagoon rock samples respond differently to supercritical CO₂.
- Rapid dissolution occurs predominantly in the reef and high energy shoal rock cores primarily because carbonates are susceptible to dissolution in the presence of CO₂.
- In addition to mineralogy, severity of the dissolution process is largely influenced by the transport properties of the rock.
- Lagoon rock sample is the most resistant to CO₂ invasion mainly because its pores are inaccessible, thus ensuring its integrity as a caprock.

Presentation Outline

Facies 1, 2, 3



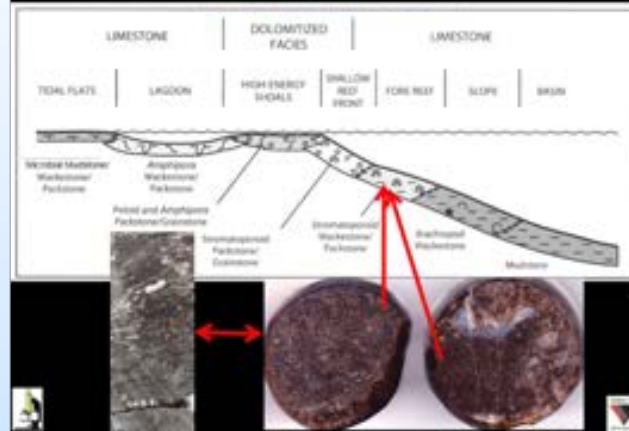
Facies 4, 5, 6



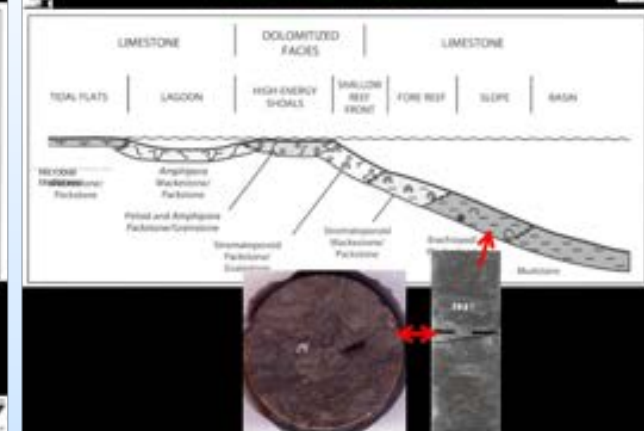
WALLEINWEIN: 4053.9 ft.



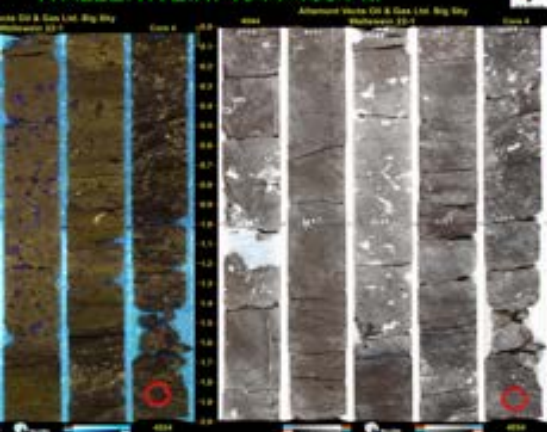
WALLEINWEIN: 4052.8 ft.



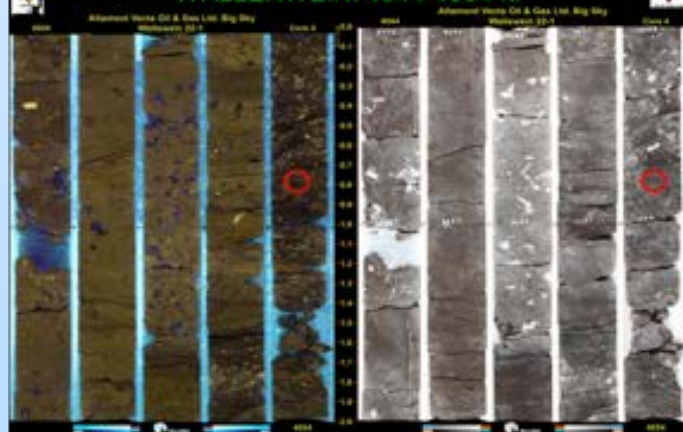
WALLEINWEIN: 3939.3 ft.



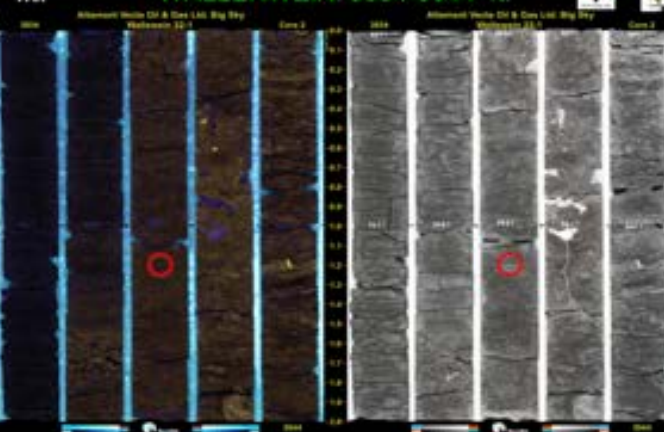
WALLEINWEIN: 4044-4054 ft.



WALLEINWEIN: 4044-4054 ft.

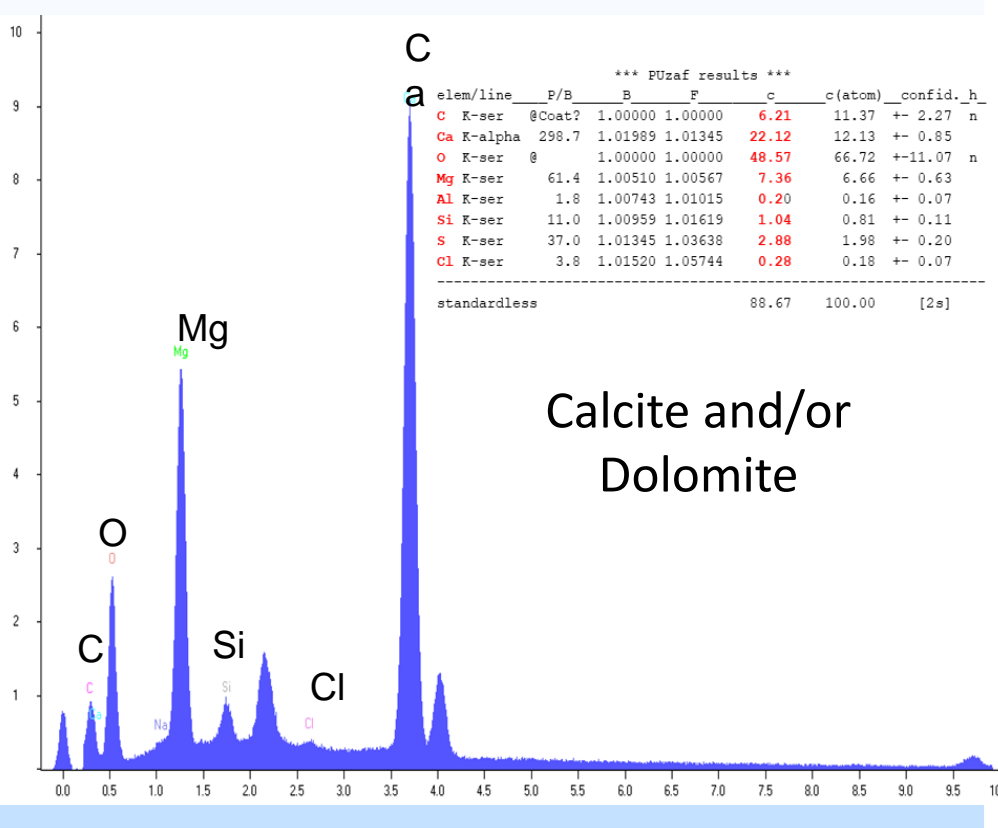


WALLEINWEIN: 3934-3944 ft.



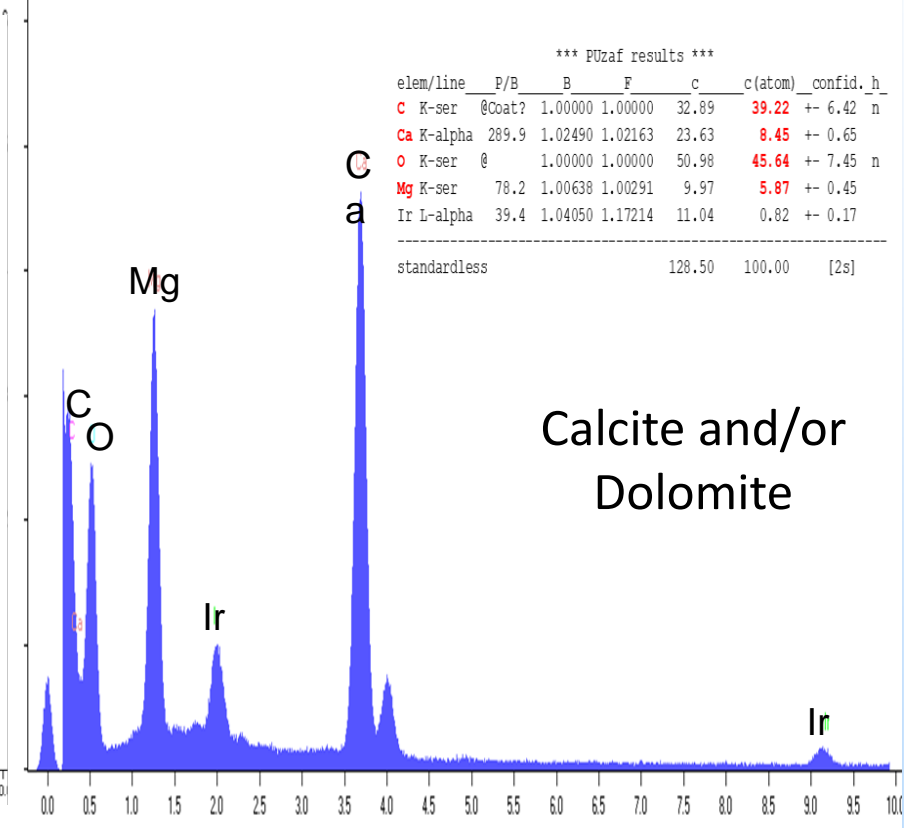
EDX Elemental Composition : High Energy Shoal

Pre-CO₂



Calcite and/or Dolomite

Post-CO₂

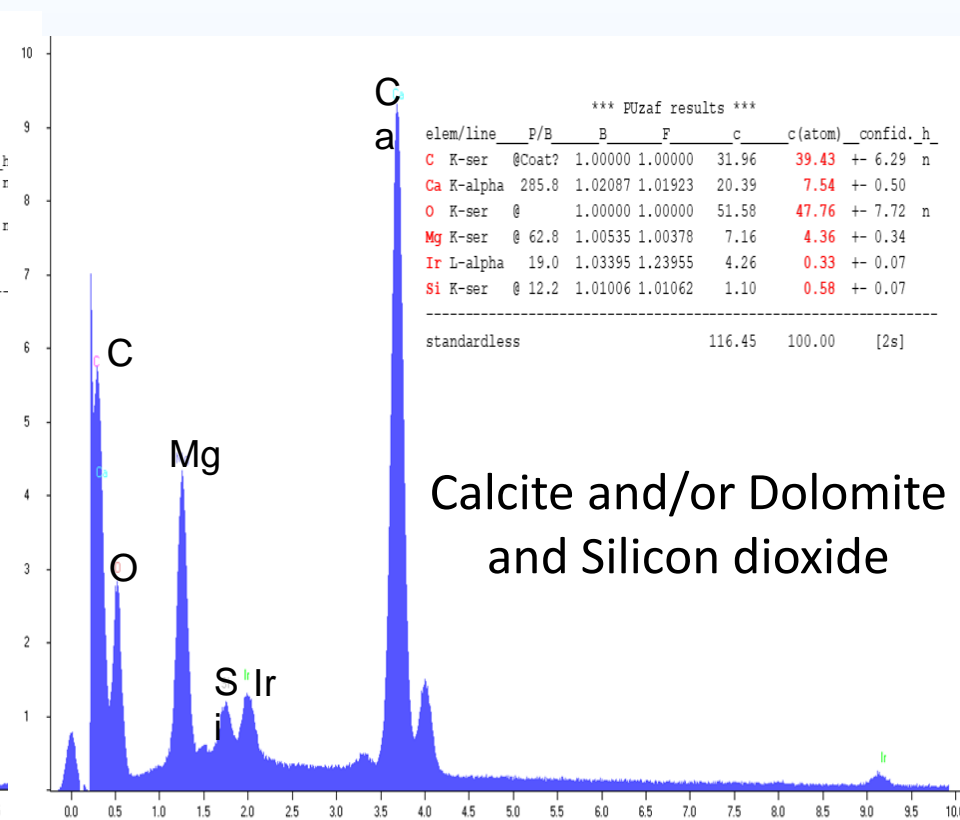
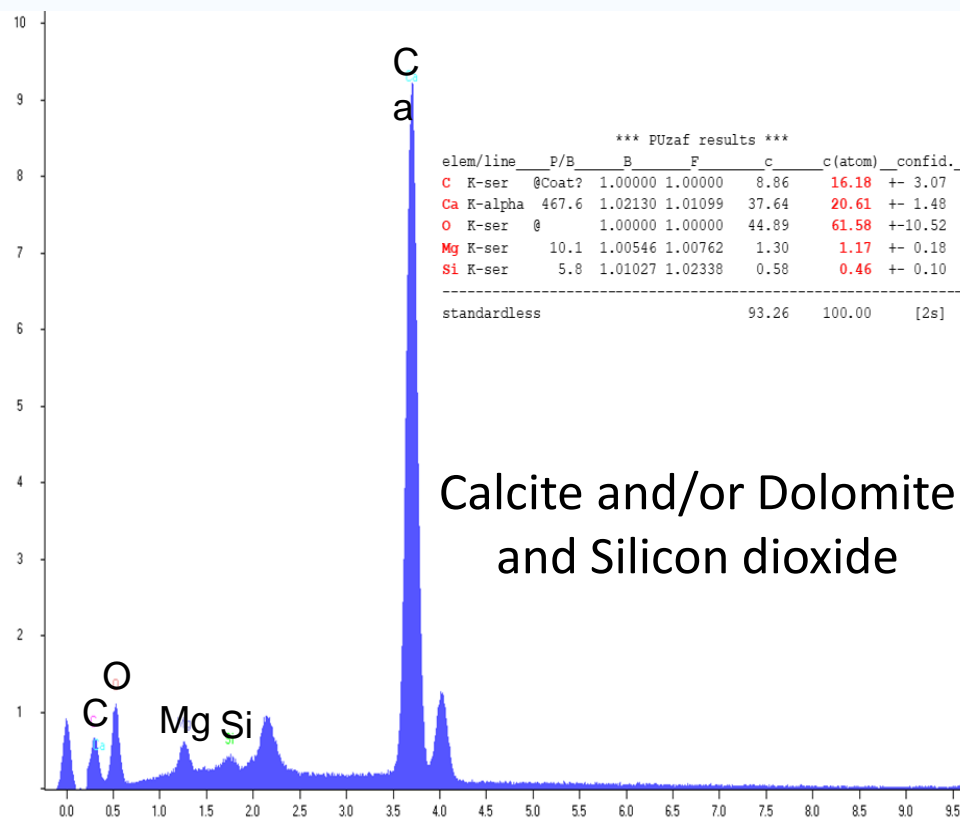


Calcite and/or Dolomite

EDX Elemental Composition : Reef

Pre-CO₂

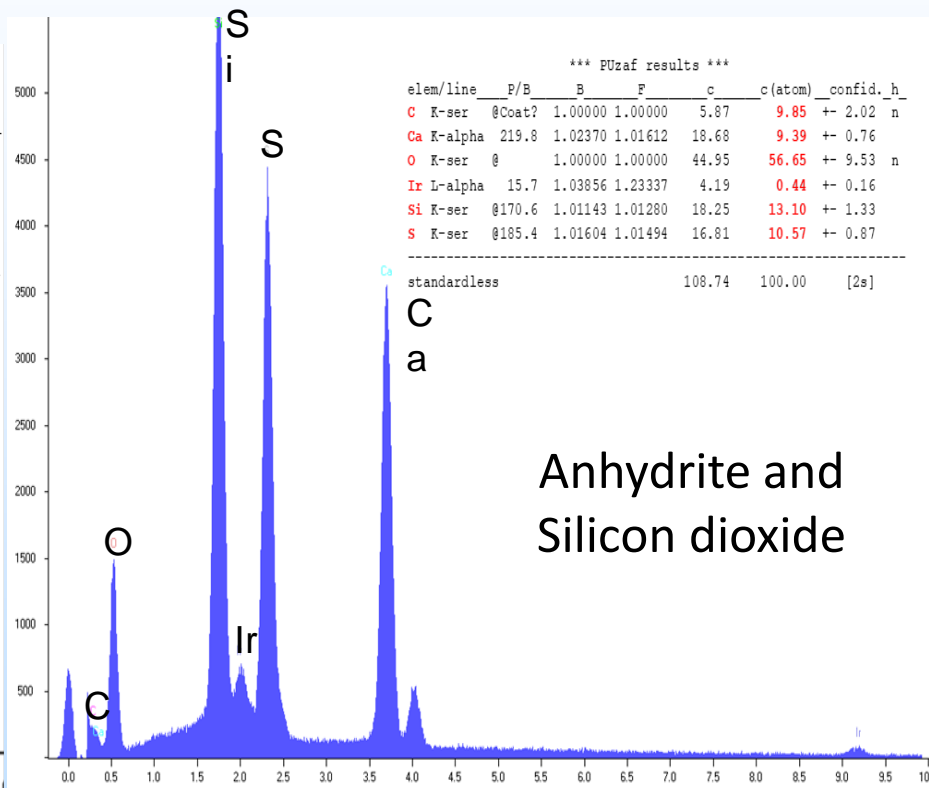
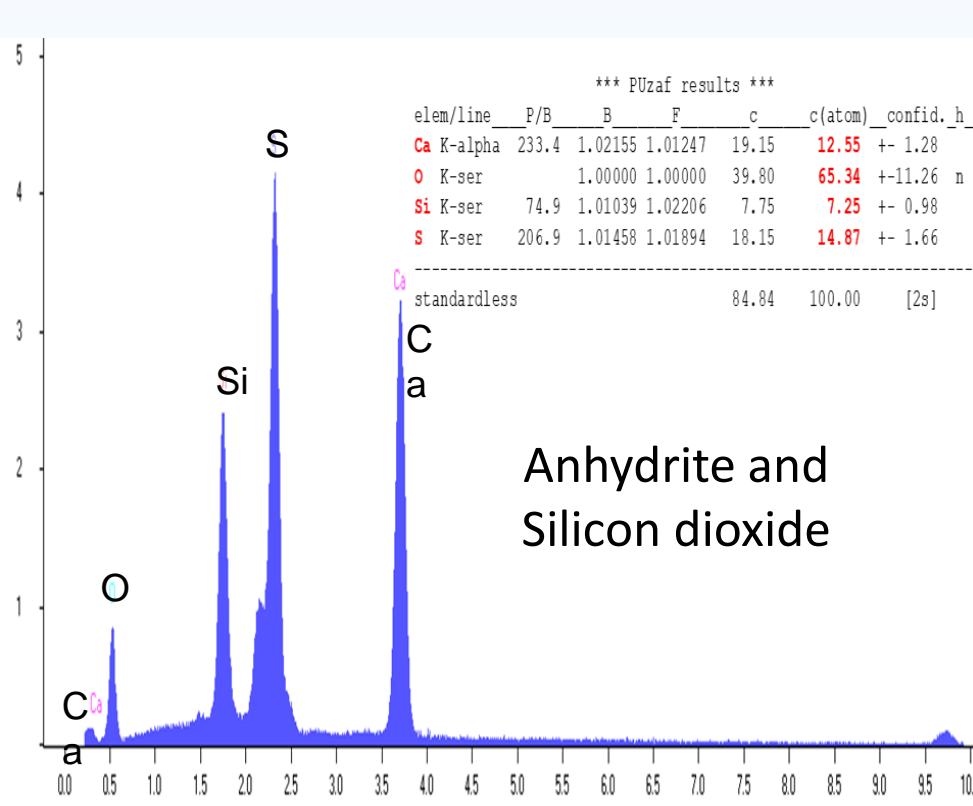
Post-CO₂



EDX Elemental Composition : Lagoon

Pre-CO₂

Post-CO₂







BSCSP ©



BSCSP®

Technical Status

- Prepare as many technical status slides as needed, but recognize the limits of the allocated presentation time.
- Use these slides to logically walk through the project. Focus on telling the story of your project and highlighting the key points as described in the Presentation Guidelines.
- Include specific information to show how your project is advancing the state-of-the-art; be as quantitative as possible in describing improvements in the performance of your technology compared to the state-of-the-art.

Accomplishments to Date

- Bullet List of Accomplishments (see Presentation Guidelines for examples).
- Multiple slides can be used if needed.

Lessons Learned

- Research gaps/challenges.
- Unanticipated research difficulties.
- Technical disappointments.
- Changes that should be made next time.
- Multiple slides can be used if needed.

Synergy Opportunities

- Discuss how collaboration among projects could have a synergistic effect on advancing the technologies described during the session in which you are presenting.

Project Summary

- Key Findings.
- Next Steps.

Appendix

- These slides will not be discussed during the presentation, **but are mandatory.**

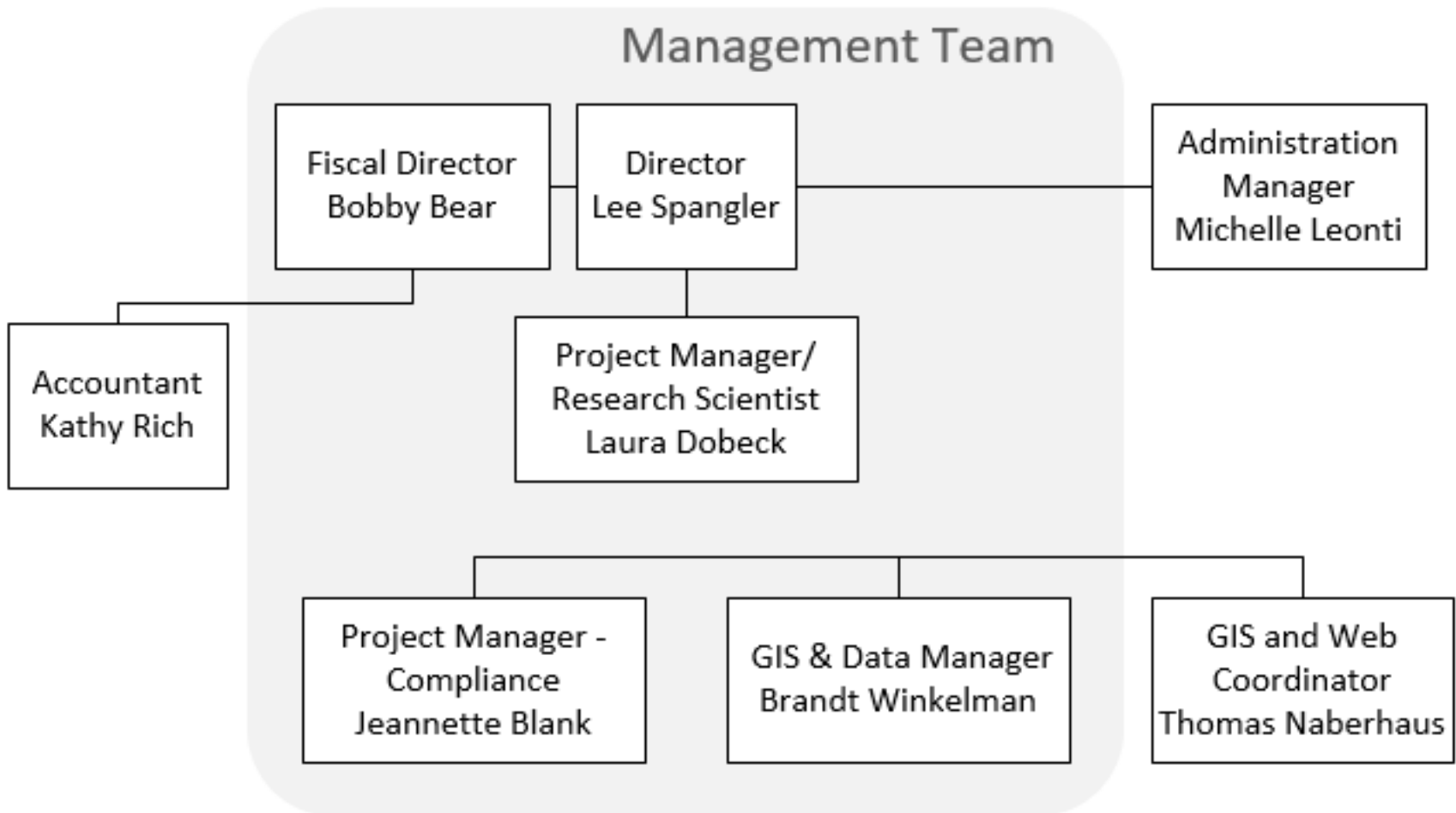
Benefit to the Program

- Identify the program goals being addressed.
-
- Insert project benefits statement.
 - See Presentation Guidelines for an example.

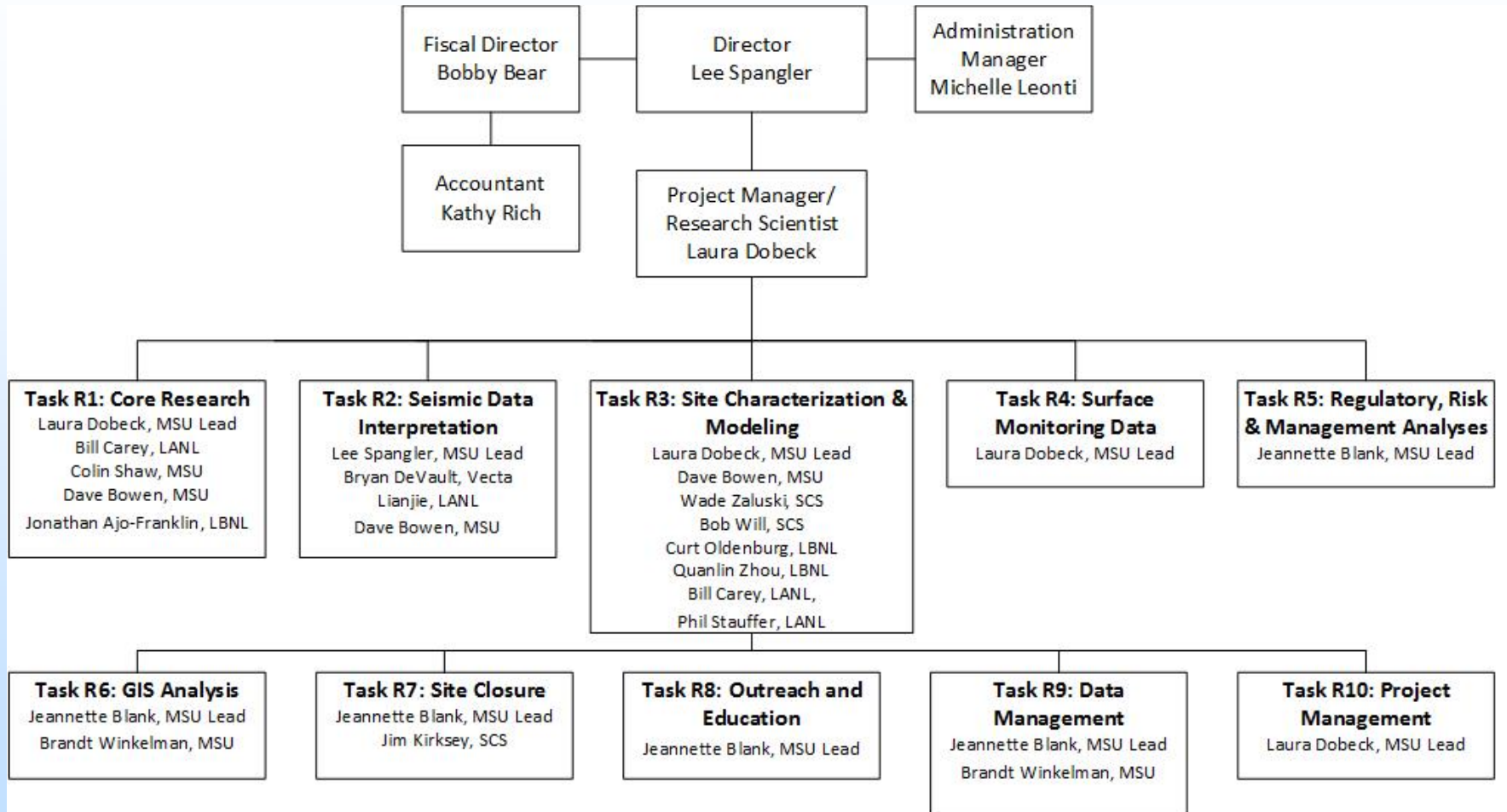
Project Overview

- Describe the project goals and objectives in the Statement of Project Objectives.
 - How the project goals and objectives relate to the program goals and objectives.
 - Identify the success criteria for determining if a goal or objective has been met. These generally are discrete metrics to assess the progress of the project and used as decision points throughout the project.

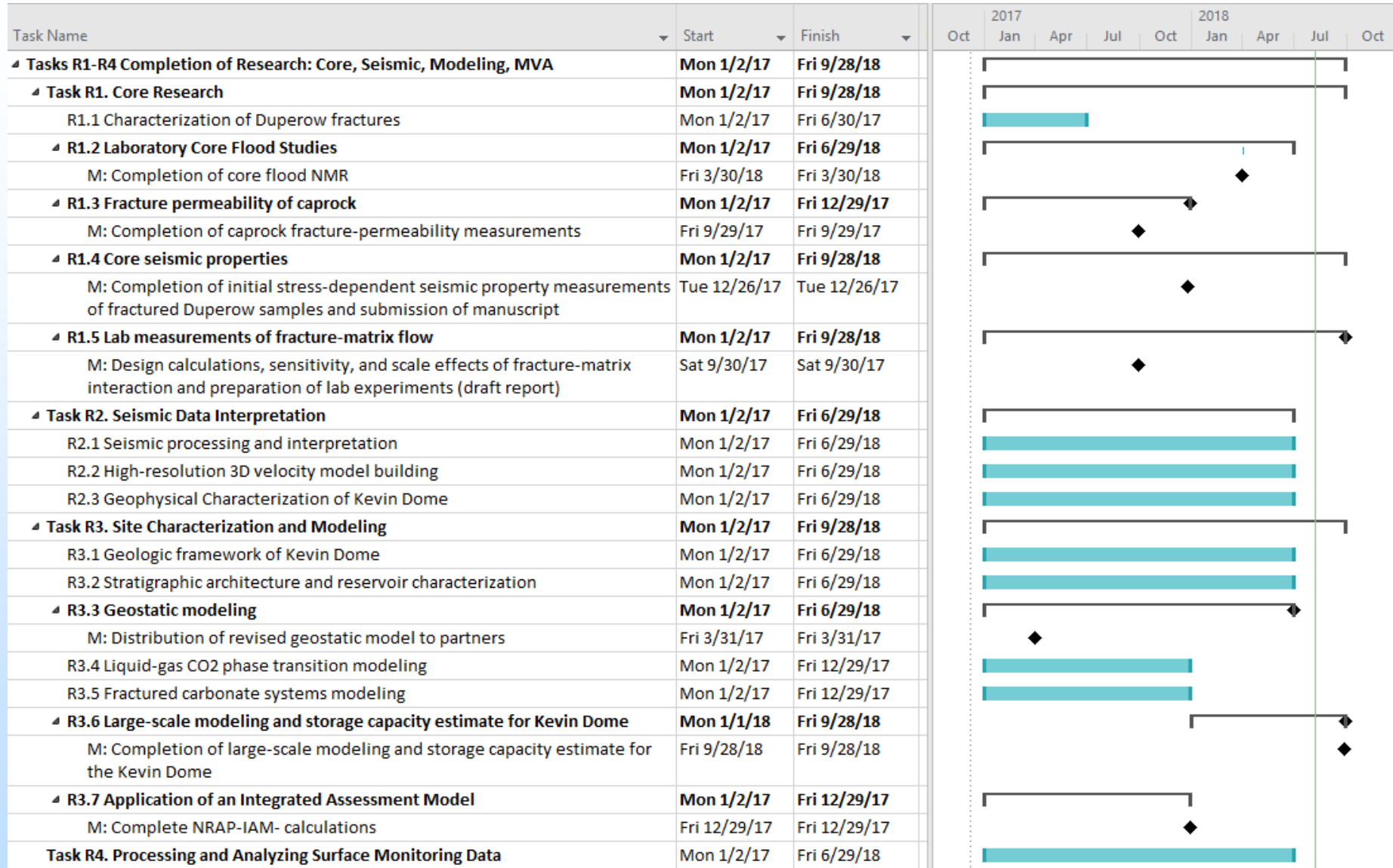
Organization Chart



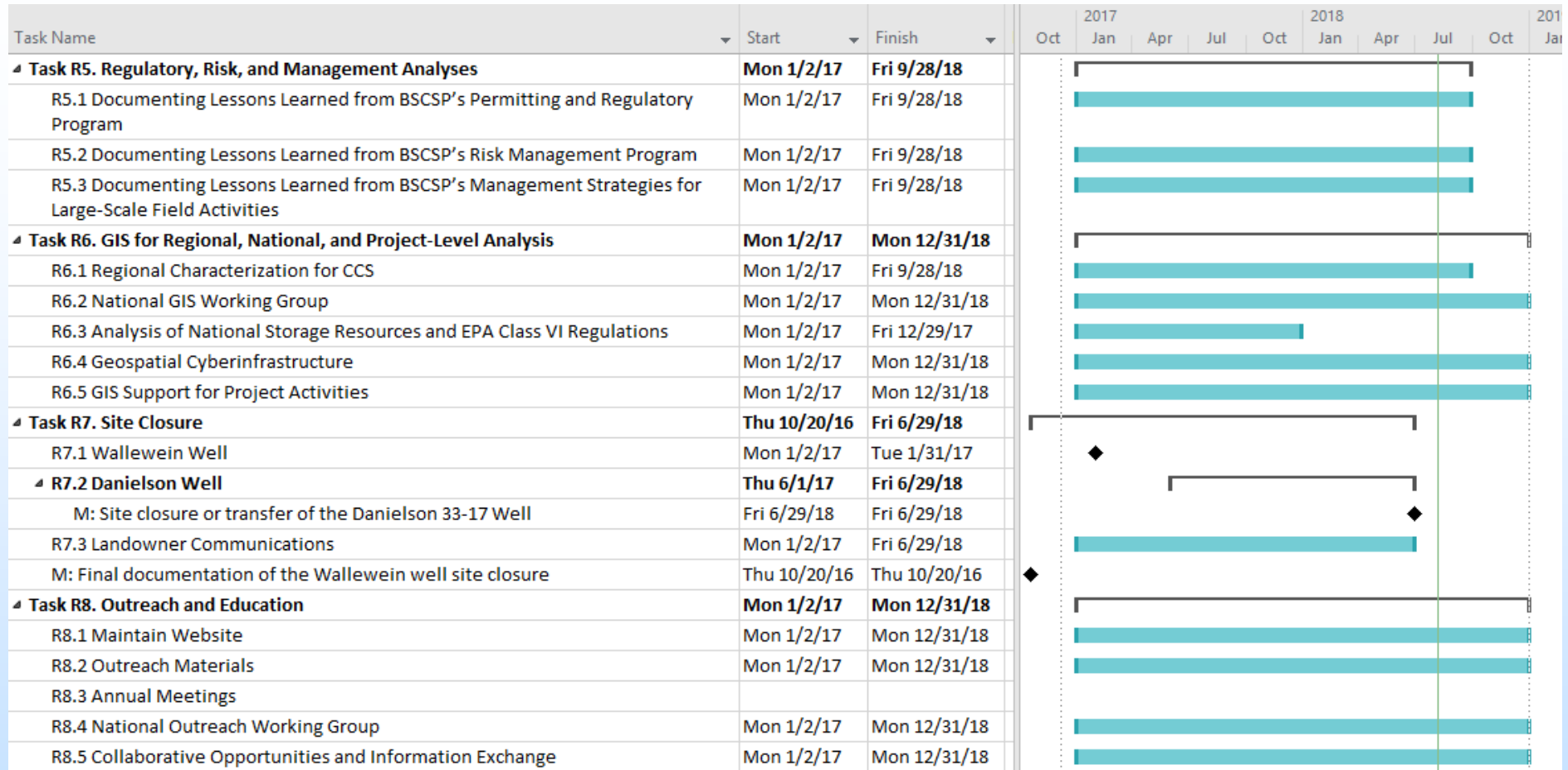
Organization Chart



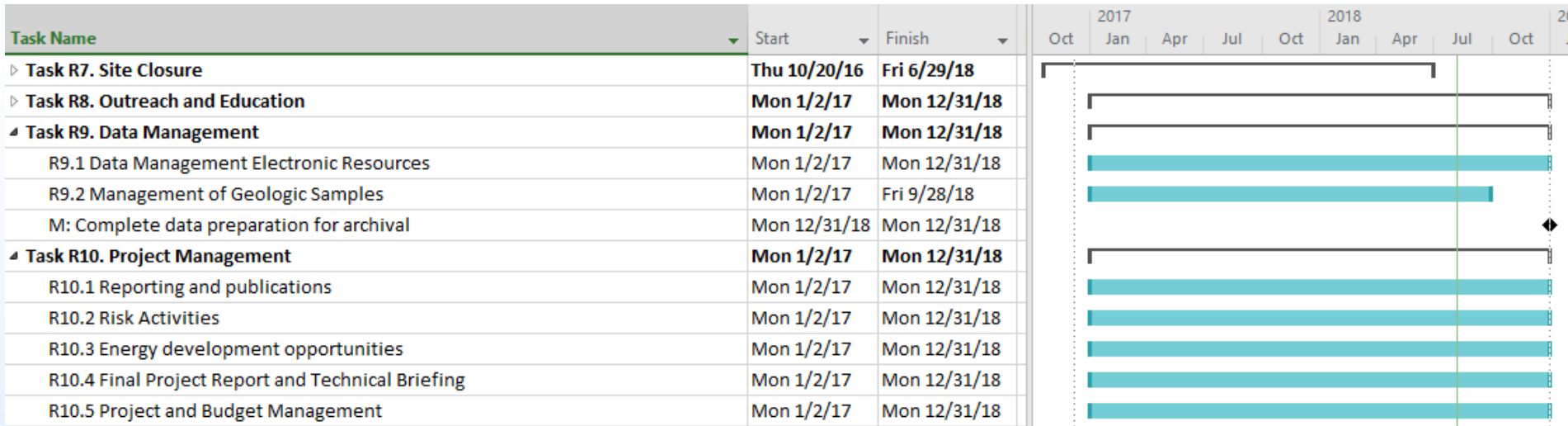
Gantt Chart



Gantt Chart



Gantt Chart



Bibliography

- DeVault, B., Bowen, D.W., Clochard, V., Delepine, N. and Wangkawong, K., Quadri-Joint inversion: Method and application to the Big Sky 9C 3D dataset in Northern Montana. *Journal Interpretation*, 2018. Revised
- Onishi, T., Nguyen, M., Carey, J.W., Will, R., Zaluski, W., Bowen, D.W., DeVault, B., Duguid, A., Zhou, Q., Fairweather, S., Spangler, L. and Stauffer, P., Potential CO₂ and brine leakage through wellbore pathways for geologic CO₂ sequestration using the National Risk Assessment Partnership tools: Application to the Big Sky Regional Partnership. *International Journal of Greenhouse Gas Control*, 2018. In Review

Bibliography

- McCann, C., Repasky, K.S., Morin, M., Lawrence, R.L. and Powell, S.L., Using Landsat surface reflectance (LaSRC) data as a reference target for multi-swath hyperspectral data collected over mixed agricultural rangeland areas. *IEEE Transactions in Remote Sensing*, 2017. 55(9): p. 5002-5014 10.1109/TGRS.2017.2699618.
- Saltiel, S., Bonner, B.P., Mittal, T., Delbridge, B. and Ajo-Franklin, J.B., Experimental evidence for dynamic friction on rock fractures from frequency-dependent nonlinear hysteresis and harmonic generation. *Journal of Geophysical Research: Solid Earth*, 2017. 122(7): p.4982-4999 DOI: 10.1002/2017JB014219.

Bibliography

- Saltiel, S., Selvadurai, P.A., Bonner, B.P., Glaser, S.D. and Ajo-Franklin, J.B., Experimental development of low-frequency shear modulus and attenuation measurements in mated rock fractures: shear mechanics due to asperity contact area changes with normal stress. *Geophysics*, 2017. 82(2): p. M19-M36 DOI: 10.1190/GEO2016-0199.1
- Spangler, L.H., Repasky, K.S., Morin, M., Lawrence, R.L. and Powell, S.L., A novel histogram based unsupervised classification technique to determine natural classes from biophysically relevant fit parameters to hyperspectral data. *IEEE Transactions in Remote Sensing*, 2017. 10(9): p. 4138-1148 10.1109/JSTARS.2017.2701360.
- Zhoua, Q., Oldenburg, C.M., Rutqvist, J. and Birkholer, J.T., Revisiting the fundamental analytical solutions of heat and mass transfer: The kernel of multirate and multidimensional diffusion. *Water Resources Research*, 2017. 53(11): p. 9960-9979 DOI: 10.1002/2017WR021040.

Bibliography

- Oldenburg, C.M., Cihan, A., Zhoua, Q., Fairweather, S. and Spangler, L., Geologic carbon sequestration injection wells in overpressured storage reservoirs: estimating area of review. *Greenhouse Gas Science and Technology*, 2016. 2016(00): p. 1-12 DOI: 10.1002/ghg.1607.
- Yoshida, N., Levine, J.S. and Stauffer, P.H., Investigation of uncertainty in CO₂ reservoir models: A sensitivity analysis of relative permeability parameter values. *International Journal of Greenhouse Gas Control*, 2016. 2016(49): p. 161-178 DOI: 10.1002/ghg.1607.
- Zdhanov, M., Endo, M., Black, N., Spangler, L., Fairweather, S., Hibbs, A., Eiskamp, G.A. and Will, R., Electromagnetic monitoring of CO₂ sequestration in deep reservoirs. *First Break - Special Topic: Unconventionals & Carbon Capture and Storage*, 2016. 31: p. 71-78.

Bibliography

- Zhoua, Q., Oldenburg, C.M., Spangler, L. and Birkholer, J.T., Approximate solutions for diffusive fracture-matrix transfer: Application to storage of dissolved CO₂ in fractured rocks. *Water Resources Research*, 2016. 53(2): p. 1746–1762 DOI: 10.1002/2016WR019868.
- Poggio, M., Brown, D.J. and Bricklemeyer, R.S., Laboratory-based evaluation of optical performance for a new soil penetrometer visible and near-infrared (VisNIR) foreoptic. *Computers and Electronics in Agriculture*, 2015. 2015(115): p. 12-20 DOI: 10.1016/j.compag.2015.05.002.
- Bellante, G.J., Powell, S.L., Lawrence, R. and Repasky, K.S., Hyperspectral Detection of a Subsurface CO₂ Leak in the Presence of Water Stressed Vegetation. *PLOS ONE*, 2014. 9(10) DOI: 10.1371/journal.pone.0108299.

Bibliography

- Dai, Z., Stauffer, P.H., Carey, J.W., Middleton, R.S., Lu, Z., Jacobs, J.F., Hnottavange-Telleen, K. and Spangler, L.H., Pre-site Characterization Risk Analysis for Commercial-Scale Carbon Sequestration. *Environmental Science & Technology*, 2014. 2014(48): p. 3908-3915 DOI: [dx.doi.org/10.1021/es405468p](https://doi.org/10.1021/es405468p).
- Long, J.A., Lawrence, R.L., Marshall, L. and Miller, P.R., Changes in field-level cropping sequences: Indicators of shifting agricultural practices. *Agriculture, Ecosystems and Environment*, 2014. 189(2014): p. 11-20 DOI: [10.1016/j.agee.2014.03.015](https://doi.org/10.1016/j.agee.2014.03.015).
- Tan, S. and Huang, L., Reducing the computer memory requirement for 3D reverse-time migration with a boundary-wavefield extrapolation method. *Geophysics*, 2014. 79(5): p. 185-194 DOI: [10.1190/GEO2014-0075.1](https://doi.org/10.1190/GEO2014-0075.1).

Bibliography

Bricklemeyer, R.S., Brown, D.J., Turk, P.J. and Clegg, S.M., Improved Intact Soil-Core Carbon Determination Applying Regression Shrinkage and Variable Selection Techniques to Complete Spectrum Laser-Induced Breakdown Spectroscopy (LIBS). *Applied Spectroscopy*, 2013. 67(10): p. 1185-1199 DOI: 10.1366/12-06983.

Lewicki, J.L., Hilley, G.E., Dobeck, L.M., McLing, T., Kennedy, B.M., Bill, M. and Marino, B.D.V., Geologic CO₂ input into groundwater and the atmosphere, Soda Springs, ID, USA. *Chemical Geology*, 2013. 339(SI): p. 61-70 DOI: doi:10.1016/j.chemgeo.2012.06.013.

Bibliography

Long, J.A., Lawrence, R.L., Greenwood, M.C., Marshall, L. and Miller, P.R., Object-oriented crop classification using multitemporal ETM+ SLC-off imagery and random forest. *GIScience & Remote Sensing*. *GIScience & Remote Sensing*, 2013. 50(4): p. 418-436 DOI: 10.1080/15481603.2013.817150.

Vogt, S.J., Shaw, C.A., Brox, T., Maneval, J.E., Skidmore, M.L., Codd, S.L. and Seymour, J.D., Magnetic Resonance Imaging of permeability enhancement in fast-flow-paths during supercritical CO₂ injection in sandstone and carbonate rock cores. *Journal of Petroleum Science and Engineering*, 2013. 122(October 2014): p. 507-514 DOI: 10.1016/j.petrol.2014.08.013.

Bibliography

- Borgia, A., Pruess, K., Kneafsey, T.J., Oldenburg, C.M. and Pan, L., Numerical simulation of salt precipitation in the fractures of a CO₂-enhanced geothermal system. *Geothermics*, 2012. 44(October 2012): p. 13-22 DOI: <http://dx.doi.org/10.1016/j.geothermics.2012.06.002>.
- Brickley, R.S., Soil carbon determination using rapid, inexpensive, non-destructive spectroscopy techniques, in Washington State University, Department of Crop and Soil Sciences. Ph.D. 2012. p. 176.
- Brickley, R.S., Brown, D.J., Barefield, J.D. and Clegg, S.M., Intact Soil Core Total, Inorganic, and Organic Carbon Measurement Using Laser-Induced Breakdown Spectroscopy. *Soil Science Society of America Journal*, 2011. 75(3): p. 1006-1018 DOI: 10.2136/sssaj2009.0244.

Bibliography

Leach, A., Mason, C.F. and van 't Veld, K., Co-optimization of enhanced oil recovery and carbon sequestration. *Resource and Energy Economics*, 2011. 33(4): p. 893-912 DOI: 10.1016/j.reseneeco.2010.11.002.

Watts, J.D., Lawrence, R.L., Miller, P.R. and Montagne, C., An analysis of cropland carbon sequestration estimates for North Central Montana. *Climate Change*, 2011. 108(1-2): p. 301-331 DOI: 10.1007/s10584-010-0009-1.

Watts, J.D., Powell, S.L., Lawrence, R.L. and Hilker, T., Improved classification of conservation tillage adoption using high temporal and synthetic satellite imagery. *Remote Sensing of Environment*, 2011. 115(1): p. 66-75 DOI: 10.1016/j.rse.2010.08.005.